COAL DESULFURIZATION BY SELECTIVE CHLORINOLYSIS

Thesis by

Nikolaos Petrou Vasilakos

In Partial Fulfillment of the Requirements
for the Degree of
Doctor of Philosophy

California Institute of Technology
Pasadena, California
1981

(Submitted October 30, 1980)

ACKNOWLEDGMENTS

It is with great pleasure that I acknowledge the inspiring guidance and the continuous support of my advisor, Professor W. H. Corcoran, throughout this work. His personal interest and encouragement along with the valuable insights and the thoughtful suggestions he offered me during the course of this investigation, and the great deal of freedom he allowed me in research, are deeply appreciated. My studies here at Caltech have been greatly enriched by my contact with him.

Dr. John J. Kalvinskas and Daniel D. Lawson of the Jet Propulsion Laboratory made significant contributions through many helpful discussions on several aspects of this research.

I am indebted to Erich Siegel of the Glassworking Shop for the skillful construction and the regular maintenance of the experimental apparatus and to George Griffith and Henry Smith of the Chemical Engineering Shop for their technical assistance in many phases of the experimental work.

The financial support of the California Institute of Technology, the Jet Propulsion Laboratory, and the Bechtel Corporation throughout this investigation is greatfully acknowledged.

Kathy Lewis did an excellent job in typing the thesis.

I thoroughly enjoyed the open and friendly atmosphere created here at Caltech by my fellow graduate students. I especially enjoyed the daily companionship of Russ Bone, Jim Kralik, Gary Whatley and Samir Barudi.

Special thanks go to my close friends Yannis Psycharis and Panos

Pananicolaou, with whom I shared so many pleasant, funny and occasionally crazy moments.

Finally, I would like to express my deepest gratitude to my parents for their love, understanding and constant support throughout the happy and the difficult times in my life. This work is naturally dedicated to them.

ABSTRACT

The desulfurization of coal by selective oxidation under slurry-phase chlorination conditions was investigated. Chemical reaction was found to be the rate-controlling step in carbon-tetrachloride chorination at 25°C for coal particles less than 150 μ in diameter. For larger particle sizes, a transition from chemical to intraparticle-mass-transfer control was observed. The nitrogen-surface area of the coal decreased significantly as a result of the chlorination reaction.

The reaction mechanism and the desulfurization patterns of chlorinolysis were studied under model-reaction and coal-chlorination conditions. Possible complete desulfurization schemes were considered.

The role of solvents both in increasing the efficiency of the coal treatment and in providing alternative paths for coal beneficiation processes was also examined. The results of this study were interpreted within the frame of the solubility-parameter theory, utilizing the new experimental technique of solubility-parameter spectroscopy.

Table of Contents

Table of Contents (continued)

Table of Contents (continued)

List of Figures

Figure No. Page

List of Figures (continued)

List of Tables

List of Tables (continued)

Table No. Page

Nomenclature

A	Frequency factor in Arrhenius equation.
c	Molar concentration, $\frac{\text{moles}}{\text{cm}^3}$.
c	Cohesive energy density, $\frac{\text{cal}}{\text{cm}^3}$.
D	Effective diffusion coefficient, $\frac{\text{cm}^2}{\text{sec}}$.
E	Activation energy, $\frac{\text{cal}}{\text{mole}}$.
E	Potential energy of a mole of material, $\frac{\text{cal}}{\text{mole}}$.
H	Heat content, $\frac{\text{cal}}{\text{g}}$.
ΔH_v	Heat of vaporization, $\frac{\text{cal}}{\text{mole}}$.
k	Reaction-rate constant.
n	Refractive index.
P	Pressure, atm.
Q	Chlorine uptake in coal, g/g.
R	Radius of a particle, cm.
R	$= 1.987 \frac{\text{cal}}{\text{mole} \cdot {}^\circ\text{K}}$, gas constant.
r	Radial position within a particle.
r	Reaction rate.
S	Surface area, $\frac{\text{m}^2}{\text{g}}$.
S	Sulfur content, wt.%.
T	Temperature, °K.
t	Time, sec.
t_D	$= \frac{R^2}{D}$, characteristic time for diffusion, sec.
V	Molar volume, $\frac{\text{cm}^3}{\text{mole}}$.
X	Fractional conversion.

Greek Symbols

γ	Surface tension, $\frac{\text{dyne}}{\text{cm}}$.
$\mathcal{D}$	Molecular diffusion coefficient, $\frac{\text{cm}^2}{\text{sec}}$.
δ	Tortuosity factor.
δ	Solubility parameter, $\frac{\text{cal}^{1/2}}{\text{cm}^{3/2}}$ (Hb).
ε	Porosity.
ϕ	Volume fraction.

Subscripts

b	Boiling point.
c	Critical state.
e	Equilibrium conditions.
f	Final.
l	Refers to liquid phase.
m	Effective.
o	Initial.
s	At surface.
T	Total.

Chapter 1

INTRODUCTION

Though coal has been a major contributor to U.S. energy needs for well over a hundred years, its growth has been limited by the availability of relatively cheap oil and natural gas. Coal production in 1975 was equivalent to 15.4 quadrillion Btu, a level first achieved in 1918, and today represents only 18% of our primary energy supply as contrasted to 75% in 1918 (1).

With increasing energy demands and uncertainties in imported oil and natural gas supplies, which in any case appear to be limited, the vast reserves of coal in the United States (almost one-third of the world's known coal reserves) are becoming an extremely important energy source, especially for electric utilities, where coal comprises 55% of the primary fuel used in electric generation. With the economy becoming more dependent on electricity and the development of effective alternatives for energy production (nuclear, solar power, etc.) not likely for various reasons in the near future, it becomes apparent that coal, either as a solid fuel, or a source of synthetic liquid or gaseous fuels, will fill a significant part of the nation's energy needs during the next few decades.

Coal utilization gives rise, however, to a number of ecological problems, the most severe of them being the air pollution from particulates, nitrogen oxides, and sulfur dioxide produced by combustion in utility boilers. It is estimated that worldwide sulfur dioxide emissions from coal combustion in 1965 amounted to 102×10^6 tons, a two-fold increase since 1940 (2). Under the 1970 amendments to the Clean Air Act, the Environmental Protection Agency (EPA) sets up national ambient-air quality standards for sulfur oxides. The latest Federal standards of performance for new coal-fired power plants call (3) for an upper sulfur dioxide emission limit of 1.2 lb per million Btu output and for 90% sulfur reduction (or 70% reduction when emissions are less than 0.6 lb per million Btu output). For a coal with a heating value of 12,000 Btu/lb, the $\frac{1.2 \text{ lb } SO_2}{10^6 \text{ Btu}}$ limit is equivalent to 0.7% maximum allowable sulfur content. Only 13% of the current run-of-mine utility coal production in the United States meets this sulfur-content requirement, mainly the Western coals and some limited tonnage of West Virginia, Kentucky and Alabama coals. The additional requirement of 90% sulfur reduction poses even more severe problems in coal utilization and stresses the urgent need for a highly effective desulfurization process which will meet both EPA standards and economic feasibility. Desulfurization of fossil fuels has become a major issue in the world's economics and politics. One can safely say that the lack of desulfurization technology is one of the major contributors to the energy crisis. Because of air pollution regulations and the lack in the United States of low-sulfur fuel, the huge U.S. energy market previously sought other sources of fuel abroad. High-sulfur fuel in the form of coal, however, does exist in the United States, and it is possible to use it if it can first be desulfurized (4).

1.1 Sulfur compounds in coal

The total amount of sulfur in coal varies from 0.2 to 10 wt.% but in most samples is in the range of 1.0 to 4.0 wt.% (5).

Two forms of sulfur are recognized in coal:

(i) Organic sulfur, which is bound to the hydrocarbon structure of the coal, and

(ii) Inorganic sulfur, which is the remainder.

The weight ratio between these two general classes of sulfur varies from 4:1 to 1:3 inorganic/organic sulfur; however, it is usually close to 2:1 (6).

Inorganic sulfur appears mainly in two forms: as pyritic sulfur (i.e. sulfur combined with iron as pyrite or marcasite crystalline forms of FeS_2) and as sulfate sulfur in the form of iron, calcium and barium sulfates. The amount of sulfate sulfur, small for freshly mined coal, increases with the length of exposure of the coal to air due to pyrite oxidation and conversion of the pyritic sulfur to sulfates.

Organic sulfur is categorized according to the type of functional group in which it appears, namely, sulfidic (R-S-R'), disulfidic (R-S-S-R'), mercaptanic (R-S-H), thiophenic (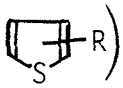), etc.

It is found that the organic sulfur is essentially uniformly distributed in the coal matrix (7). No organic sulfur compounds can be isolated from coal without changing the organostructure, and that is why organic sulfur is the most difficult form of sulfur to remove from coal. The random distribution of sulfur in coal is then attributed to the pyritic sulfur which is present in the form of a network of foreign material and can be separated by physical means.

1.2 Coal desulfurization

Current desulfurization processes can be classified into two categories: (1) processes for the removal of sulfur from the gaseous coal-combustion products and (2) processes for the desulfurization of coal prior to combustion.

Post-combustion or flue-gas desulfurization of coal involves stack-gas treatment with scrubbing with lime solution being the most common. Because the resistance to SO_2 mass transfer is in the gas phase, the particular solution or solid used for scrubbing is of secondary importance only (4). On the other hand, the concentration of SO_2 in the combustion products is generally small. These factors result in large capital investments for huge processing units and in large operating costs for gas-phase desulfurization.

An additional disadvantage of flue-gas desulfurization by scrubbing is that it can produce large amounts of sludge, thus not really solving the SO_2 pollution problem but rather shifting it to a solid-waste problem.

Precombustion desulfurization of coal can be classified into three groups: (i) physical separation (depyriting), (ii) conversion of coal to low-sulfur (and low-ash) liquid and gaseous fuels (hydrodesulfurization), and (iii) chemical desulfurization.

The coarse particles of pyritic (and sulfate) sulfur can be removed from coal by one of the following physical-separation techniques

(<u>8</u>):

(1) Density-based separation of pyrite (density 5.0 g/cm^3) from coal (density 1.2 - 1.6 g/cm^3),

(2) Stage crushing of the coal,

(3) Froth flotation,

(4) Gravity concentration,

(5) Microwave and high-intensity magnetic separation, and

(6) Electronic separation.

These methods remove part of the ash and the inorganic sulfur from coal but are completely ineffective for organic sulfur. Therefore, they are not suitable for high-sulfur coals, which contain substantial amounts of organic sulfur.

Hydrodesulfurization processes (<u>9</u>) can remove both inorganic and organic sulfur as H_2S by hydrogenation of the coal in a solvent at high temperatures and pressures (450°C, ∿200 atm), and in the presence or absence of a catalyst. Hydroprocessing is effective but costly in terms of equipment, investments and resources (high cost of hydrogen). This assessment, however, is not really accurate, because hydroprocessing of coal is almost never used for desulfurization purposes alone, but at the same time for liquefaction; that is, for production of low-ash (and low-sulfur) liquid and gaseous fuels from coal (EXXON, SRC processes, etc.). The two costs, for hydrodesulfurization and for liquefaction, cannot be separated easily.

Chemical desulfurization processes, which in the author's opinion are the most promising in terms of sulfur removal and processing costs, use specific reagents, either oxidizing agents or basic media, to selectively attack and remove both inorganic and organic sulfur from coal.

Some nine processes under development, in the laboratory or on pilot-plant scale, are currently considered serious contenders for chemical coal cleaning (10). Five of them are well documented, and they are assessed briefly below.

The TRW Meyer's process (11,12) uses a regenerable aqueous ferric sulfate solution to oxidize the pyritic sulfur in coal to elemental sulfur and sulfate at low temperatures and pressures (100 - 130°C, 0 - 100 psig). The process removes only the inorganic sulfur, which is a serious drawback in treatment of high-sulfur coals.

The Battelle Hydrothermal Process (13) involves heating of a slurry of coal in $NaOH/Ca(OH)_2$ solution in an autoclave to a temperature of 225 - 350°C at pressures of 350 - 2500 psig. Part of the inorganic minerals in coal dissolves, and some of the sulfur is converted into sodium sulfide. The process operates at elevated temperatures and pressures with the implications of being costly.

Partial oxidation of coal at elevated temperatures and pressures (150°C, 400 - 500 psig) is employed in the DOE process (10) to convert both inorganic and organic sulfur to sulfuric acid. The oxidation takes place by contacting air with a slurry of coal in aqueous Na_2CO_3 solution. Almost all the pyrite and up to 40% of the organic sulfur can be removed as sulfuric acid, but at the expense of significant, up to 50%, losses in the heat content of the coal because of the co-current oxidation of the hydrocarbon matrix. This loss is a very serious disadvantage of the DOE process, which has also received unfavorable economic estimates (14).

The KVB process (15) involves heating of the coal in the presence of NO-NO_2-air mixtures in a fluidized bed reactor under mild reaction conditions (100°C and ambient pressure). Sulfur is converted to SO_2 and sulfates, which are subsequently extracted from coal in an alkaline-wash step. Pyritic-sulfur removal up to 100% and organic sulfur removal up to 40% have been claimed. The process is plagued by the same problem present in the DOE process, namely, the nonselective reaction of NO_2 with the coal matrix resulting in significant nitration and oxidation of the coal with significant losses in heat content. Work along the same line of coal desulfurization by selective oxidation with nitrogen oxides has also been conducted independently by our research group at the California Institute of Technology (16,17).

Finally, the JPL chlorinolysis process (18) employs the Cl_2/H_2O system to oxidize selectively and remove both inorganic and organic sulfur from coal as water-soluble sulfates under mild reaction conditions (50 - 100°C, 0 - 100 psig). This process, which has received (14) the most favorable estimate of all the chemical desulfurization processes considered so far, both in terms of economics and performance, will be described in detail in the next section.

Other processes in the same general area of chemical desulfurization include (10,19): the Ledgemont process (ammonia/oxygen/water system), fluidized-bed combustion, the Institute of Gas Technology (IGT) process (combination of oxidative pretreatment and hydrodesulfurization), the General Electric Microwave process (alkaline, with a microwave shock treatment) and the ARCO process (information withheld). These processes are at the early stages of development and thus not sufficiently documented to allow for thorough assessment.

It is apparent from the above discussion that there is a pressing need for significant improvement in the effectiveness and the economics of coal desulfurization. A low-cost, technically simple, coal-pretreatment process that removes the organic as well as inorganic sulfur in coal effectively without having to destruct the carbon matrix will be a major breakthrough in coal utilization. Of particular interest among potential processes is one at moderate temperatures (<300°C) and pressures (<20 atm) wherein coal is attacked by an oxidizing agent, such as Cl_2/H_2O or NO_2, with hydrolysis or pyrolysis as a later step to split off relatively low-molecular-weight sulfur compounds from the organic matrix (20).

1.3 Coal desulfurization by low temperature chlorinolysis

The JPL chlorinolysis process involves three steps:

(1) Slurry-phase chlorination of coal

Chlorine gas is bubbled through a slurry of ground moist coal in an organic solvent (methyl chloroform in most cases) under mild conditions. The pressure never exceeds 100 psig, nor the temperature 90°C with the solvent present. The reaction of chlorine with pyritic and organic sulfur in coal produces sulfuric and hydrochloric acids which should also be counted as reagents because they attack the accessory minerals of the coal, extract sodium from the organic phase of the coal, and perform other functions as well (10).

The overall desulfurization scheme involved in "wet" chlorination of coal may be described as follows (21):

(i) $FeS_2 + \frac{15}{2} Cl_2 + 8H_2O \rightarrow FeCl_3 + 2H_2SO_4 + 12HCl$

(ii) $R\text{-}S\text{-}R' + 3Cl_2 + 3H_2O \rightarrow RSO_3H + R'Cl + 5HCl$

(iii) $R\text{-}S\text{-}R' + 4Cl_2 + 4H_2O \rightarrow RCl + R'Cl + H_2SO_4 + 6HCl$

Under the mild reaction conditions, little chlorine becomes strongly bound to the organomatrix, for most residual chlorine in the treated coal can be removed by steam stripping.

(2) Hydrolysis

The chlorinated coal is hydrolyzed, producing hydrochloric acid according to the reaction:

(iv) $RCl + H_2O \rightarrow ROH + HCl$

The sulfur converted to sulfonates or sulfates in the chlorination step is water soluble and is leached out by water washing at 60°C.

(3) Dechlorination

After hydrolysis, the treated coal is dechlorinated by heating at 350 - 550°C and ambient pressure in a steam:

(v) $RCl(s) + H_2O(g) \rightarrow ROH(s) + HCl(g)$

or in an inert gas atmosphere:

(vi) $RCl + R'H \rightarrow RR' + HCl$

Laboratory-scale results for coal samples which have undergone complete process treatment (22,23) indicated the following levels of sulfur reduction: pyritic sulfur 13 to 98%, organic sulfur 27 to 74%, total sulfur 43 to79%. A number of the coals tested achieved a total sulfur reduction down to ∿0.7 wt.% sulfur which meets the EPA limit of 1.2 lb $SO_2/10^6$ Btu in stack emissions. Attendant chlorine levels in treated coal samples after dechlorination were from 0.06 to 1.0 wt. %.

Work on the chlorinolysis process is being funded by DOE and is already progressing rapidly on the pilot-plant level (24). Chlorinolysis owes its favorable economics (14) and unique sulfur-extractive abilities to the power of the reagent which permits action at low temperatures in contrast with oxygen, water, etc. Under these mild conditions, the reagent is rather selective, and little of it is taken up by the coal. Even that amount is removed easily by hydrolysis and dechlorination. The reagent is thus rapidly recovered and reactivated, while the fuel value of the coal is preserved, and, indeed, on a per-ton basis, enhanced in the finished product (10).

Clearly, the most important step in the whole process is the chlorination of coal where most of the physical and chemical changes in the organomatrix take place. Hydrolysis is just a leaching step for the water-soluble sulfonates and sulfates formed in the chlorination step, and dechlorination is the step for the removal of any additional chlorine incorporated in the coal matrix during chlorination (25).

The main goals of this present research work were to:

(1) Determine the physical and chemical changes that take place in coal during chlorination and their effect on the desulfurization efficiency of chlorinolysis. Model chlorination studies would provide additional insight to the reaction mechanisms and desulfurization paths of the chlorinolysis process and help select optimum reaction conditions.

(2) Describe the nature of the mass transfer of reactants through the complex coal structure and its coupling with the chemical rate during chlorination of coal (<u>26</u>), and

(3) Examine and refine the role of certain physicochemical parameters of the slurry system in maintaining the structural integrity of the coal in the presence of the exothermic, oxidative chlorinolysis reactions and in enhancing the desulfurization rate. Interfacial tension of the slurry liquid on the coal surface (<u>28</u>), compressibilities $\left(\frac{\partial V}{\partial P}\right)_T$ and expansivities $\left(\frac{\partial V}{\partial P}\right)_T$ for both the coal and the liquid, and the solubility parameter of the liquid as it relates to the swelling and extraction characteristics of the coal matrix are some of the parameters that should receive careful consideration in this area (<u>26</u>).

Chapter 2

CHLORINATION OF COAL

2.1 Introduction

Most of the early studies on using chlorine to treat coal had different objectives other than desulfurization, such as the production of a non-coking fuel suitable for burning and the production of chlorohydrocarbons from coal.

The most comprehensive studies of halogenation of coal using gaseous chlorine have been made by McCulloch and co-workers (29), although other studies have been reported. Gaseous chlorine was found to react vigorously with coal, the reaction producing considerable heat. The gaseous products of chlorination contained large quantities of hydrogen chloride. Chlorination thus seemed to give rise to substitution as well as addition. McCulloch reported a negative temperature dependence for the rate of chlorination over the range of 20 - 60°C. Chlorinated coal was found to be completely non-coking and yielded no tar upon distillation. The chlorine incorporated in the coal during chlorination was evolved practically quantitatively as hydrogen chloride upon heating at temperatures below 550°C. The highly condensed nucleus of the coal molecule did not appear to be significantly altered by chlorination. Decomposition of the residue above a temperature of 500 - 600°C gave essentially the same results as the residue from unchlorinated coal. Finally, chlorinated coal was found to be much more extractable in the same solvents than raw coal.

Beyers and van Rooyen (30) found a positive temperature dependence for the rate of reaction of gaseous chlorine with coal over the range 90 - 150°C, zero dependence from 150° to 340°C, and a negative dependence at temperatures above 340°C.

In an attempt to obtain chlorinated products from coal, Weiler (31) treated coal with chlorine and antimony pentachloride for six days at 200°C and then four more days at 400°C. The volatile products obtained were carbon tetrachloride, hexachloroethane, hexachlorobenzene, and other unidentified, highly chlorinated hydrocarbon derivatives, but these products accounted for only 5% of the carbon originally present in the coal.

Under extremely severe chlorination conditions and in the presence of ferric chloride as catalyst, Kung (32) obtained carbon tetrachloride from coal in high yields (77 to 86%). Boyk and Hass (33), on the other hand, employed the reaction of gaseous chlorine with a bituminous coal to produce activated carbon.

Pinchin (34) studied the chlorination of a medium rank coal in the temperature range 0 - 1100°C under various conditions, both with gaseous chlorine and in the slurry phase. He found that with increasing temperatures of chlorination, the chlorine remaining in the product coal was more firmly bound, though much was still removed on hydrolysis. Chlorination was shown to remove hydrogen and peripheral organic groups. Substitution predominated over incorporation of chlorine into the coal nucleus. Chlorination even under relatively severe conditions (700 - 1100°C) did not substantially alter the major part of the coal structure. Subsequent carbonization of coals treated at lower temperatures did not produce chlorinated tars but only hydrogen chloride and some volatile matter.

Moschopedis *et al*. (35) reported the absence of carbon-chlorine bands from the infrared spectra of chlorinated coals and hypothesized that this absence was caused either by the extreme dependence of C-Cl absorptions on molecular environments, and thus the possible occurrence of such absorptions outside the spectral region examined, or by a general "smearing out" of absorptions in the relevant regions owing to several simultaneous addition and substitution reactions. Wielopolski *et al*. (36), however, reported a new band at 13.3 μm for coal residues containing 22 - 42% chlorine.

Macrae and Oxtoby (37) studied the chlorination of bituminous and anthracite coals in aqueous and nonaqueous liquid media at temperatures below 60°C. The reaction of chlorine with coal was characterized mainly by the progressive removal of hydrogen, dehydrogenation effects being much greater in aqueous than in nonaqueous solutions. This dehydrogenation was shown to lead to a condensation of the coal structure rather than to a controlled degradation to small molecular species. The extent of chlorination was progressively lower with increasing coal rank. Again, on being heated, chlorinated coals readily lost hydrogen chloride and at 500°C virtually all of the chlorine had been lost in that way. No tar was evolved. A large proportion of the chlorine was only loosely bound in the coal matrix and could be removed by mild hydrolysis. The more stable coal materials were those produced under the more severe reaction conditions, which confirmed Pinchin's results.

Chlorinated coals containing 15 - 20 wt.% chlorine were appreciably more soluble in solvents than untreated coals. This increased solubility was attributed largely to a weakening of cohesive, secondary forces in the coal rather than to a rupture of primary chemical linkages. The infrared spectra of the untreated, the chlorinated, and the extracted coals were very similar which led to the conclusion that chlorinated or extracted coal materials had a structure not fundamentally different from that of the unmodified coal. Absorption due to C-Cl bonds in the spectra of chlorinated coals was not apparent here as well.

Finally, Ball and Mitchell (38) reported recently the results of a study on chlorination of a low-rank bituminous coal with gaseous chlorine at temperatures between 19° and 300°C. The amount of chlorine taken up and the proportion evolved as hydrogen chloride were found to be controlled by mass-transfer processes at temperatures up to 200°C. At higher temperatures, a change in the reaction mechanism was apparent. Solvent extraction and infrared studies showed that the chlorinated derivatives were basically similar to the raw coal. In contrast to the results of McCulloch (29) and Macrae and Oxtoby (37), chlorinated coals were found to be only slightly more extractable in the same solvents than the raw coal. The infrared spectra indicated reductions in several important bands including those ascribed to hydrogen-bonded phenolic groups and nonaromatic carbon-hydrogen groups. Again, there was no evidence of the existence of C-Cl bonds. Hydrolysis showed that much of the chlorine was readily removed from chlorinated coal.

2.2 Experimental system

The laboratory apparatus used throughout this investigation for the study of slurry-phase chlorination of coal and related compounds is shown in Figure 1.

The chlorination unit consists of the following parts:

(1) Chlorine line - chlorine tank, $CaCl_2$ dehydrator and flow meter. High purity (Union Carbide, 99.5% minimum purity) chlorine gas was used.

(2) Chlorinator - a 500-ml, double-bottomed, cylindrical glass vessel with an inside diameter of 6 cm. Chlorine at ambient pressure was bubbled through the upper bottom, which is a fritted glass disk of medium (10 - 15 μ) size pores, into the liquid medium. The reactor is equipped with a thermometer immersed in the liquid phase, a temperature controlling element (thermocouple, on-off temperature controller, heating tape) and magnetic stirring.

(3) Reflux condenser - suitable for total solvent reflux.

(4) Cold trap - a Dewar container filled with a dry ice-acetone mixture (-78°C) for collecting the excess chlorine (b.p. -34.6°C) off the chlorinator.

(5) Scrubber - containing a 3N sodium hydroxide solution for absorption and determination by titration of the hydrogen chloride (b.p. -84.9°C) produced by the chlorination reaction.

(6) Gas holder - for collecting and analyzing gaseous compounds, other than chlorine and hydrogen chloride, produced by coal chlorination.

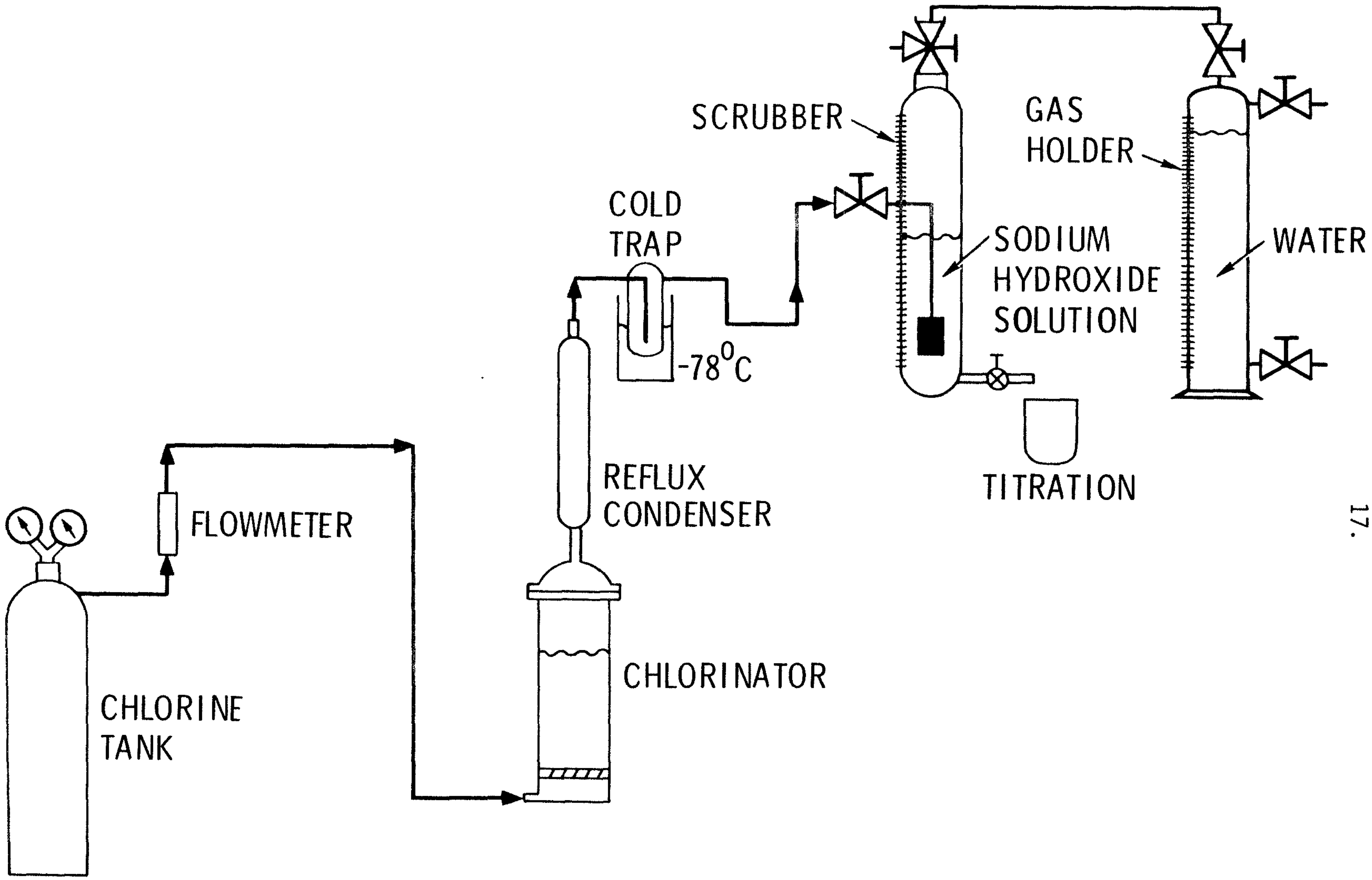

Figure 1. Laboratory glassware apparatus for the slurry-phase chlorination of coal.

2.3 Kinetic and mass-transfer effects in the slurry-phase chlorination of coal

2.3.1 The reaction system

The PSOC 190 coal, obtained from the Pennsylvania State University Coal Bank, was used throughout this investigation. It was an Illinois No. 6, high volatile C, bituminous coal. Two different lots, representing two different samplings of the coal from the mine and having slightly different compositions, were received from the Coal Bank and were designated as A and B.

The PSOC 190B coal used in the present study showed the following ultimate-analysis composition (on a dry basis):

Ash: 7.5 wt.%
Carbon: 69.5 wt.%
Hydrogen: 4.9 wt.%
Nitrogen: 1.09 wt.%
Sulfur: 3.06 wt.%
Oxygen: 13.9 wt.%
Chlorine: 0.05 wt.%

The moisture content of this coal was about 14 wt.%. Before each experimental run, the coal sample was dried in vacuum at 115°C for two hours. The moisture content was reduced by this procedure to less than 0.08 wt.%.

To study kinetic and mass-transfer effects experimentally in slurry-phase chlorination of coal, approximately five grams of raw predried PSOC 190B coal of a certain (narrow) particle-size range were suspended in 350 ml of reagent-grade carbon tetrachloride presaturated with chlorine and were chlorinated at 25°C and at a (dry) chlorine flow rate of 0.75 g/min under intense (1100 r.p.m.) and constant stirring for a certain period of time. The chlorinated coal was then filtered, dried in vacuum at 115°C for four hours, and the weight increase of the sample because of chlorination was noted. The chlorine content of the treated coal was determined by the Eschka method (Section 5.2.1).

Four different particle-size ranges were kinetically studied: (i) -400 Tyler mesh (<37μ), representing negligible intraparticle mass-transfer resistance and thus displaying kinetic effects only, (ii) 100 x 200 mesh (74 x 149μ; $\bar{d} \simeq 112\mu$), (iii) 20 x 24 mesh (707 x 841μ; $\bar{d} \simeq 774\mu$), and (iv) 12 x 14 mesh (1190 x 1410μ; $\bar{d} \simeq 1300\mu$).

2.3.2 Results and discussion

The results for chlorine uptake Q (in grams of chlorine incorporated in the coal matrix during chlorination per gram of raw dry coal) for the various coal samples are given in Table 1 and depicted in Figures 2 (-400 mesh: kinetic effect) and 3 (coupled kinetic and mass-transfer effects).

In reference to Table 1, the following observations can be made:

(i) Chlorine uptake in coal for the -400 mesh particle size (kinetic effect) is very satisfactorily described by an Elovitch-type equation:

$$\frac{dQ}{dt} = Ae^{-BQ} \qquad (1)$$

Table 1. Chlorine uptake for the PSOC 190B coal chlorinated in carbon tetrachloride at 25°C.

Reaction Time (min)	Chlorine Uptake (g of chlorine/g of raw dry coal)			
	-400 mesh	100 x 200 mesh	20 x 24 mesh	12 x 14 mesh
0	0	0	0	0
5	0.208	0.214 (6)[1]	0.054	0.038 (7)
10	0.230	0.267 (11)	0.080	-
20	0.257	0.284	0.141	0.082
40	0.276	0.336 (42)	0.212	0.150
60	0.289	0.347	0.270	0.200
120	0.310	0.365	0.359	0.312
180	0.328	0.374	-	-

[1] The numbers in parentheses indicate reaction times (in minutes) for the cases where they are slightly different from the ones indicated in the first column.

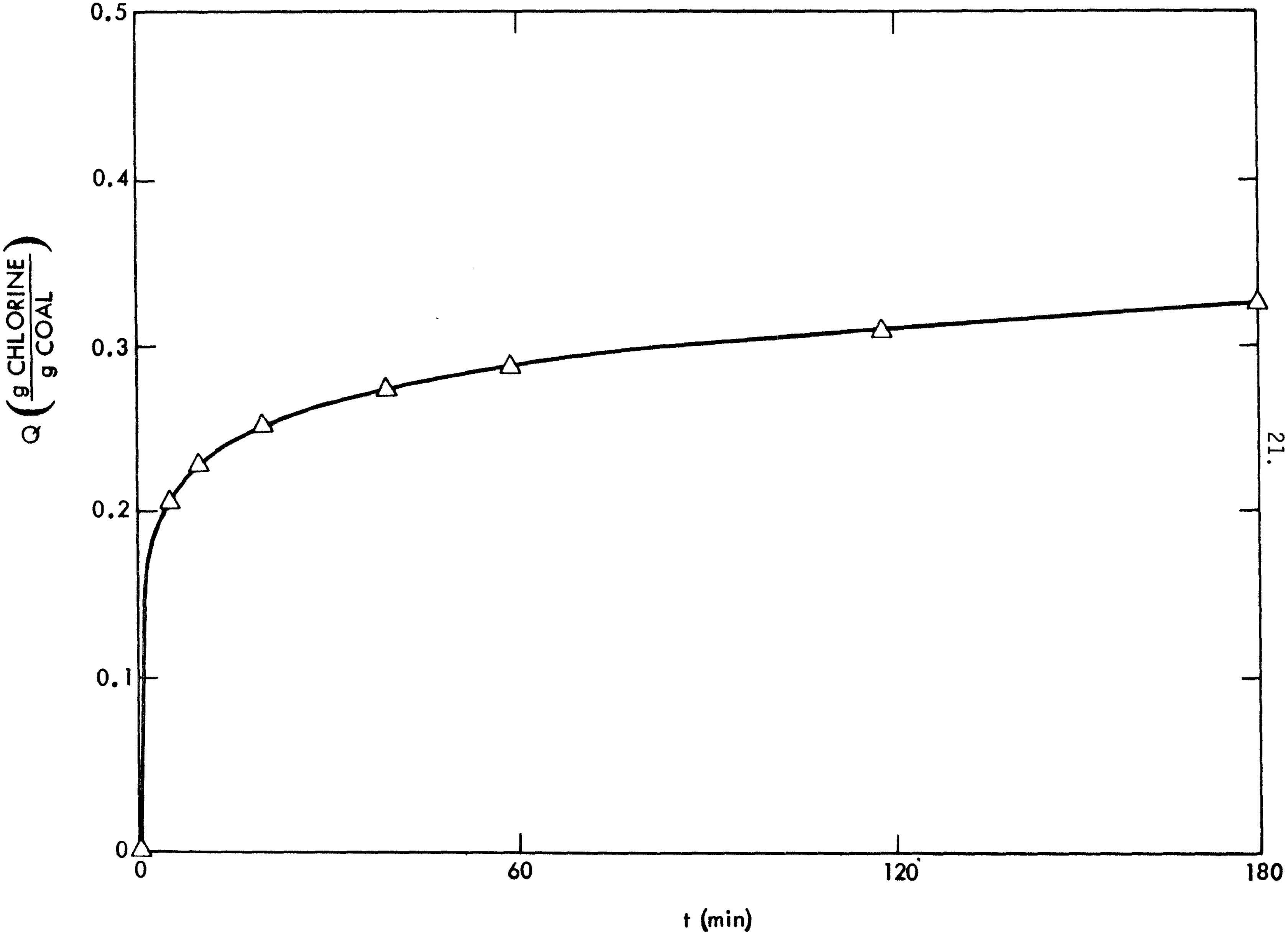

Figure 2. Chlorine uptake for the -400 mesh particle size of the PSOC 190B coal chlorinated in carbon tetrachloride at 25°C.

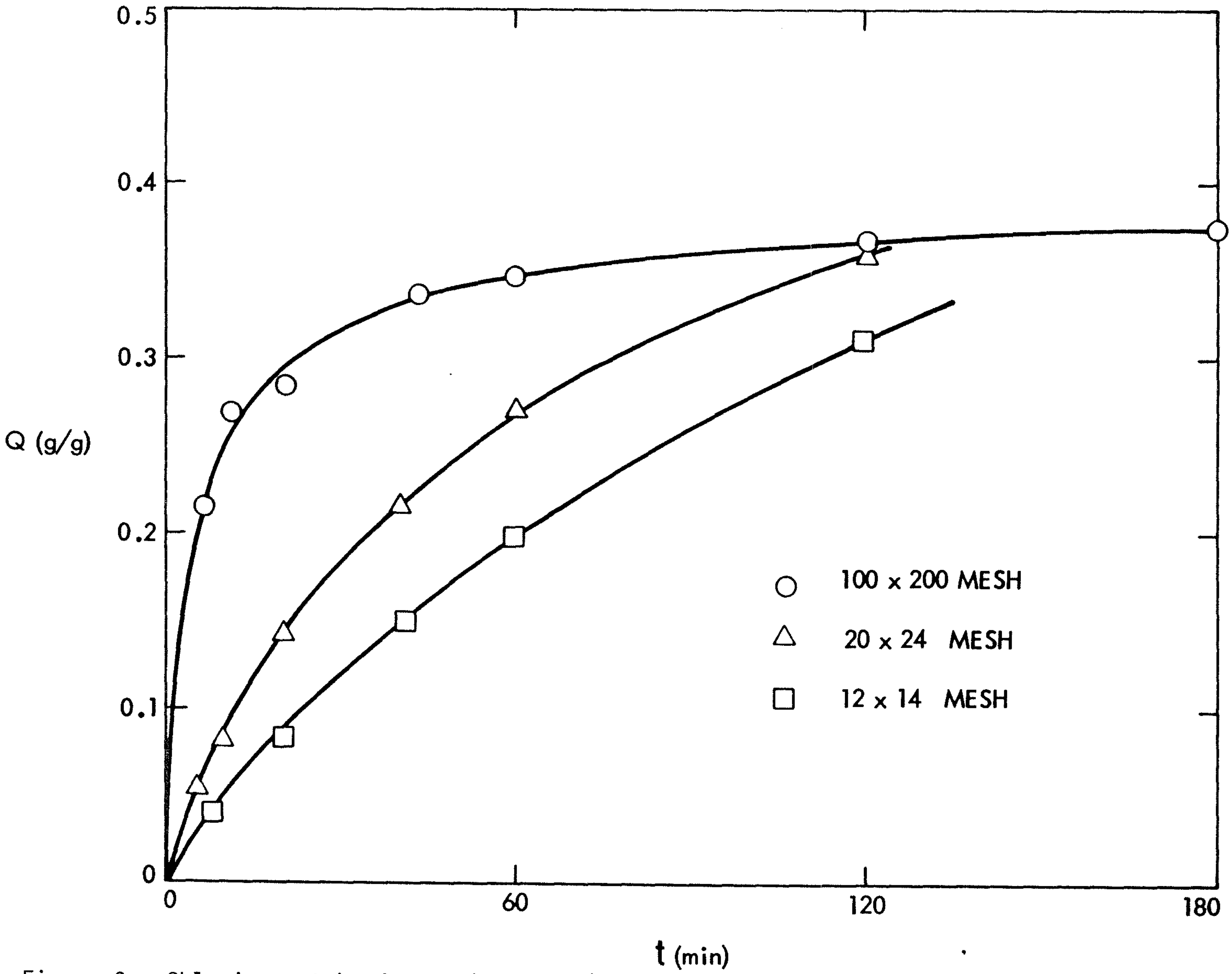

Figure 3. Chlorine uptake for various particle sizes of the PSOC 190B coal chlorinated in carbon tetrachloride at 25°C.

or

$$Q = \frac{1}{B}\ln(1 + ABt) \qquad (2)$$

or

$$\frac{dt}{dQ} = \frac{1}{A} + Bt \quad , \qquad (3)$$

t = chlorination time, min.

The best least-squares fit of the experimental data on equation (2) was obtained using the following values for the parameters A,B:

$$A = 3.706 \, \frac{\text{g of chlorine}}{\text{(g of raw dry coal)(min)}}$$

$$B = 30.419 \, \frac{\text{g of raw dry coal}}{\text{g of chlorine}}$$

Both the experimental data points and the Elovitch equation are depicted in Figure 2.

The Elovitch equation is frequently found to apply to chemisorption processes and has been used to describe coal-oxygen reactions at 40°C (119), chlorination of coal with gaseous chlorine at temperatures up to 250°C (38), and chlorination of coal in aqueous and carbon tetrachloride suspensions at 20° and 60°C (37). The problem in applying this equation to coal-chlorination is that it projects the limit $Q \rightarrow \infty$ for $t \rightarrow \infty$ [see equation (2)], while of course in real situations $Q \rightarrow Q_e$ as $t \rightarrow \infty$, Q_e (in grams of chlorine per gram of coal) being the equilibrium value describing the state where all the available under the given reaction conditions chlorination sites in coal have been saturated. For example, an upper limit for Q_e in benzene chlorination would be that corresponding to hexachlorobenzene, namely $Q_e = \frac{6 \times 35.5}{78} \simeq 2.73 \frac{\text{g of chlorine}}{\text{g of benzene}}$.

The modified [compared with equation (3)] Elovitch equation (37):

$$\frac{t}{Q} = a + bt \tag{4}$$

which yields:

$$Q = Q_e = b^{-1} \quad \text{for} \quad t \to \infty$$

was used to determine the equilibrium value Q_e for coal chlorination in carbon tetrachloride at 25 C. A linear-regression analysis of the experimental data for the -400 mesh size (Table 1) in the form $(\frac{t}{Q}, t)$ gave the following best fit ($r^2 \simeq 0.9982$) values:

$$Q_e \simeq 0.333 \frac{\text{g of chlorine}}{\text{g of raw dry coal}}$$

(ii) The experimental data for chlorine uptake for the other three particle sizes are depicted in Figure 3. Measurements of particle-size distribution on raw and the corresponding chlorinated coal samples showed no significant change in particle size, except in the cases of extended reaction periods (>2 hours) and large particle sizes (>100 μ). In these cases, severe fracturing of the particles because of swelling (Section 2.5) resulted in considerable reduction in particle size. These data points were not included in Table 1.

The rate-controlling step for the slurry-phase chlorination of coal was determined on the basis of the following arguments:

(1) Chlorine flow rate and stirring rate for the coal slurry were found to have no effect on the chlorine uptake in coal. Therefore, diffusion of chlorine through the liquid film surrounding the coal particle to its surface was not the rate-controlling step.

(2) To determine, on the other hand, whether intraparticle diffusion of chlorine was the rate-controlling step, the diffusion equation in the absence of chemical reaction for a spherical particle and uniform surface concentration of the diffusing species was considered. This equation may be written as (<u>121</u>):

$$\frac{\partial c}{\partial t} = D\nabla^2 c = \frac{D}{r^2}\frac{\partial}{\partial r}\left(r^2 \frac{\partial c}{\partial r}\right) \tag{5}$$

with the boundary and initial conditions:

$$\begin{aligned} c &= c_s \quad \text{at} \quad r = R \quad (t \geq 0) \\ c &= 0 \quad \text{for} \quad t < 0 \quad (0 \leq r \leq R) \end{aligned} \tag{6}$$

where

c = concentration of the diffusing species at time t and position r in the spherical particle,

c_s = constant concentration of the diffusing species at the particle's surface,

R = radius of the particle, and

D = effective diffusion coefficient.

Non-dimensionalization of (5) and (6) gives:

$$\frac{\partial \bar{c}}{\partial \bar{t}} = \frac{1}{\bar{r}^2}\frac{\partial}{\partial \bar{r}}\left(\bar{r}^2 \frac{\partial \bar{c}}{\partial \bar{r}}\right) \tag{8}$$

with $\bar{c} = 1$ at $\bar{r} = 1$ $(\bar{t} \geq 0)$

and $\bar{c} = 0$ for $\bar{t} < 0$ $(0 \leq \bar{r} \leq 1)$,

where $\bar{c} \triangleq \frac{c}{c_s}$, $\bar{r} \triangleq \frac{r}{R}$ and $\bar{t} = \frac{t}{t_D}$

$\left(t_D \triangleq \frac{R^2}{D}\right.$ = characteristic time for intraparticle diffusion$\left.\right)$.

The solution of (8) is (121):

$$\bar{c}(\bar{r},\bar{t}) = \frac{c(r,t)}{c_s} = 1 + \frac{2}{\pi\cdot\bar{r}} \sum_{n=1}^{\infty} \frac{(-1)^n}{n} [\sin(n\pi\bar{r})] e^{-n^2\pi^2\bar{t}} \tag{9}$$

For the concentration of the diffusing species at the particle's center ($\bar{r} = 0$) as a function of time, equation (9) gives:

$$\bar{c}(o,\bar{t}) = \frac{c(o,t)}{c_s} = 1 + 2\sum_{n=1}^{\infty} (-1)^n e^{-n^2\cdot\pi^2\cdot\left(\frac{t}{t_D}\right)} \tag{10}$$

The relative concentration $\frac{c}{c_s}$ of the diffusing species at the center of the spherical particle as a function of the relative time $\frac{t}{t_D}$, described by equation (10), is plotted in Figure 4.

The plot basically shows that the concentration of the diffusing species at the center of the particle becomes practically equal to the concentration at the particle's surface within a time period $t \simeq 0.7\ t_D$.

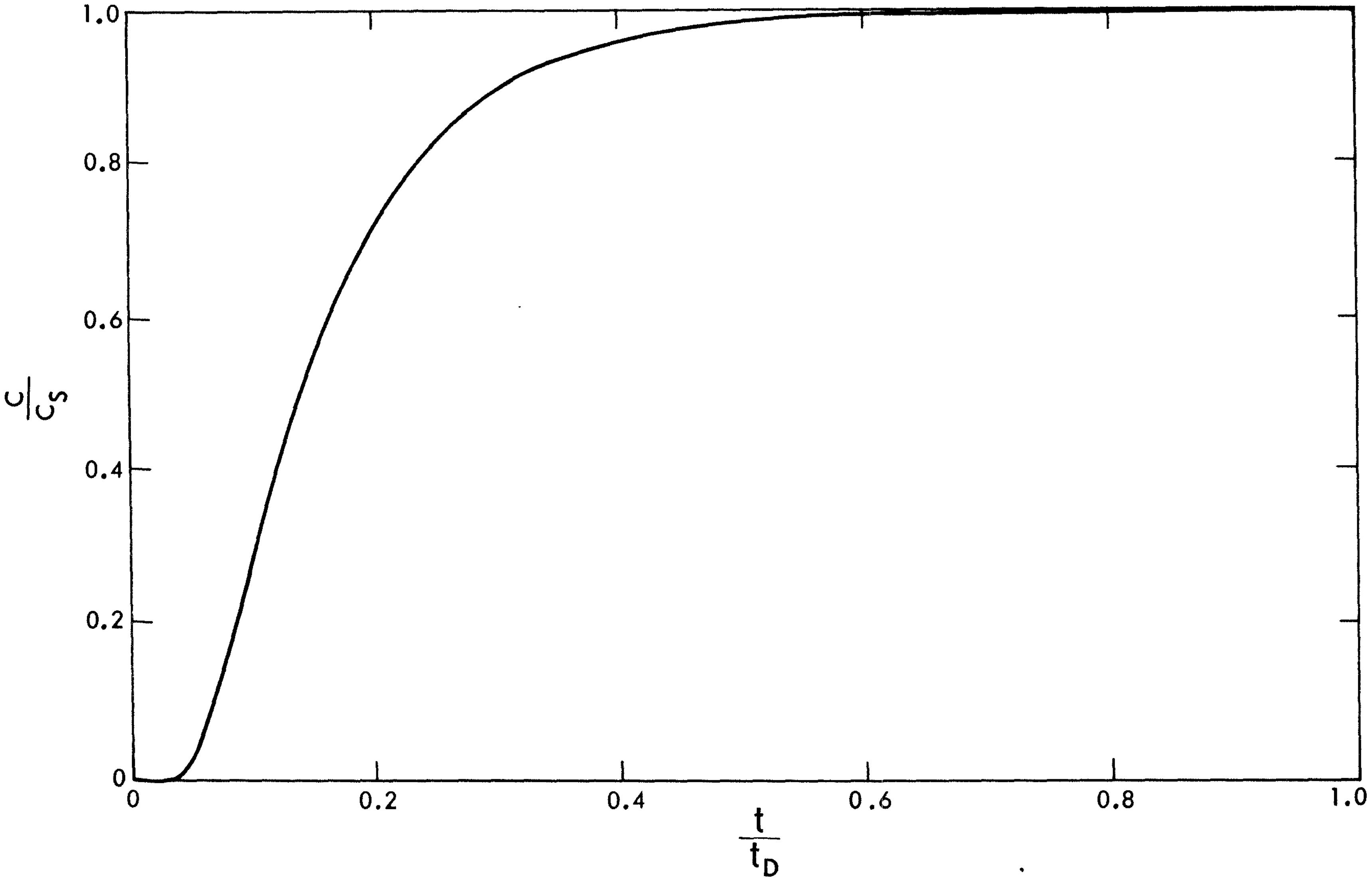

Figure 4. Relative concentration $(\frac{c}{c_s})$ of the diffusing species at the center of a spherical particle as a function of relative time $(\frac{t}{t_D})$ for the case of constant surface concentration (values calculated from equation 10).

To estimate $t_D \triangleq \frac{R^2}{D}$ one has to assign a value for D, the effective coefficient of diffusion of chlorine in the coal particle. Adopting the parallel-pore model for a monodisperse system (122), one can write:

$$D = \frac{\varepsilon \cdot \mathcal{D}}{\delta} \tag{11}$$

where ε = porosity of the coal particle,

δ = tortuosity factor, taken approximately equal to 4 when surface diffusion is insignificant (122), and

$\mathcal{D}$ = chlorine diffusivity in the coal particle.

For the PSOC 190 coal, $\varepsilon \simeq 0.23$.

If the pores of the coal particle are assumed to be completely filled with liquid carbon tetrachloride, one can use the value (123) of $\mathcal{D} \simeq 10^{-5} \frac{cm^2}{s}$ (liquid diffusivity of chlorine in carbon tetrachloride at 25°C).

Then,

$$D = \frac{\varepsilon \cdot \mathcal{D}}{\delta} \simeq 5.8 \times 10^{-7} \frac{cm^2}{s}$$

For a particle-size range of 100 x 200 mesh (74 x 149μ), the average particle radius is:

$$R \simeq 56\ \mu = 5.6 \times 10^{-3}\ cm$$

Therefore:

$$\underline{t_D = \frac{R^2}{D} \simeq 54s}\ .$$

Similarly, for a particle-size range of 12 x 14 mesh (1190 x 1410), one finds:

$$\underline{t_D \simeq 2 \text{ hours}}\ .$$

The very small characteristic time for intraparticle diffusion of chlorine inside the 100 x 200 mesh particles suggests that chemical reaction is most probably the rate-controlling step in this case. Fast intraparticle-mass transfer in chemical-control situations establishes a uniform concentration of chlorine throughout the coal particle within a very short period of time so that chlorine uptake at any given time is independent of the particle size. Table 1 and Figures 2 and 3 show that this is the case for the -400 and the 100 x 200 mesh sizes. Slightly higher chlorine uptake at relatively long reaction times for the 100 x 200 mesh size compared wtih the -400 mesh size is attributed to temperature gradients inside the coal particle because of the high exothermicity of the chlorination reaction.

For particle sizes greater than about 150μ, Figure 3 shows that there is a strong dependence of the chlorine uptake in coal on the particle size. Intraparticle diffusion of chlorine becomes important (≡ large characteristic times for diffusion) and a transition from chemical to mass-transfer control occurs.

2.4 Temperature, solvent and concentration effects

The temperature and solvent effects in slurry-phase chlorination of coal were studied in a series of experiments where approximately 11.6 g of raw PSOC 190A coal (100 x 200 mesh size) were suspended in 350 ml of solvent and chlorinated for one hour at a chlorine flow rate of 0.3 g/min and at various temperatures. The chlorinated coal was filtered and dried in vacuum for two hours at 100°C.

The results for chlorine uptake for the various coal samples are given in Table 2. In reference to this table, the following observations can be made:

(1) Only small differences exist in chlorine uptake between methyl chloroform and carbon tetrachloride under the same reaction conditions. For both solvents, chlorine uptake increases slightly with temperature up to 45°C and then decreases slightly up to 60°C. The same trend is also observed with another chlorinated solvent, tetrachloroethylene, up to 100°C (74).

The higher chlorine uptake in coal at intermediate temperatures is consistent with the fact that low temperatures favor high chlorine concentrations in the liquid phase but at these temperatures the coal-chlorination rate constant is relatively small, while at high temperatures this constant increases considerably (37), but then chlorine solubility in the solvent is severely reduced.

(2) Chlorine uptake in coal chlorinated in water is significantly

Table 2. Chlorine uptake for the PSOC 190A coal (100 x 200 mesh) chlorinated for one hour in various solvents and at various temperatures.

Solvent	Reaction Temperature (°C)	Chlorine Uptake $\left(\frac{\text{g of chlorine}}{\text{g of raw dry coal}}\right)$
CH_3CCl_3	30	0.358
	45	0.378
	60	0.365
CCl_4	30	0.334
	45	0.355
	60	0.344
H_2O	30	0.289
	60	0.288

lower than in methyl chloroform or carbon tetrachloride, obviously a result of the significantly lower solubility of chlorine in water (for example, chlorine solubility at 60°C: water 0.0032 $\frac{g}{cm^3}$, carbon tetrachloride 0.061 $\frac{g}{cm^3}$). No temperature dependence is observed here, at least for the temperature range examined (30 - 60°C).

The effect of the slurry-phase concentration of coal on chlorine uptake was studied in a series of experiments where a certain amount of raw PSOC 190A coal (100 x 200 mesh size) was suspended in 350 ml of methyl chloroform and chlorinated for one hour at a chlorine flow rate of 0.3 g/min and at 60°C. The chlorinated coal was filtered and dried in vacuum for two hours at 100°C. Results for chlorine uptake are given in Table 3.

These results indicate that under the experimental conditions employed here chlorine uptake in coal approaches a more or less constant value (0.358 $\frac{\text{g of chlorine}}{\text{g of raw dry coal}}$) for coal concentrations lower than 11.6 g coal/350 cm^3 methyl chloroform. For higher concentrations, a significant decrease in chlorine uptake is observed. This effect is most probably due to the high solubility of chlorine in the organic solvent which, at low concentrations of coal particles, results in a sufficient supply of dissolved reactant for mass transfer to each particle to be independent of the number of particles. As the coal concentration increases to higher values, there is a competition for chlorine between particles and chlorine uptake decreases.

Table 3. Chlorine uptake for the PSOC 190A coal (100 x 200 mesh) . chlorinated at various concentrations in methyl chloroform for one hour at 60°C.

Coal Concentration ($g/350\ cm^3$ of solvent)	Chlorine Uptake (g of chlorine/g of raw dry coal)
2.9	0.351
5.8	0.358
11.6	0.359
23.2	0.321
34.8	0.277

Finally, results of ultimate analyses on raw and chlorinated PSOC 190 coal samples indicate a small ($\sim$12%) reduction in sulfur content and a considerable ($\sim$25%) reduction in hydrogen content because of the dehydrochlorination effect noted as follows:

$$\text{Coal(s)} + \text{Cl}_2\text{(g)} \rightarrow \text{Chlorinated coal(s)} + x\text{HCl(g)} .$$

Carbon, nitrogen, oxygen and ash contents remain unchanged during the course of the chlorination reaction.

2.5 Scanning-Electron-Microscope (SEM) and Energy-Dispersive-Analyzer-of-X-rays (EDAX) analysis of raw and chlorinated coal

To obtain a qualitative idea of the alterations the coal undergoes in both its physical structure and the elemental composition of its surface as a result of the chlorination reaction, representative samples of raw and chlorinated PSOC 190A coal were examined under the scanning-electron microscope (SEM) to which an energy-dispersion analyzer of X-rays (EDAX) was attached. The results are presented in Figures 5, 6 and 7.

The SEM uses secondary electrons emitted from the surface of the sample to form seemingly three-dimensional images. The SEM has a wide range of magnification (30 to 100,000x) and a resolution of approximately 70 Angstroms. The EDAX system allows a semiquantitative anlaysis of elemental composition. When the specimen is scanned by the electron beam, each constituent element radiates a unique X-ray energy spectrum. These X-rays are separated in a multichannel analyzer. A complete spectrum from all elements can be displayed on a fluorescent

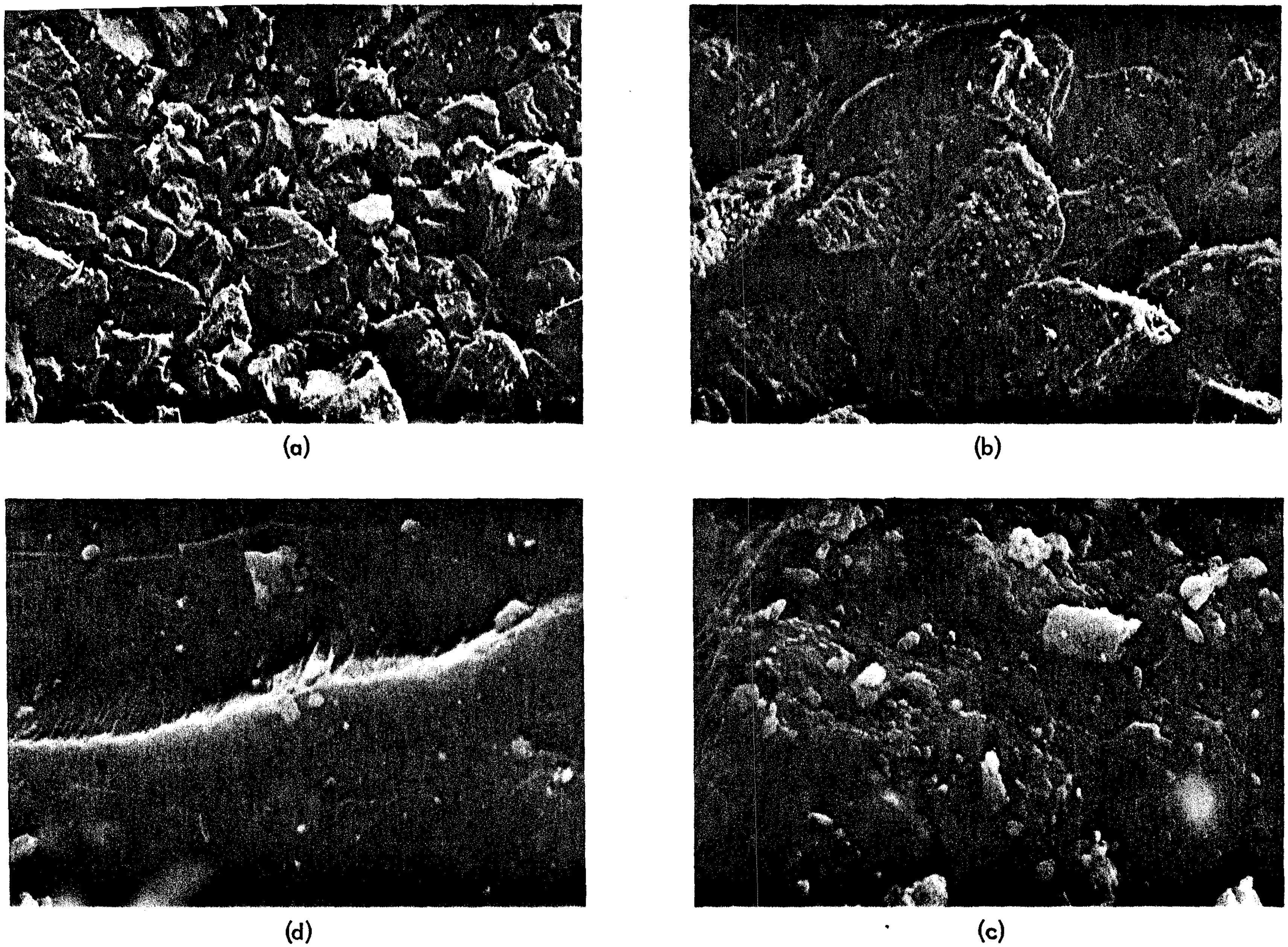

(a) (b)

(d) (c)

<u>Figure 5.</u> Scanning electron micrographs of raw PSOC 190A coal (100 x 200 mesh); (a) 100x, (b) 200x, (c) and (d) 2000x .

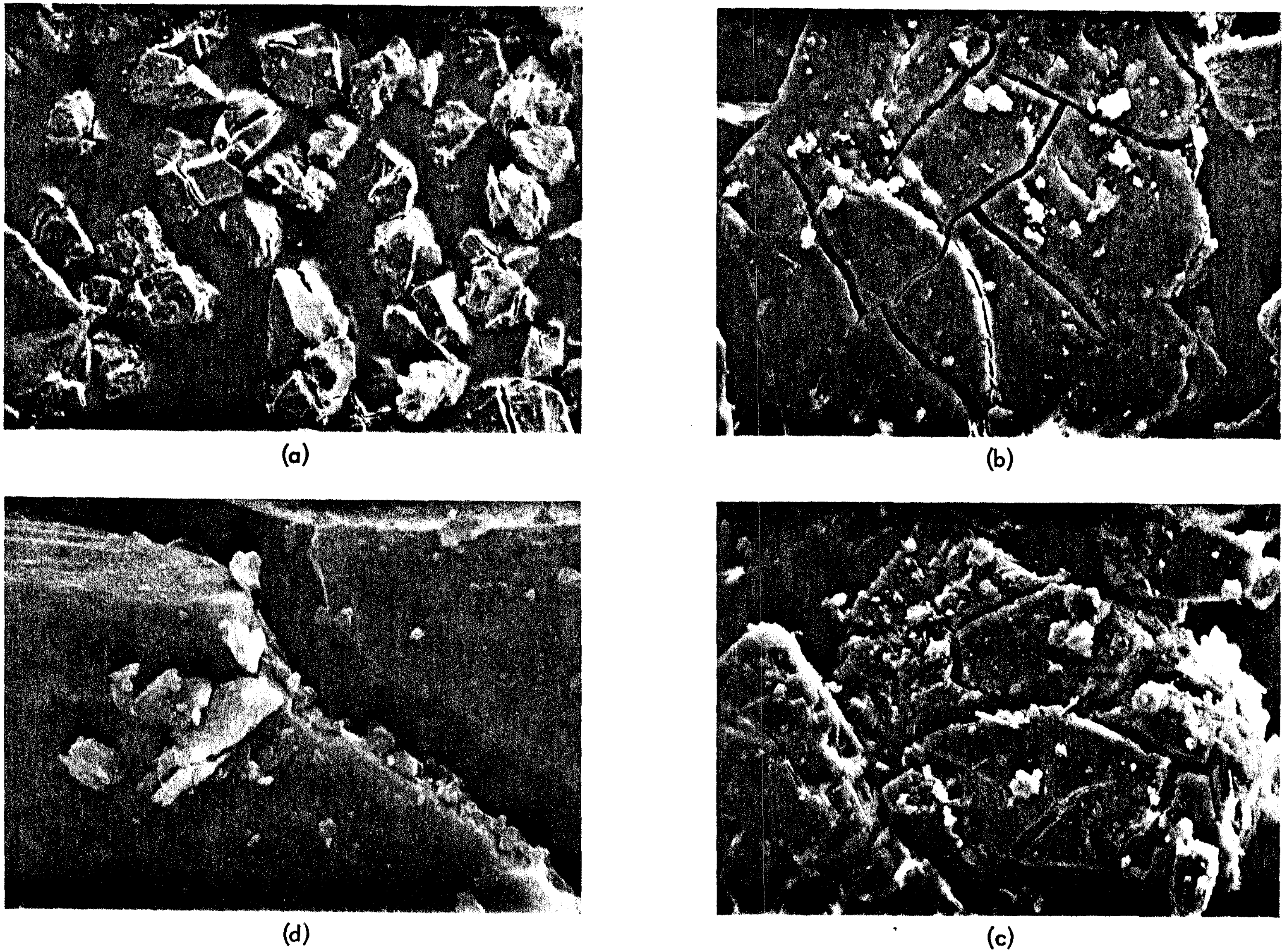

Figure 6. Scanning electron micrographs of chlorinated PSOC 190A coal (100 x 200 mesh); (a) 100x, (b) and (c) 500x, (d) 2000x .

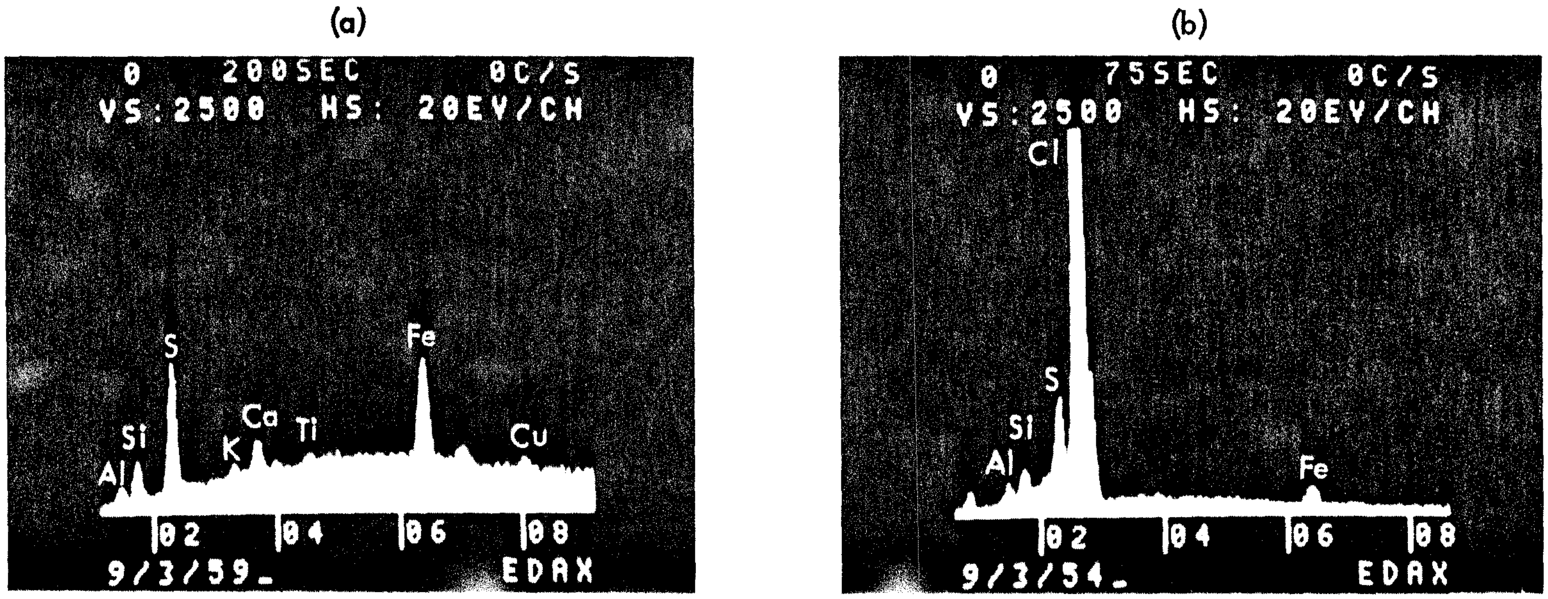

Figure 7. EDAX spectrum of the PSOC 190A coal (100 x 200 mesh); (a) raw, (b) chlorinated .

screen and photographed (39). EDAX has only recently been used for examining, non-destructively, the inorganic matter in coals (40).

Raw and chlorinated coal samples were examined on an AMR 900 Scanning Electron Microscope. All the samples were mounted on aluminum discs and coated with a thin (∿100 Å) layer of carbon to prevent charging. Carbon coating was preferred over gold coating as it does not obscure some important peaks, like the sulfur Ka peak, as gold does, and at the same time it provides greater sensitivity.

In reference to the pictures, Figure 5 shows raw coal particles. The small particles on the coal surfaces are inorganic compounds containing (EDAX spectrum, Figure 7a) aluminum, silicon, sulfur, iron and, in smaller quantities, potassium, calcium, titanium and copper. From the examination, the inorganic constituents were found to vary considerably in distribution from point to point on the coal's surface.

Figure 6 shows chlorinated coal particles. The large amount of chlorine present is indicated by the large peak at 2.62 keV (Figure 7b). Other than the chlorine, the elemental analysis was more or less the same. Furthermore, the surfaces appeared to be similar to those of the raw coal. But the most spectacular effect of chlorination was the extensive fissuring it produced on the coal grain. Almost every single particle shows multiple surface fractures with gaps of a few microns, which in many cases are so deep that the particle barely holds together. Particle-size reduction because of the chlorination reaction has already been mentioned in Section 2.3. The fissuring of the coal particles was observed under any chlorination condition examined and it was not a result of solvent action but rather a result of chlorine incorporation in the coal matrix. Coal samples which have undergone solvent treatment under conditions similar to chlorination conditions, but with no chlorine present, showed no fracture effect at all.

2.6 The liquid phase after chlorination

Chlorination of the coal in an organic solvent, especially under relatively severe conditions (finely divided coal, extended chlorination periods, etc.), was always found to yield a liquid phase possessing a dark red color, completely different from the color of the chlorinated solvent. Because this result was a clear indication of the presence of coal-chlorine reaction products in the liquid phase and because very few references exist in the literature on this aspect of coal-chlorination, and all of them for the reaction with gaseous chlorine (31,32), it was decided to examine the matter more closely.

Fifty grams of raw PSOC 190 A coal, 200 x 395 mesh size, were suspended in 350 ml of reagent-grade CCl_4 and were chlorinated for two hours with a flow rate of dry chlorine of 0.6 g/min and in a temperature range of 25 - 50°C. The weight increase of the (dried) chlorinated coal over the raw coal was approximately 42%. The liquid phase of the slurry after chlorination was isolated by filtration.

Analysis of this phase on a Perkin-Elmer 3920 gas chromatograph, equipped with a flame-photometric detector which had a 394 nm optical filter for sulfur detection, showed no sulfur compounds present in solution.

The liquid phase was then evaporated under reduced pressure. Approximately 0.6 gram (≡ "extraction" yield: ∼1%) of a viscid brown-red solid possessing a penetrating odor were isolated. It was very soluble in acetone but sparingly soluble in water. It has a melting-point range of 90 - 120°C. Examination of this solid in a Spectraphysics Model 3500B liquid chromatograph using a reverse-phase column of 10 μ Spherisorb ODS and a solvent program of water and acetonitrile, gave only a small double peak (relative retention times of 1 and 1.157). No additional analysis was attempted at that point.

Chapter 3

SURFACE-AREA MEASUREMENTS ON RAW AND CHLORINATED COAL

3.1 Introduction

The principles of gas adsorption on solid surfaces and their application to the determination of surface areas and pore-size distributions of porous solids [BET (41) and Dubinin-Polanyi (42) approaches] are well known and will not be discussed here. Rather, a review of the literature on the pore structure and the internal surface area of coal materials will be presented.

Zwietering and Van Krevelen (43) first applied Ritter and Drake's method of mercury penetration to the study of coal. Their work suggested that coal contains two pore systems, one of macropores and the other of micropores.

Mercury can penetrate the macropores but even at high pressures is unable to penetrate the micropore system. Both pore systems, however, are accessible to helium at room temperature. Generally, pores in the size range below 12 Å are described as micropores and those above about 200 Å as macropores. Those in between are referred to as transitional or intermediate pores. Depending on the rank of coal, the pore-size distributions can vary greatly (44).

Gan, Nandi and Walker (45) measured the gross pore-size distribution for a number of American coals using nitrogen adsorption isotherms at -196°C. They determined the cumulative pore volume in the pore range of 12 - 29600 Å and showed that coals in general have a very fine micropore system with an average pore diameter of less than 12 Å.

Lamond and Marsh (46) employed N_2 adsorption at -196°C and CO_2 adsorption at -78°C and 0°C on 4 Å and 5 Å molecular sieves to show that coal possesses an ultrafine molecular-sieve structure with an average pore diameter of 4 Å. That result confirmed earlier observations by Anderson et al. (47).

The molecular-sieve characteristics of coal and chars have been discussed by Walker et al. (48), and the porosity has been described as of the aperture-cavity type. A large proportion of the total surface area and of the pore volume in coal is accessible through apertures 4.9 - 5.2 Å in size. Slight changes in aperture openings can have a profound effect on the surface area and porosity of such materials (49).

In contrast to the pore structure of the coal, which can be satisfactorily described in the above more or less generally accepted terms, considerable controversy and continuing discussion exist in the literature about the values for the internal surface area of coal. Depending on the conditions of the gas adsorption (temperature, specific gas), surface-area values from 1 to 200 m^2/g have been reported for the same coal sample.

Nitrogen adsorption at -196°C was the first and by far the most extensively used method for obtaining surface areas and pore-size distributions for coal materials (44,45). The adsorption of rare gases on coal has also been reported. Lahiri et al. (50) studied the adsorption of argon at -183°C, and Kini (51) studied the adsorption of xenon at 0°C on several coals and cokes. Lahiri obtained surface areas ranging from 13 to 51 m^2/g using the BET equation. Kini, using a pressurized system for xenon adsorption, observed surface areas from 140 to 200 m^2/g depending on the coal sample studied.

The surface areas obtained from nitrogen and rare-gas adsorptions at low temperatures have been criticized as too low, a result of the inability of these molecules to diffuse into the ultrafine pore structure of the coal because of activation phenomena. Nandi and Walker (52) measured the unsteady-state diffusion of nitrogen and carbon dioxide in several coals over the temperature range of 25° to 140°C. From a questionable extrapolation of the Arrhenius plots, from this temperature range to the liquid nitrogen temperature of -196°C and the dry-ice temperature of -78°C, they concluded that only a very small fraction of the ultrafine pore structure of the coal is accessible to nitrogen at -196°C, whereas a substantial fraction of these pores is accessible to carbon dioxide at -78°C.

Carbon dioxide as the adsorbate on coal has been used extensively in recent years to measure internal surface areas. Anderson et al. (53) have obtained surface-area values for a low-volatile bituminous Pittsburgh coal of 114 and 140 m^2/g from CO_2 isotherms at -78°C. Walker and Geller (54), also using CO_2 as the adsorbate, obtained 175 m^2/g for an anthracite coal. Walker and Nandi (45) compared carbon-dioxide adsorption at -78°C and nitrogen adsorption at -196°C for several types of coal. For all of the samples, the areas obtained using nitrogen were lower than those obtained using carbon dioxide. For some coals, the nitrogen surface-area values were less than 1 m^2/g. For other coal samples they varied up to 90 m^2/g. The carbon dioxide areas ranged from 100 to 430 m^2/g, depending on the particular coal sample.

Carbon-dioxide surface areas have also been criticized lately, because of the accumulating evidence that the mechanism of CO_2 adsorption in coal includes permeation <u>through</u> the solid coal matrix which yields high values for surface areas. Surface-area measurements on coal using numerous other gases have also been reported (<u>44</u>,<u>54</u>).

3.2 Experimental system

The effects of reaction time, solvent and temperature of chlorination on the internal-surface area of coal were studied. Approximately 11.6 grams of raw PSOC 190A coal of 100 x 200 mesh were suspended in 350 ml of solvent and chlorinated at a chlorine flow rate of 0.3 g/min for a certain period of time and at a certain temperature. The chlorinated coal was filtered and dried in vacuum for two hours at 100°C. It was then further outgassed for 48 hours at room temperature in high ($>10^{-5}$ mm Hg) vacuum.

Surface areas of samples of raw and chlorinated coal were measured on a Quantasorb Sorption Apparatus. This apparatus uses the dynamic technique (flow method) to determine the BET surface area of a sample. The procedure (<u>56</u>) is to pass a mixture of known composition of helium and the gas to be adsorbed (nitrogen in this case) continuously over the solid sample at constant total pressure and at the desired adsorption temperature (-196°C here). This procedure is followed until equilibrium is reached, that is, until the solid has adsorbed an amount of the adsorbable component corresponding to equilibrium at its partial pressure in the mixture. Then the gas is desorbed by heating the sample while a stream of pure helium flows over it. The amount desorbed is measured with a thermal-conductivity cell, and this result gives one point on the isotherm. Then the process is repeated at successively different compositions of the mixture until the whole isotherm is obtained. Prior to the BET determination, all the coal samples were degassed for one hour in a stream of nitrogen at 120°C in a degassing station connected with the apparatus. The surface-cleaning technique of Lopez-Gonzalez et al. (57) involving a series of consecutive adsorptions at low temperatures and desorptions at room temperature was also employed and led to reproducible (within 1%) isotherms. The surface areas of the samples were determined using the BET equation and a value of 16.2×10^{-16} cm^2 for the cross-sectional area of the nitrogen molecule.

3.3 Results and discussion

The results for the surface-area measurements are given in Tables 4 (kinetic study) and 5 (temperature and solvents).

In reference to Table 4, the following observations can be made:

(i) The raw PSOC 190A coal has a relatively high nitrogen-surface area of 70.6 m^2/g. Gan et al. (45) reported a value of 83.0 m^2/g for the same coal but for a particle size of 40 x 70 mesh. This coal shows a unimodal pore-size distribution in the diameter range 20 - 200 Å with the peak value at 36 Å (58), but a significant fraction of the pores is in

Table 4. Surface-area measurements for PSOC 190A coal samples chlorinated in methylchloroform at 60°C for various periods of time.

Reaction Time, t (min)	Chlorine Uptake, Q $\left(\frac{\text{g of chlorine}}{\text{g of raw dry coal}}\right)$	Surface Area, S $\left(\frac{m^2}{\text{g of raw dry coal}}\right)$
0	0	70.6
5	0.080	32.8
10	0.120	22.7
20	0.193	16.2
40	0.293	11.7
60	0.359	8.1
80	0.385	5.8
100	0.415	5.0
120	0.421	5.1
180	0.457	5.1

Table 5. Surface-area measurements for PSOC 190A coal samples chlorinated for one hour in various solvents and at various temperatures.

Solvent	Reaction Temperature (°C)	Chlorine Uptake $\left(\frac{\text{g of chlorine}}{\text{g of raw dry coal}}\right)$	Surface Area $\left(\frac{\text{m}^2}{\text{g of raw dry coal}}\right)$
CH_3CCl_3	30	0.358	3.4
	45	0.378	5.1
	60	0.365	7.9
CCl_4	30	0.334	7.0
	60	0.344	15.8
H_2O	30	0.289	6.3
	60	0.288	18.8

the micropore region (pore-diameters <12 Å) (45).

(ii) There is a sharp decrease in the nitrogen-surface area of the coal with reaction time. This decrease is accompanied by a shift in the pore-size distribution towards larger pore sizes (58). After the first five minutes of chlorination approximately 54% of the coal's surface area is not accessible for nitrogen adsorption any more. The reduction in surface area continues up to 100 minutes and then levels off, though chlorine uptake continues at a reasonable rate even after 180 minutes.

(iii) The experimental data on chlorine uptake versus reaction time (Table 4) were correlated using an Elovitch-type equation:

$$\frac{dQ}{dt} = Ae^{-BQ} \tag{1}$$

or the equivalent:

$$Q = \frac{1}{B}\ln(ABt + 1) \quad , \tag{2}$$

where

Q = chlorine uptake in coal $\left(\frac{\text{g of chlorine}}{\text{g of raw dry coal}}\right)$, and

t = reaction time (min),

with the following best-fit results:

$$A = 0.023 \frac{(\text{g of chlorine})}{(\text{g of raw dry coal})(\text{min})}$$

$$B = 7.08 \frac{\text{g of raw dry coal}}{\text{g of chlorine}}$$

The chlorination rate $r \overset{\Delta}{=} \frac{dQ}{dt}$ was then calculated from the equation:

$$r = \frac{A}{ABt + 1} \tag{3}$$

and the relative reaction rate $\frac{r}{r(t = 0)}$ from the equation:

$$\frac{r}{r_o} = \frac{1}{ABt + 1} = \frac{1}{0.1628t + 1} \tag{4}$$

It is interesting to note that equation (3) can also be written as:

$$\frac{1}{r} = \frac{1}{A} + Bt \ , \tag{5}$$

implying a linear relationship between the inverse of the reaction rate and time. If, for a moment, one assumes that:

$$r \propto S$$

S = coal's surface area, $\frac{m^2}{\text{g of raw dry coal}}$,

then a similar linear relationship should hold for $\frac{1}{S}$ and t, namely:

$$\frac{1}{S} = \frac{1}{A'} + B't \tag{6}$$

Linear-regression analysis of the experimental data in the form $(\frac{1}{S}, t)$, excluding the level portion of the curve (points 120 and 180 min), gave the following best-fit results:

$$A' = 50.0 \ \frac{m^2}{\text{g of raw dry coal}}$$

$$B' = 1.814 \times 10^{-3} \ \frac{(\text{g of raw dry coal})}{(m^2)\cdot(\text{min})}$$

with a correlation coefficient very close to unity:

$$r_c^2 \approx 0.9928 .$$

Both $\frac{r}{r_o}$ calculated from equation (4) and $\frac{S}{S_o}$ (experimental) are depicted in Figure 8 as functions of time.

An interesting behavior of the surface area with chlorination temperature is revealed in Table 5. With all the other chlorination conditions being the same, surface-area reduction decreases significantly with temperature, and this effect is independent of the amount of chlorine uptake in coal. Chlorine uptake for the PSOC 190A coal, for example, is higher in chlorination in carbon tetrachloride at 60°C than at 30°C, but the resulting surface area of the chlorinated coal at 60°C is more than twice that at 30°C.

Finally, for comparison purposes, the surface areas of a raw and a chlorinated (26.0 wt.% chlorine) coal sample were determined by adsorption of three different gases: nitrogen (-196°C), Krypton (-196°C), and carbon dioxide (-78°C). The results are given in Table 6.

These results show that the surface-area reduction is approximately the same for nitrogen and krypton adsorption, despite the lower absolute surface-area values for krypton (most probably a result of the low adsorption temperature, well below krypton's normal boiling point: -152.3°C).

In contrast, the results on carbon-dioxide adsorption show a small increase in the surface area of the chlorinated sample over that of the raw coal. This result is puzzling because, despite the different

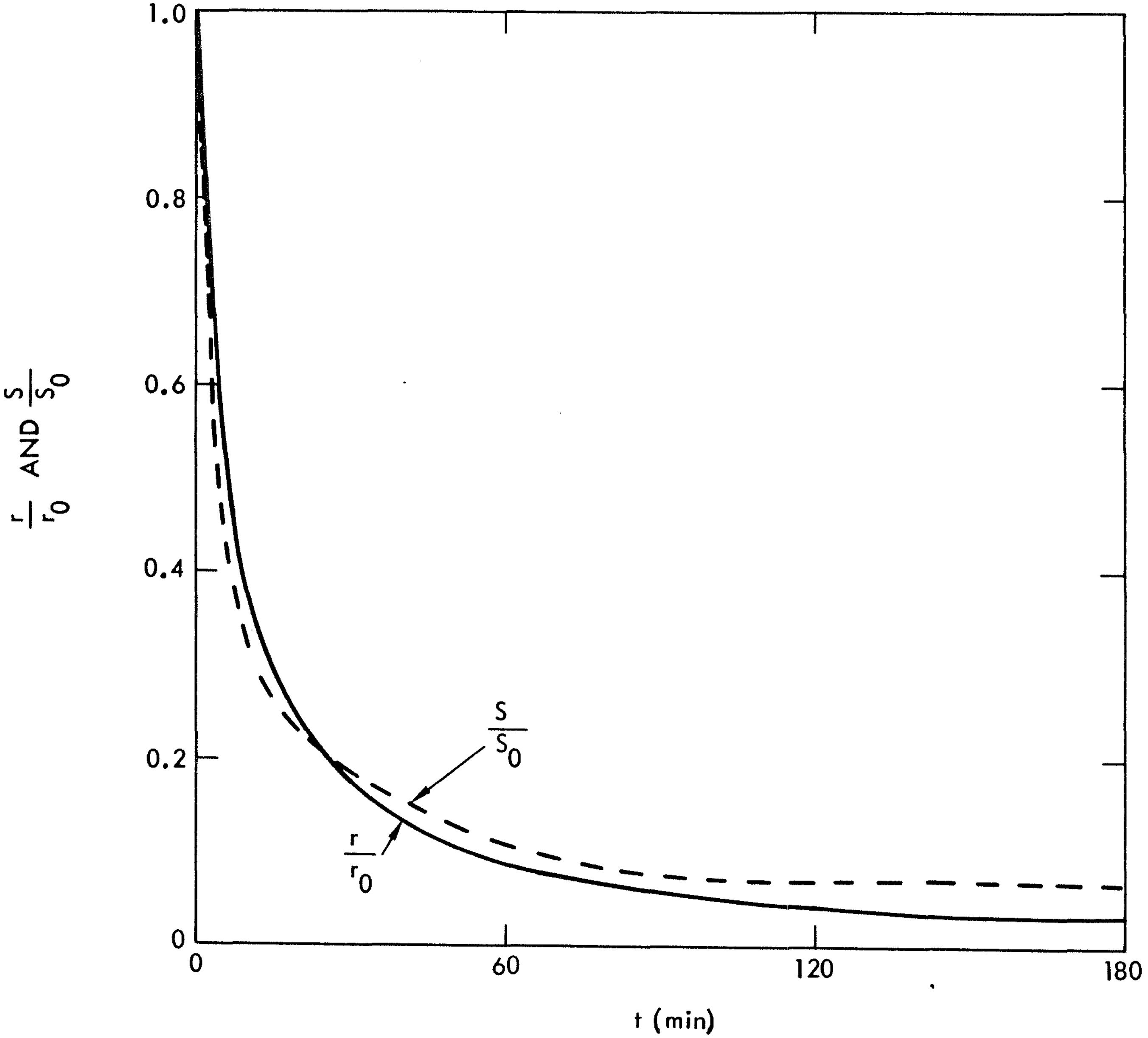

Figure 8. Relative reaction rate (r/r_0) and relative nitrogen-surface area (s/s_0) versus time in the slurry-phase chlorination of PSOC 190A coal in methyl chloroform at 60°C.

Table 6. Surface-area values determined by adsorption of different gases.

	Surface Area $\left(\frac{m^2}{\text{g of raw dry coal}}\right)$		
	N_2 (-196° C)	Kr(-196° C)	CO_2 (-78° C)
Raw PSOC 190A Coal	70.6	45.0	213.0
Chlorinated PSOC 190A	17.0	13.5	224.7
Surface Area Reduction (%)	75.9	70.0	-5.5

absolute surface-area values (for example, the CO_2 surface area for raw coal is more than three times that of nitrogen), all three gas adsorptions describe <u>the same</u> physical change (loss of porosity) that has occurred in <u>the same</u> coal sample. Therefore, surface-area reduction should be the same for all three adosrbates. Walker and co-workers (49) have also noted these discrepancies in nitrogen and carbon-dioxide adsorptions on treated coals.

A possible explanation is based on the fact mentioned in Section 3.1, namely, that the porosity of coal is of the aperture-cavity system with a large proportion of the total surface area and pore volume accessible through apertures about 5 Å in size. Slight changes in aperture openings can have a profound effect on the surface area of such materials. Since the minimum dimension of an N_2 molecule (3.65 Å) is larger than that of a CO_2 molecule (3.30 Å), N_2 areas are more sensitive to slight changes in aperture sizes (49). The discrepancies in N_2- and CO_2-determined changes in surface area are, however, too big to be attributed to the above effect only. This result seems to support the possibility mentioned in Section 3.1 that CO_2 adsorption in coal includes direct permeation through the coal matrix, and, of course, this adsorption component is not affected by pore blocking.

Before any attempt is made to interpret the trends in surface-area measurements discussed in the previous pages, the following question on the reported experimental data should be answered first. To what extent is the observed sharp decrease in the surface area of the coal during chlorination caused by solvent interference in the BET determinations? Insufficient drying of the chlorinated coal sample would not empty the pores from the solvent and thus at the very low (-196°C) temperature of the BET determination, the solvent would solidify acting as an extension of the coal surface and result in a large, but only apparent, drop in accessible pore volume.

To test this possibility, approximately 10.5 g of raw PSOC 190A coal, 100 x 200 mesh size, were suspended in 400 ml of three different solvents (methylchloroform, carbon tetrachloride and water) and stirred intensely for two hours at room temperature. Then the sample was filtered and dried in the usual way (Section 3.2) along with a sample of raw coal serving as a comparison. The results on nitrogen-surface areas of the treated samples were as follows:

(i) Raw coal: 70.6 $\left(\frac{\mathrm{m}^2}{\mathrm{g\ raw\ dry\ coal}}\right)$
(ii) Coal soaked in CH_3CCl_3: 68.1 "
(iii) Coal soaked in CCl_4: 65.3 "
(iv) Coal soaked in H_2O: 96.9 "

The results for methylchloroform and carbon tetrachloride indicate that there is a slight decrease in coal-surface area caused by the insufficiency of the drying procedure in removing the last traces of the solvent from the coal after treatment. But this decrease is not comparable in any way with the 93% decrease in surface area occurring in two hours of chlorination (Table 4).

The significant increase in the surface area of the coal after treatment with water is most probably due to the removal of water-soluble, low-surface-area inorganic material from the small apertures of the pore-network in coal.

Therefore, solvent interference because of insufficient drying is not responsible for the reported severe loss of porosity of the coal, at least in the absence of chlorination. The situation is more complicated in the presence of chlorination, where the highly chlorinated internal coal surfaces can adsorb and sustain solvent molecules like CCl_4 or CH_3CCl_3 much more effectively than raw coal surfaces, because of the increased degree of interaction between these surfaces and the solvent. And then, even the highest vacuum would not be able to remove the last traces of the solvent from the microporous coal matrix, resulting again in a sharp apparent decrease in accessible surface area.

A strong argument against this last possibility was provided by a coal-chlorination experiment using gaseous chlorine, where, of course, no solvent or solvent effects were present. Raw PSOC 190A coal was chlorinated in a fluidized-bed reactor under conditions similar to the slurry-phase chlorination conditions employed so far. One might argue that the mechanism of coal chlorination with gaseous chlorine may be different from that in the slurry phase, but thorough analysis of the coal product and surface-area measurements gave the same results and the same reduction in available surface area with that of slurry-phase experiments in the presence of a solvent.

Therefore, the reported loss of porosity during chlorination of coal is a result of the chlorination reaction itself and not of the solvent interference, and can be envisioned as occurring through swelling of the coal matrix, especially in the apertures, because of the high chlorine uptake. Swelling phenomena leading to fissuring and reduction in size of the coal particles during chlorination have already been discussed in Chapter 2 (Sections 2.3 and 2.5). The apertures can become effectively blocked or reduced in size, because of the swelling of the pore walls. That can result in a large drop in the accessible surface area because a whole network of pores in the aperture-cavity system accessible only through these apertures is also lost from surface-area determinations.

Finally, the reduced blocking at higher temperatures can be explained by the significantly increased intrinsic reaction rate at higher temperatures. Chlorine is readily consumed at the entrance of the larger pores before diffusing into the apertures and causing extensive blocking. In contrast, at low temperatures, chlorine has enough time to diffuse into the smaller pores before being completely reacted, so that a more uniform and severe blocking of the pores occurs.

Chapter 4

MODEL - REACTION STUDIES

4.1 Pyritic sulfur

4.1.1 Introduction

The earlier work on chlorination of iron pyrite has been reviewed by Mellor (59). Brown (60) reported that dry hydrogen chloride did not attack the pyrite at room temperature. When the HCl was passed over pyrite for an hour, the percentage amounts of sulfur lost were 0.93% (15°C), 10.73% (310°C), and 17.13% (325°C). Also, pyrite was not easily attacked by hydrochloric acid. When treated for an hour with the boiling concentrated acid, only 2.56 out of 46.67 percent iron passed into solution (∿5.5% conversion). No evolution of H_2S was observed. Crookes (61) obtained ferric chloride and elemental sulfur from the reaction of FeS_2 with a mixture of hydrochloric and nitric acids. Deville (62) reported the conversion of iron pyrite to iron sulfates by treatment with hypochlorous acid. Rivot *et al*. (63) decomposed finely divided FeS_2 by reacting with gaseous chlorine in alkaline lye.

Kangro and Flügge (64) observed complete removal of the iron when pyrite was chlorinated with gaseous chlorine at 900°C for 30 minutes. The distillate contained ferric chloride and sulfur monochloride.

The chlorination of pyrite with gaseous chlorine was also studied by Ezdakov (65). He found that dry chlorine did not react with dry pyrite below 100°C. The reaction proceeded energetically and with the evolution of large amounts of heat when finely ground moist pyrite was used. Without heating, the mass baked together, and fumes of $FeCl_2$ and Fe complexes with S_2Cl_2 were formed. On heating, the reaction proceeded energetically and a liquid condensate was formed. Optimum temperature conditions were determined to be between 300° and 400°C.

Luft and Todhunter (66) used a fluidized-bed reactor for pyrite chlorination. Heating the reaction mixture to 350° - 420°C converted the FeS_2 to $FeCl_3$ and S_2Cl_2. Raising the temperature to 480° - 520°C and reducing the chlorine-to-pyrite ratio led to the formation of $FeCl_3$ and S.

The utilization of pyrite ores as an industrial source of elemental sulfur via chlorination with gaseous chlorine follows the reaction:

$$FeS_2 + Cl_2 \xrightarrow{\Delta} FeCl_2(FeCl_3) + S(S_2Cl_2, SCl_2)$$

The process has been described in a number of patents and papers (67). In general, chlorination reactions were found to be thermodynamically favorable and highly exothermic. Hydrogen chloride was less effective than chlorine in the reaction with FeS_2.

The chlorination of iron pyrite in nonaqueous solvents was studied by McElroy and Peters (68). They found that iron pyrite reacted with chlorine dissolved in carbon tetrachloride or dichloroethane to produce ferric chloride and sulfur dichloride at ambient temperature according to the reaction:

$$2FeS_2 + 7Cl_2 \rightarrow 2FeCl_3 + 4SCl_2$$

Both products of this initial reaction could in turn be used as reactants with additional pyrite to produce ferrous chloride and elemental sulfur:

$$FeS_2 + 2FeCl_3 \rightarrow 3FeCl_2 + 2S$$

$$FeS_2 + SCl_2 \rightarrow FeCl_2 + 3S$$

Boros et al. (69) studied the same reactions in a variety of solvents. The expected reaction of chlorine with iron pyrite to produce ferric chloride and sulfur monochloride was not achieved to any significant extent. Recycling the solvents through pyrite beds and use of elevated temperatures and ultraviolet radiation (70) gave only slight improvements in the reaction rate.

The aqueous chlorination of iron pyrite was studied by Strickland et al. (71). Pyrite under all conditions examined (10° - 40°C) produced only ferric and sulfate ions:

$$2FeS_2 + 15Cl_2 + 16H_2O \rightarrow 2Fe^{3+} + 30Cl^- + 32H^+ + 4SO_4^{2-}$$

The reaction was found to be diffusion-controlled with an activation energy of about 5 Kcal/mole.

Amio (72) also reported that treatment of powdered pyrite with chlorine in water produced an aqueous solution of H_2SO_4, sulfates, HCl and chlorides.

Finally, Lopatin and Girdasova (73) studied the behavior of pyrite in alkaline solutions containing a sulfur-oxidizing agent (a weak hypochlorite solution). At concentrations less than

$50 \frac{\text{g hypochlorite}}{\text{lt of concentrated alkali}}$ the degree of oxidation was small. The rate of oxidation increased with increasing temperature.

4.1.2 Experimental section

The anhydrous slurry-phase chlorination of iron pyrite was examined in the following experiment:

Approximately 15 g of FeS_2 (Matheson grade), ground so that an 85% minimum passed through 50 mesh, were suspended in reagent-grade carbon tetrachloride presaturated with chlorine and were chlorinated under intense stirring for two hours at 60°C and at a dry chlorine flow rate of 2 g/min. The solid was then filtered and dried in vacuum for two hours at 110°C. It possessed a dark brown color, characteristic of $FeCl_3$ presence, and showed a weight increase of 2.7% over the original pyrite. EDAX scan confirmed the presence of chlorine on its surface. The elemental compositions of the iron pyrite and the solid product were determined and are given as follows:

	Fe(wt%)	S(wt%)	Cl(wt%)
FeS_2	43.2	49.5	0
Solid Product	42.1	47.4	0.43

Mass balances on the above elements indicated that, while there was no loss of iron, about 1.6% of the sulfur present in the original pyrite was lost to the liquid phase of CCl_4. A sample of this phase after chlorination was run through a Perkin-Elmer 3920 gas chromatograph equipped with a sulfur detector (Section 2.6). A single sulfur peak was detected confirming the presence of a small amount of sulfur in solution. A standard solution of sulfur monochloride (S_2Cl_2) in carbon tetrachloride gave a similar peak at the same retention time, indicating the presence of an S-Cl species (SCl_2 or S_2Cl_2) in the reaction mixture.

It is very likely that the limited extent of pyrite chlorination in CCl_4, even under vigorous reaction conditions, was due to a mass-transfer constraint rather than to some kinetic limitation. Chlorination of iron pyrite, a nonporous solid, results in the formation of a ferric-chloride layer on its surface. Due to the inability of CCl_4 to dissolve appreciable amounts of $FeCl_3$ (69), this layer eventually attaches to the surface prohibiting the exposure of fresh pyrite for further chlorination, and thus the reaction ceases.

To test this hypothesis, iron pyrite should be chlorinated in a non-aqueous solvent capable of readily dissolving both the reactant and the products of chlorination. A 50/50 volume mixture of carbon tetrachloride and methanol was selected, because of the high solubility of chlorine (reactant) and SCl_2 or S_2Cl_2 (products) in CCl_4 and the very high solubility of ferric chloride (product) in MeOH $\left(1.55 \frac{\text{g FeCl}_3}{\text{g MeOH}}\right)$ (69).

Chlorination of the iron pyrite in this mixture, under reaction conditions similar to those in the (pure) carbon tetrachloride experiment, resulted in about 35% conversion of the FeS_2 to CCl_4-MeOH soluble products. This extent of reaction is considerably higher than the extent of the same reaction in CCl_4 alone (1.6%) and is also comparable with the extent of aqueous chlorination, discussed below, of iron pyrite under similar conditions. Therefore, mass-transfer limitations, in the previously discussed sense, seem to control the rate of anhydrous slurry-phase chlorination of FeS_2.

The aqueous chlorination of iron pyrite, where of course no such limitations exist, was kinetically studied in a series of experiments. Approximately 15 grams of FeS_2 were suspended in 350 ml of distilled water presaturated with chlorine and were chlorinated under intense (1300 r.p.m.) and constant stirring at a high chlorine flow rate of 2g/min for a certain period of time. Two different initial reaction temperatures were studied, 23°C and 59°C. No attempt was made to control the temperature once the very exothermic reaction was initiated. The temperature for the first set of experiments (initial temperature of 23°C) ranged between 23° and 38°C and for the second (initial temperature of 59°C) ranged between 59° and 91°C.

At the end of each run, the pyrite was filtered and dried in vacuum for two hours at 110°C. The weight loss because of the chlorination reaction was determined. The aqueous phase after chlorination was analyzed for iron (on a Varian AA6 atomic absorption spectrophotometer) and sulfur (gravimetric analysis). Mass balances on these elements indicated that only Fe^{3+} and SO_4^{2-} ions were produced in the aqueous chlorination of FeS_2 under all conditions examined. The amounts of iron and sulfur found in solution matched exactly the weight loss of iron pyrite due to the chlorination reaction. No elemental sulfur was detected in the reaction products by the KOH-acetone test (74).

The results for pyrite conversion as a function of time are given in Table 7 and are shown in Figure 9.

The experimental data were reduced using a first-order rate expression similar to the one determined by Sherman and Strickland (71) in their study of the aqueous chlorination of pyrite:

Table 7. Pyrite conversion as a function of time in aqueous chlorination.

Reaction Time, t (min)	Pyrite Conversion, X (%)	
	T_o = 23°C	T_o = 59°C
0	0	0
15	29.7	34.6
30	48.1	53.0
60	61.1	76.6
90	69.8	84.5
120	74.3	87.0

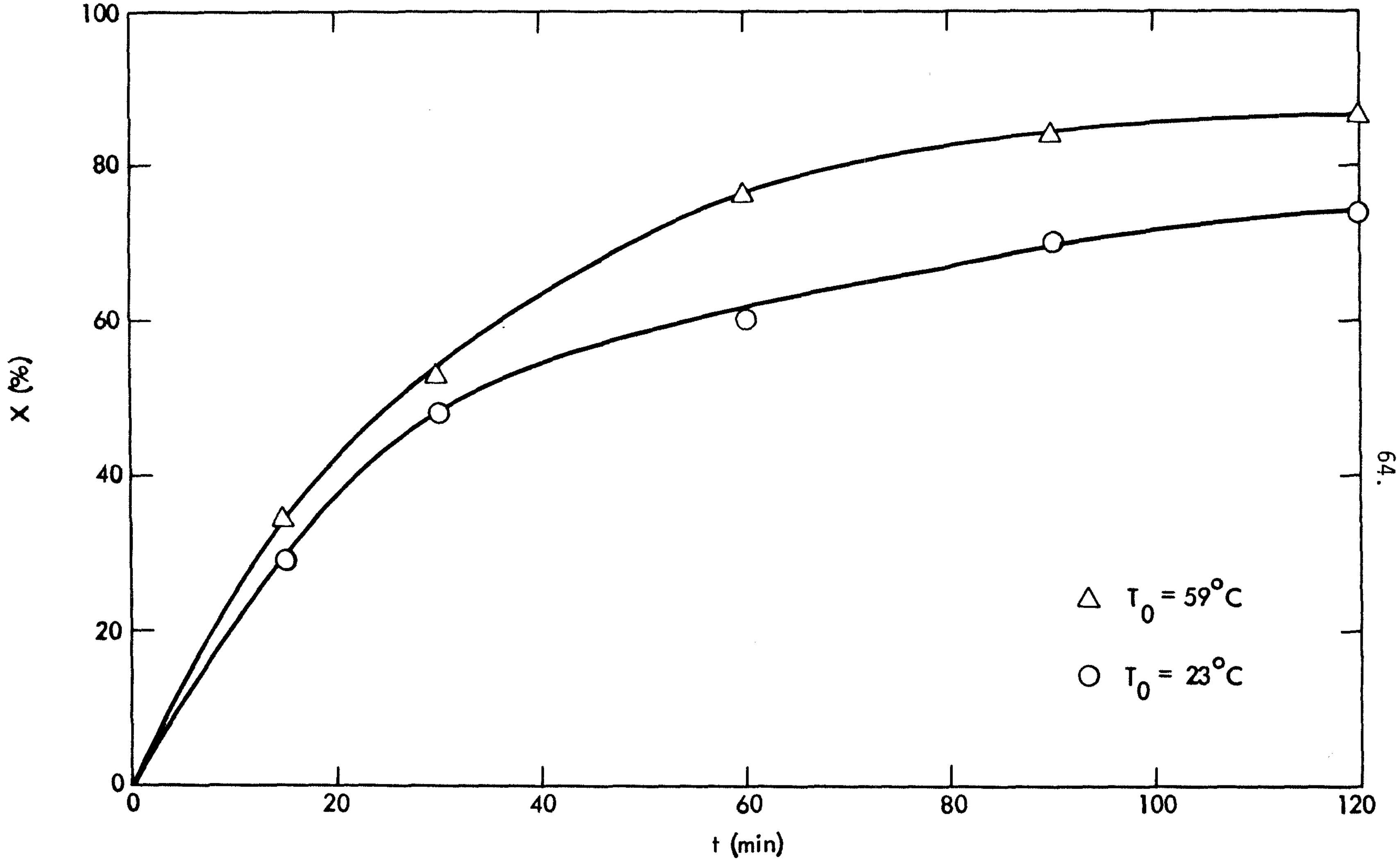

Figure 9. Pyrite conversion X(%) as a function of time in aqueous chlorination.

$$\frac{dX}{dt} = k[Cl_2] \qquad (1)$$

where

X = pyrite conversion (dimensionless).

t = reaction time, min.

k = rate constant, min^{-1}.

$[Cl_2]$ = concentration of molecular chlorine in the aqueous solution,

$$\frac{\text{cm}^3 \text{ chlorine}^*}{\text{cm}^3 \text{ water}} \quad \text{(dimensionless)}.$$

Equation (1) may also be written as:

$$k = \frac{1}{[Cl_2]} \cdot \frac{dX}{dt} \qquad (2)$$

The concentration $[Cl_2]$ of molecular chlorine in aqueous solution at saturation and at various temperatures can be determined from the total solubility $[Cl_2]_T$ of chlorine in water (Figure 10, from data of reference 75) and from the hydrolysis constant for the reaction:

$$Cl_2(aq.) + H_2O \rightleftharpoons Cl^- + H^+ + HClO \quad .$$

This hydrolysis constant as a function of temperature has been determined experimentally by Yakovkin *et al*. (76).

The experimental data in Table 7 cannot be utilized directly for the calculation of $\frac{dX}{dt}$ and thus of rate constants through equation (2) because of the nature of the present experiments. The initial

---

[*] Under standard conditions, 1 atm - 0°C.

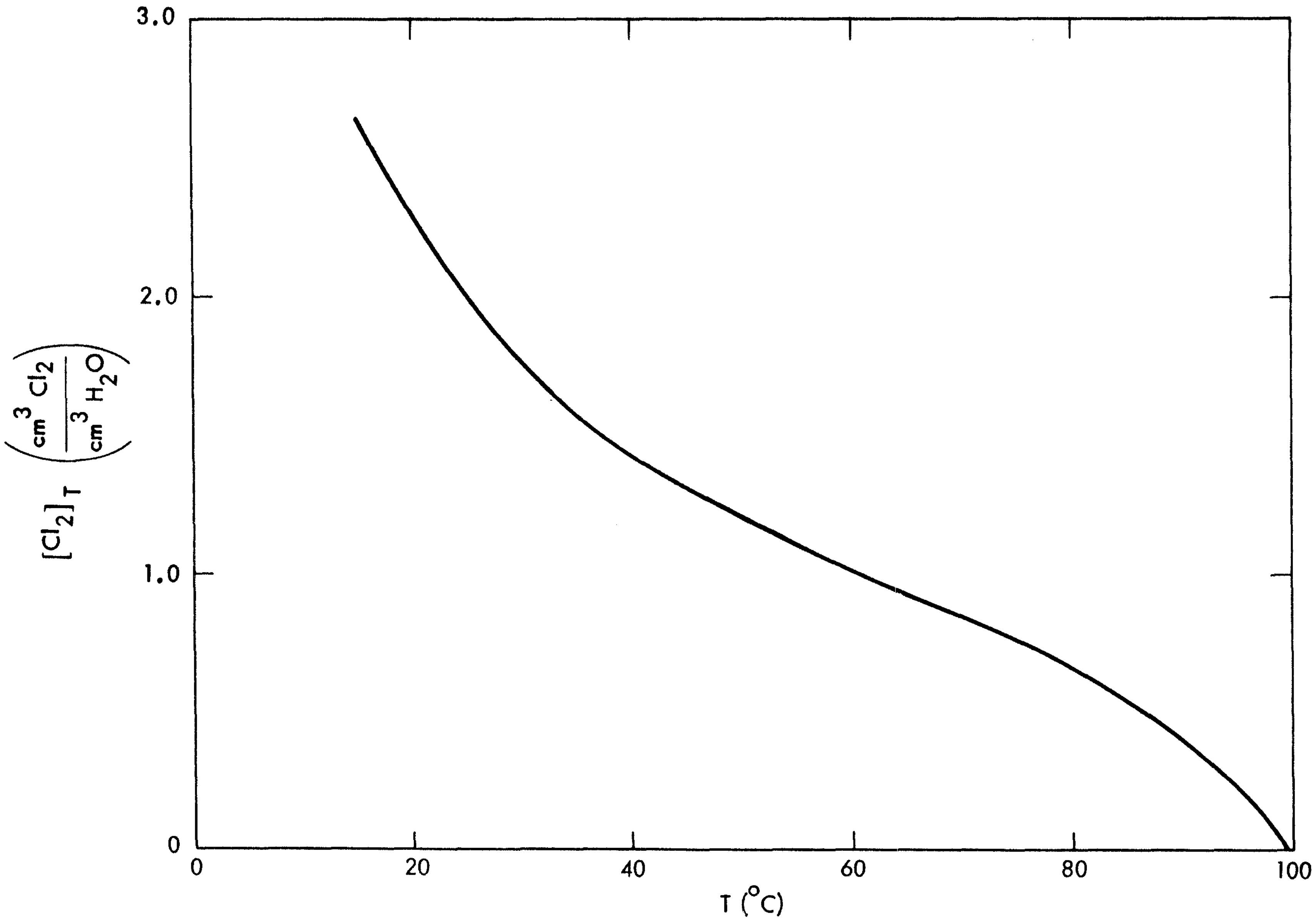

Figure 10. Total solubility $[Cl_2]_T$ of chlorine in water as a function of temperature (P = 1 atm).

temperature changes considerably during the course of the exothermic chlorination reaction (page 62) and affects the total solubility and the aqueous equilibrium of chlorine in solution. On the other hand, the formation of significant quantities of iron and sulfate ions has a pronounced effect on the ionic strength of the aqueous solution and thus on chlorine equilibrium as well.

Therefore, the experimental data can be utilized for calculating $\frac{dX}{dt}$ only in the cases where controlled and well-known conditions exist. Such conditions are, of course, the initial conditions, i.e. $t = 0$ and (pure) saturated aqueous chlorine solutions at 23° and 59°C.

Cubic interpolation on the pyrite conversion-versus-time curves gave the following values for $\frac{dX}{dt}$ at $t = 0$:

$$23^\circ\text{C:} \quad \frac{dX}{dt} = 2.141 \text{ min}^{-1}$$

$$59^\circ\text{C:} \quad \frac{dX}{dt} = 2.575 \text{ min}^{-1} \quad .$$

Since the two values are sufficiently close to each other (±19%), linear interpolation was employed to calculate $\frac{dX}{dt}$ values for a series of temperatures within the 23° - 59°C.

The results of this interpolation, along with total and molecular chlorine solubility values (from data of references 75 and 76) are given in Table 8, where the rate constants calculated from equation (2) are also included.

The Arrhenius plot for these rate constants was highly linear (correlation coefficient $r_c^2 = 0.9996$) and gave the following values for

Table 8. Calculation of first-order rate constants for the aqueous chlorination of iron pyrite at various temperatures.

Temperature (°C)	$\frac{dX}{dt}$ (min^{-1})	$[Cl_2]_T$ (cm^3Cl_2/cm^2H_2O)	$[Cl_2]$ (cm^3Cl_2/cm^3H_2O)	k (min^{-1})
23	2.141	2.09	1.41	1.52
30	2.225	1.77	1.11	2.01
40	2.346	1.41	0.77	3.05
50	2.467	1.20	0.57	4.29
59	2.575	1.03	0.44	5.90

the activation energy and the preexponential factor:

$$E = 7.384 \frac{\text{Kcal}}{\text{mole}}$$

$$A = 4.284 \times 10^{5} \text{ min}^{-1} .$$

Sherman and Strickland (71), using a different experimental approach, determined the activation energy to be about 4.9 $\frac{\text{kcal}}{\text{mole}}$ and concluded that liquid diffusion of chlorine in the aqueous solution was the rate-controlling step.

4.2 Organic sulfur

4.2.1 Introduction

The chlorination of organic sulfides has been reviewed by Reid (77). The primary reaction of chlorine with alkyl sulfides is an addition: $R_2S + Cl_2 \rightleftharpoons R_2SCl_2$. With the simpler alkyl sulfides, the addition is quantitative and may be used for their estimation. Chlorination frequently involves the alkyl or aryl group of the sulfide as well. Alkyl sulfides take up chlorine more readily than aryl sulfides.

Just what happens in a particular case depends on the conditions of chlorination. Pierre (78) reported that by passing chlorine into ethyl sulfide, much heat was evolved, ethyl chloride was produced and sulfur separated. Propyl sulfide gave 1,1,1-trichloropropane and a pentachloropropane, i-butyl sulfide gave 2-methyl-1,1,1-trichloropropane, a dichloro- and a tetrachlorobutane and i-amyl sulfide gave 2-methyl-4,4,4-trichlorobutane and other chlorinated pentanes (79).

The oxidation of sulfides to sulfoxides and sulfones by chlorine, in the presence of water, must involve addition of chlorine and hydrolysis of the dichloride. Fries and Vogt (80) reported the formation of phenyl sulfoxide by chlorination of phenyl sulfide in benzene at 0°C and hydrolysis of the unstable intermediate dichloride. Lee and Dougherty (81) converted di-n-butyl and dibenzyl sulfides to n-butane- and toluene-alpha-sulfonyl chlorides, respectively, by chlorination in aqueous acetic acid. Dronov et al. (82) studied the oxidative chlorination of di-n-propyl, n-butyl-n-octyl, di-n-decyl, n-propyl phenyl and dibenzyl sulfides in water, methanol and acetic acid. Sulfones or sulfonyl chlorides were the final products of chlorination depending on the particular sulfide. For the nonsymmetric alkyl sulfides, the chain was broken between the sulfur atom and the larger alkyl group.

Sulfonyl chlorides have also been obtained from mercaptans, disulfides, thiol esters and other types of sulfur compounds by using chlorine, in the presence of water, as the oxidizing agent for the organic sulfur (83).

Finally, hypochlorite takes a sulfide all the way to the sulfone (84). Alkaline calcium hypochlorite may destroy the sulfide, oxidizing the sulfur to the sulfate ion (85).

4.2.2 Oxidative chlorination of dibenzothiophene (86)

Introduction

Though the Cl_2-H_2O system is widely used as an oxidizing agent, very few references exist in the literature on the use of this system for the oxidation of dibenzothiophene (DBT). Most of these references are concerned with the first step of the oxidation, i.e. the formation of the sulfoxide.

In a method which was first proposed by Fries and Vogt (80), Brown et al. (87) treated a solution of 15 g of dibenzothiophene in 150 ml of CCl_4 at 0° - 5°C with chlorine until 6 g had been added. The addition compound which was produced was hydrolyzed by vigorously shaking the reaction mixture with ice and water in accord with the reaction:

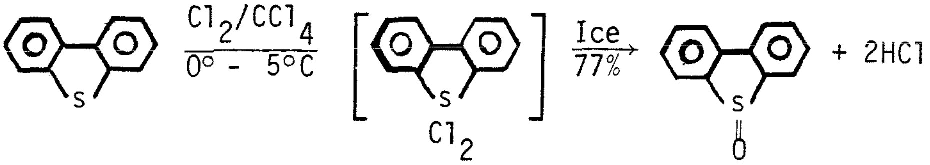

The intermediate dichloride was not isolated. The yield of dibenzothiophene sulfoxide (DBTO) melting at 174° - 180°C was 15.8 g (97%). It was crystallized from benzene and the yield of pure compound was 12.5 g (77%). It had a melting point of 185° - 187°C.

Using the same method, Attar and Corcoran (88) employed chlorine to oxidize dibenzothiophene in a solution of CCl_4 at -10°C and then hydrolyzed the product at 15°C. They observed that substantial chlorination of the phenyl groups occurred.

Baciocchi and Mandolini (89) investigated the kinetics of the reaction of dibenzothiophene with chlorine in 99.1% acetic acid at 20°C to give dibenzothiophene sulfoxide. The reaction was found to follow second-order kinetics. It was first-order in chlorine and first-order in dibenzothiophene. The production of HCl did not affect the rate constants which were also insensitive to the presence of LiCl. NaOAc showed a very strong accelerating effect. In the presence of sodium acetate, chlorine and dibenzothiophene gave dibenzothiophene sulfoxide even when the reaction was carried out in anhydrous acetic acid. The results were consistent with a reaction scheme in which the formation of the dibenzothiophene-chlorine adduct occurs in a fast pre-equilibrium step which is nearly completely shifted toward the reactants. The formation of dibenzothiophene sulfoxide was rapid and practically quantitative when dibenzothiophene was treated with chlorine in 99.1% acetic acid, but a slow ring chlorination of dibenzothiophene was observed when the reaction mixture was allowed to stand for some time.

Finally, Dronov *et al*. (82,90) reported that passing chlorine through 5 g of dibenzothiophene in 50 ml of 90% by volume methanol or in aqueous acetic acid at 0° - 14°C gave the dibenzothiophene sulfone ($DBTO_2$) in very high yields (>90%).

Experimental section

Oxidative chlorination was conducted by passing chlorine at a flow rate of 0.3 g/min through 15 g of dibenzothiophene (Aldrich grade, >95% purity) in 350 ml of a reagent grade solvent (CCl_4, $MeOH/H_2O$, H_2O) for an appropriate period of time and at a chosen temperature. Dibenzothiophene was completely dissolved in CCl_4. It was mostly in slurry form with H_2O or $MeOH$-H_2O because of its low solubility in water.

With an anhydrous solvent such as CCl_4, the reaction mixture after chlorination was hydrolyzed by vigorous shaking with ice and water for three minutes. No hydrolysis was necessary after chlorination when aqueous solvents were used. The time for the hydrolysis period was chosen to be small enough to prevent further reaction between the unreacted dibenzothiophene and the chlorine dissolved in the water. After chlorination and hydrolysis of the reaction mixture and filtering of the solid product, the CCl_4 phase was evaporated. Only small amounts (less than 0.5 g) of solid residue were obtained after evaporation in the low temperature (0°C) runs. However, a significant amount of residue was obtained in the high temperature (60°C) run and therefore its analysis was included in Table 9.

In all cases, the solid product (or residue) was washed with water and dried under vacuum for 48 hours at 50°C. It was analyzed with a Spectraphysics Model 3500 B liquid chromotograph using a reverse-phase column of 10μ Spherisorb ODS and a solvent program of water and acetonitrile. Identification of the main compounds present in the solid sample and determination of its composition were made by comparison of retention times and peak areas of the sample with standard solutions of dibenzothiophene, dibenzothiophene sulfoxide, and dibenzothiophene sulfone.

Under the conditions of the analysis, the relative retention times were 1 (DBTO) to 1.12 ($DBTO_2$) to 1.44 (DBT), and the relative $\frac{\text{mole}}{\text{peak area}}$ ratios were 1 (DBTO) to 0.235 ($DBTO_2$) to 0.325 (DBT).

Further identification of the solid products included melting-point determinations, infrared spectra of the solid phase and elemental analyses for sulfur and chlorine.

Table 9. Experimental conditions and analysis of products of chlorination of dibenzothiophene in carbon tetrachloride.

Experimental Conditions		Analysis of the Solid Product			
Temperature (0°C)	Reaction Time (min)	Weight[a] (g)	DBT/DBTO/DBTO$_2$ (mole ratio)	Relative Retention Times of Byproducts[c]	Chlorine (% wt.)
0	30	14.9	1/20.3/2.0	None Detected	0
0-2	120	14.3	1/2.6/23.1	1.23	1.4
60	30	2.5	1/7.5/27.2	1.23, 1.50, 1.57	8.8
60	30	11.4[b]	1/2.9/4.3[b]	1.23, 1.50, 1.57, 1.63[b]	14.5[b]

[a] For an initial amount of dibenzothiophene of 15 grams.

[b] This line presents the analysis of the solid residue obtained by evaporation of the CCl$_4$ phase after chlorination and hydrolysis of the reaction mixture and filtering of the solid product. The analysis for the solid product of the hydrolysis is given on line 3.

[c] Relative retention times with respect to dibenzothiophene sulfoxide (retention time = 1).

Results and discussion

Chlorination of dibenzothiophene in carbon tetrachloride

The experimental conditions and the analyses of the products obtained by chlorination of dibenzothiophene in CCl_4 followed by hydrolysis of the chlorinated solution are summarized in Table 9. Chlorination of dibenzothiophene in CCl_4 at 0°C beyond the stoichiometric requirement for the formation of the sulfoxide, a reaction time of 20 minutes for the given conditions, leads in the subsequent hydrolysis step to the formation of dibenzothiophene sulfone. Continuous addition of chlorine in excess of the amount required for complete conversion of dibenzothiophene to the corresponding sulfoxide yields a solid in the hydrolysis step which is progressively richer in sulfone.

Whether the sulfone is produced by direct hydrolysis of a tetrachloride:

$$\left.\begin{array}{l} \mathrm{DBT} + \mathrm{Cl_2} \rightarrow \mathrm{DBT\text{-}Cl_2} \xrightarrow{\mathrm{H_2O}} \mathrm{DBTO} + 2\mathrm{HCl} \\ \mathrm{DBT\text{-}Cl_2} + \mathrm{Cl_2} \rightarrow \mathrm{DBT\text{-}Cl_4} \xrightarrow{\mathrm{2H_2O}} \mathrm{DBTO_2} + 4\mathrm{HCl} \end{array}\right| \quad \mathrm{I}$$

or by chlorination and subsequent hydrolysis of the sulfoxide:

$$\left.\begin{array}{l} \mathrm{DBT} + \mathrm{Cl_2} \rightarrow \mathrm{DBT\text{-}Cl_2} \xrightarrow{\mathrm{H_2O}} \mathrm{DBTO} + 2\mathrm{HCl} \\ \mathrm{DBTO} + \mathrm{Cl_2} \rightarrow \underset{\underset{\mathrm{O}}{\|}}{\mathrm{DBT}}\mathrm{\text{-}Cl_2} \xrightarrow{\mathrm{H_2O}} \mathrm{DBTO_2} + 2\mathrm{HCl} \end{array}\right| \quad \mathrm{II}$$

is not yet clear. The feasibility of route II was demonstrated in a separate experiment, where 10 grams of the solid product of the 0°C, 30-minute run, noted on the first line of Table 9, were suspended in

350 ml of CCl_4 and chlorinated for 20 minutes at 0°C and at a feed rate of chlorine of 0.3 g/min. The reaction mixture was hydrolyzed the usual way, and the solid product was filtered, water-washed and dried as before. The analysis for this solid is given as follows:

Weight: 9.5 grams.
DBT/DBTO/$DBTO_2$ mole ratio: 1/12.9/25.5.
No other compounds detected.
Chlorine: 0 wt.%.

The results show that chlorination of dibenzothiophene sulfoxide in CCl_4 followed by hydrolysis of the new addition compound, presumably $\mathrm{DB}\underset{\underset{\mathrm{O}}{\|}}{\mathrm{T}}\text{-}\mathrm{Cl}_2$, leads to a significant (∿60%) conversion of the sulfoxide to the corresponding sulfone. This conversion is considerably slower than the dibenzothiophene → dibenzothiophene sulfoxide conversion under similar reaction conditions.

Higher chlorination temperatures result in drastically reduced yields of oxidized dibenzothiophene. The amount of solid product was 14.9 g for the 0°C, 30-minute experiment and only 2.5 g for the one at 60°C, 30 minutes. This result is consistent with the equilibrium:

$$\mathrm{DBT} + \mathrm{Cl}_2 \rightleftarrows \mathrm{DBT}\text{—}\mathrm{Cl}_2$$

which at low temperatures (0°C) is shifted towards the DBT-chlorine adduct. These addition compounds are generally unstable and can liberate chlorine (<u>77</u>). Thus, at higher temperatures, the equilibrium is shifted more towards the reactants so that the yield of $\mathrm{DBT}\text{—}\mathrm{Cl}_2$ and of DBTO or $DBTO_2$ in a subsequent hydrolysis step is substantially decreased.

Finally, chlorination of the phenyl groups is very slow at 0°C but becomes the main reaction path at higher temperatures such as 60°C, as indicated by the appearance of a series of new compounds in the solid product and the very high chlorine content of both the product and the residue after evaporation. It should be noted that 100% conversion of dibenzothiophene to chlorodibenzothiophene

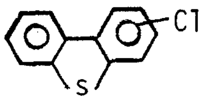

would yield a product with a chlorine content of 16.2 wt.%. These new compounds are most probably mono- or di-chloro derivatives of dibenzothiophene, dibenzothiophene sulfoxide and dibenzothiophene sulfone.

Aqueous chlorination of dibenzothiophene

No hydrolysis step was employed here. The results are summarized in Table 10.

In all cases, the only compounds present in the reaction products were DBT, DBTO and $DBTO_2$. No chlorine was detected in any of the solid samples. Ring chlorination of dibenzothiophene during the DBT $\xrightarrow{Cl_2/H_2O}$ $DBTO_2$ conversion did not occur under the experimental conditions employed, even at the highest temperature examined (70°C).

The overall rate of oxidation of dibenzothiophene in water is higher at higher temperatures despite the lower chlorine concentration at these temperatures.

The unfavorable equilibrium at high temperatures of the reaction:

Table 10. Experimental conditions and analysis of products of chlorination of dibenzothiophene in aqueous phase.

Experimental Conditions			Analysis of the Solid Product		
Temperature (°C)	Reaction Time (min)	Solvent	Weight[a] (g)	DBT/DBTO/$DBTO_2$ (mole ratio)	Sulfone Yield (% of Theoretical)
10	60	H_2O	14.8	1/0.79/5.05	64.0
10	60	MeOH[b]-H_2O	16.6	0/1/16.15	89.2
70	60	H_2O	16.4	0/0/1	93.2

[a] For an initial amount of dibenzothiophene of 15 grams.

[b] 90% by volume of MeOH.

$$DBT + Cl_2 \rightleftarrows DBT{-}Cl_2$$

did not appear to affect the overall rate as it did in the case of CCl_4, probably because in the presence of water the DBT-chlorine adduct is hydrolyzed readily, and so the equilibrium is shifted continuously towards the products.

Use of methanol in the DBT-chlorine/H_2O system improves the yield of the oxidized products significantly, even at a low reaction temperature such as 10°C.

Finally, slurry-phase chlorination of dibenzothiophene in water at 70°C proved to be an excellent method for the preparation of the dibenzothiophene sulfone. The sulfone was obtained in very high yields (>93%) and was 100% pure as proved by the melting-point determination (231° - 233°C), the liquid-chromatograph analysis (only a single $DBTO_2$ peak), the elemental analysis for sulfur (calculated for $DBTO_2$: S, 14.8; found: S, 14.8), and the solid-phase IR spectrum. Under the experimental conditions of the 70°C run conversion of DBT to $DBTO_2$ was complete after 40 minutes of reaction as indicated by the appearance of a stable yellow-green color (excess chlorine).

To determine whether the chloride ion (Cl^-) was an active species in the aqueous oxidation of dibenzothiophene by chlorine, a separate experiment was conducted. Fifteen grams of dibenzothiophene were suspended in 350 ml of a concentrated HCl solution for 120 minutes at room temperature and under intense stirring. The treated solid was filtered, water-washed, and dried by the usual method. Analysis of this solid showed no other compound present except for the original dibenzothiophene.

No chlorine was detected in the product. Thus, the chloride ion was not active in the conversion of DBT to $DBTO_2$.

4.2.3 Oxidative chlorination of other sulfides

Introduction

Reaction mechanism and products of chlorination were also studied for another sulfide, namely, phenyl sulfide.

As has already been mentioned in Section 4.2.1, Fries and Vogt (80) chlorinated phenyl sulfide in benzene at 0°C to obtain the very unstable dichloro-additive compound Ph_2SCl_2, which gradually evolved HCl and decomposed into a mixture of mono- and dichlorodiphenyl and phenyl sulfides. In the presence of water, the additive compound formed HCl and phenyl sulfoxide. Otto and Ostrop (91) reported the conversion of phenyl sulfone to phenyl sulfonyl chloride by treatment with dry chlorine at 120° - 130°C. Phosphorus pentachloride also served as the source of chlorine.

Experimental section

The solid products of chlorination of phenyl sulfide were analyzed on the Spectraphysics Model 3500B liquid chromatograph cited previously (Section 4.2.2). Identification of the main compounds present in solid samples and determination of their composition were made by comparison of retention times and peak areas for the samples with those from standard solutions of phenyl sulfide, sulfoxide, sulfone and sulfonyl chloride. Under the conditions of the analysis, the relative retention times were 1(Ph_2SO) to 1.055(Ph_2SO_2) to 1.084($PhSO_2Cl$) to 1.226(Ph_2S), and the relative $\frac{\text{mass}}{\text{peak area}}$ ratios were 1(Ph_2SO) to 0.986(Ph_2SO_2) to 0.543($PhSO_2Cl$) to 0.370(Ph_2S).

Chlorination of phenyl sulfide was first carried out in a dispersed phase in water at room temperature and up to a point of 100% chlorine excess over the stoichiometric requirement for complete conversion of the sulfide to the corresponding sulfone. The only compounds present in the solid product of chlorination were phenyl sulfoxide and phenyl sulfone in a 1(Ph_2SO) to 0.6(Ph_2SO_2) mole ratio. The overall conversion for phenyl sulfide was 88% with a sulfone yield of 55% of the theoretical. No chlorination of the aromatic nucleus was observed under the above reaction conditions.

In an attempt to carry the oxidation of phenyl sulfide a step beyond the sulfone to the phenyl sulfonyl chloride, more severe reaction conditions were employed. Phenyl sulfone, in a slurry phase in water, was chlorinated at 80°C for an extended period of time. No scission of the carbon-sulfur bond occurred; no chlorination of the phenyl group was observed; and the sulfone was recovered pure (>95% recovery).

Finally, anhydrous chlorination of phenyl sulfide was carried out in solution in carbon tetrachloride at room temperature and up to a point of 100% chlorine excess over the stoichiometric requirement for complete formation of the intermediate dichloride. A yellow solid (most probably the dichloride Ph_2SCl_2; see reference 80) started forming after the first few minutes of chlorination. It was very unstable and could not be isolated by filtration of the CCl_4 phase. No further attempt was made to isolate this solid. After chlorination, the CCl_4 phase was hydrolyzed by shaking with an ice-water mixture. The yellow solid disappeared and no solid product was formed. The water and carbon-tetrachloride phases were separated and then evaporated under reduced pressure. Only minute amounts of a white solid were recovered from the water phase. On the other hand, the evaporation of the CCl_4 phase yielded a significant amount (0.73 g per g of Ph_2S) of a white syrupy solid, which was extracted with ether and dried.

The liquid chromatogram of this solid gave two peaks at relative retention times of 1.070 and 1.136 (retention time of Ph_2SO = 1). No phenylsulfide, sulfoxide, or sulfone was detected in the sample. The two peaks most probably correspond to nuclei-chlorinated phenyl sulfide compounds, as the chlorine analysis of the sample also suggested (chlorine content: 12.8 wt.%).

Discussion

The results for the oxidative, aqueous and anhydrous, chlorination of both dibenzothiophene and phenyl sulfide indicate that no scission of carbon-sulfur bond occurs, at least under reaction conditions similar to coal-chlorinolysis conditions (Chapter 5), the final product of chlorination being the sulfone.

Complete desulfurization by chlorinolysis would require, at a first stage, scission of a carbon-sulfur bond of the sulfone to yield a sulfonyl chloride and a (desulfurized) chloride according to the following mechanism:

(1) 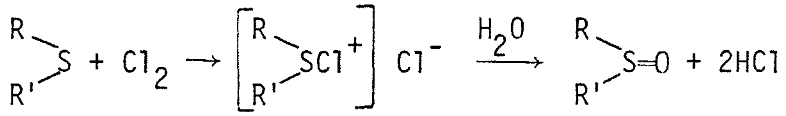

(2) 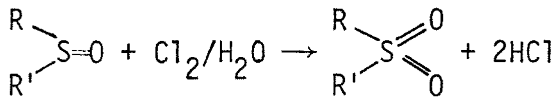

(3) 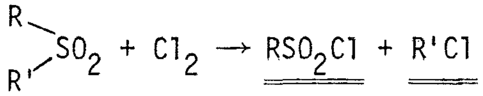

The scission of a carbon-sulfur bond in the sulfone state is in many cases considerably easier than the scission of the same bond in the original sulfide because of the increased selectivity of the decomposition at that state. With oxidation of the sulfur to sulfone, the bond energy between the carbon and the sulfur is reduced on the average by 5.2 $\frac{\text{Kcal}}{\text{mole}}$ for aliphatic sulfides and by 11.8 $\frac{\text{Kcal}}{\text{mole}}$ for aromatic sulfides and thiophenes (<u>88</u>).

The same products mentioned above, namely, a sulfonyl chloride and a chloride can also be formed during chlorination of an organic sulfide via an alternative reaction path depicted below:

(4) $R{-}S{-}R' + Cl_2 \rightarrow RSCl + \underline{\underline{R'Cl}}$

(5) $R{-}S{-}S{-}R' + Cl_2 \rightarrow RSCl + R'SCl$

(6) $R{-}S{-}H + Cl_2 \rightarrow RSCl + HCl$

(7) 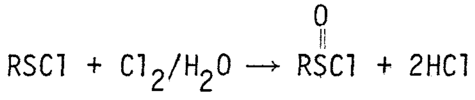

$$RSCl + Cl_2/H_2O \rightarrow R\overset{\overset{O}{\parallel}}{S}Cl + 2HCl$$

(8) 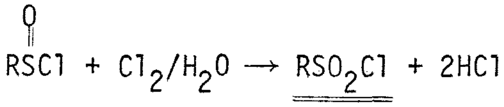

$$R\overset{\overset{O}{\parallel}}{S}Cl + Cl_2/H_2O \rightarrow \underline{\underline{RSO_2Cl}} + 2HCl$$

This reaction path involves a scission of a carbon-sulfur bond at the state of the sulfide to produce a chloride and a sulfinyl chloride, rather than an intermediate dichloride as in the case of the previous mechanism.

Sulfinyl chloride can also be formed by a scission of a sulfur-sulfur or a sulfur-hydrogen bond during chlorination of a disulfide and a mercaptan, respectively (92). This sulfinyl chloride is then oxidized by the Cl_2/H_2O system, an oxygen carrier, to sulfenyl (RSOCl) and finally to sulfonyl (RSO_2Cl) chloride. Thus, the two mechanisms predict the same final products (RSO_2Cl, R'Cl) for the chlorination of the sulfide RSR', but they differ relative to the state at which the scission of a C-S bond occurs (state of the sulfone for the first, state of the sulfide for the second). There is no sulfoxide or sulfone formed intermediately in the second mechanism.

Which of the two mechanisms a particular sulfide will follow obviously depends on the nature of the sulfide, that is, the stability of its carbon-sulfur bonds, and on the degree of destabilization that the conversion

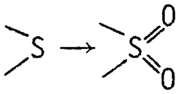

will establish for these bonds. Our experimental results for dibenzothiophene and phenyl sulfide indicate that the first mechanism is applicable for these two sulfides.

On the other hand, normal and aryl-substitued alkyl sulfides have been found (81) to follow the second mechanism. But even in the case where, for a certain sulfide, oxidative chlorination results in a carbon-sulfur bond rupture and in the formation of a sulfonyl chloride, desulfurization is not yet complete. The sulfonyl chloride can in principle be hydrolyzed to yield a sulfonic acid, which in turn can be completely desulfurized in a subsequent step by combined chlorine-water attack:

$$(9)\quad RSO_2Cl + H_2O \rightarrow RSO_3H + HCl$$

$$(10)\quad RSO_3H + Cl_2 + H_2O \rightarrow RCl + H_2SO_4 + HCl\ .$$

Reaction (10) has been demonstrated for simple aromatic (<u>but not for aliphatic</u>) sulfonic acids. Thus, an overall desulfurization reaction for organic sulfides can be written as follows:

$$(11)\quad RSR' + 4Cl_2 + 4H_2O \rightarrow RCl + R'Cl + H_2SO_4 + 6HCl.$$

A significant problem is that so far we have not been able to demonstrate this complete desulfurization effect under model reaction conditions with common sulfides (dibenzothiophene or phenyl sulfide). But we <u>do</u> know that this effect is present in coal chlorinolysis, if not with above sulfides, at least with some other organic-sulfur compounds, since coal subjected to the chlorinolysis process shows a very significant reduction in organic sulfur content in some cases (Chapter 5). This apparent contradiction may be explained by an effect, which has been proposed many times in the literature (<u>34</u>,<u>38</u>) but has not been definitely proven, namely, possible catalytic action of the mineral matter in coal during chlorination. Coal contains iron compounds in the mineral matter sufficient to form about 1 - 2% of ferric chloride. This quantity would be sufficient to catalyze ionic chlorination reactions and thus reduce the severity of the conditions needed for the desulfurization scheme to be carried to completion.

In a final attempt to demonstrate complete desulfurization of an organic sulfide under (uncatalyzed) chlorinolysis conditions, tert-butyl sulfide was chlorinated in a dispersed phase in water at 60°C and up to a point of slight chlorine excess over the stoichiometric requirement for complete desulfurization (reaction 11, page 85). The colorless sulfide phase turned yellow during chlorination, then deep orange, and finally disappeared. After chlorination, a small ($\sim$0.4 gram) amount of elemental sulfur was found adhered to the reactor's walls. Apart from that, the final product was a single, clear water phase which was analyzed for sulfur forms. Within the detection limits, all the sulfur in solution was in the sulfate form. A mass balance on sulfur showed a 60% conversion of the sulfide to sulfate ion, finally demonstrating the elusive complete desulfurization effect discussed previously.

Chapter 5

COAL DESULFURIZATION BY CHLORINOLYSIS

5.1 Introduction

Work on desulfurization of coal by chlorine treatment has been limited previously. Nelson et al. (93) reported that a large portion of the pyritic sulfur was removed from coal in experiments where small amounts of chlorine gas were added to an air stream passing through a coal-water slurry at temperatures between 22° and 70°C. No organic sulfur was removed, in contrast with earlier results obtained by Ochi (94).

The major disadvantage of earlier chlorination work directed at coal desulfurization was the use of relatively high temperatures (∿400°C) and pressures (95). Strong chlorine bonding in the organomatrix left an unacceptably high residual-chlorine content in the processed coal. Another disadvantage of the high temperature, high pressure process was the high (∿20%) loss of coal in processing because of attendant oxidation.

In a desulfurization attempt at low temperatures (25°C), chlorine gas was bubbled through a coal slurry in water for 0.5 to 6 hours (96). Chlorination for six hours resulted in 10 to 18% organic sulfur removal, 30 to 40% total sulfur removal and 23% chlorine in the coal matrix for a coal having 2.1% total sulfur, 1.5% organic sulfur and 22% ash.

Finally, along the same procedure as the JPL chlorinolysis process, Vasilakos et al. (97) have recently patented a process for the desulfurization of coal by aqueous chlorination at low temperatures (<120°C) and pressures (<100 psig).

5.2 Experimental section

5.2.1 Preliminary results

In a series of screening experiments, samples of the raw PSOC·190A coal, 100 x 200 mesh size, were chlorinated in four different solvents (methyl chloroform, carbon tetrachloride, tetrachloroethylene and water) at various temperatures and for various periods of time. Chlorinated coal samples were dried in vacuum at 100°C for two hours. The Eschka method (ASTM-D-3177) for chlorine and total-sulfur contents and the ASTM-D-2492 wet method for forms of sulfur were employed for the analysis of raw and chlorinated coals (98).

The Eschka method consists basically of incinerating an intimate mixture of coal with a mixture of one part sodium carbonate with two parts of light calcined magnesium carbonate. The sulfur compounds evolved during combustion react with the sodium carbonate and under oxidizing conditions are retained as sodium sulfate. This sulfate in the residue is extracted in either alkaline or acid solution and determined gravimetrically as barium sulfate. Chlorine on the other hand is converted during combustion to chlorides, which can also be extracted from the residue and determined by one of the usual analytical techniques.

Sulfate sulfur in coal is determined in the ASTM-D-2492 method by extracting a weighed sample of the coal with dilute hydrochloric acid followed by precipitation with barium chloride and weighing as barium sulfate. Sulfate sulfur is soluble in dilute hydrochlric acid; pyritic and organic forms of sulfur are insoluble.

Pyritic sulfur is determined in the same method by extracting the coal sample, already extracted with dilute hydrochloric acid for sulfate-sulfur determination, with dilute nitric acid followed by titrimetric determination of iron in the extract as a measure of the pyritic sulfur.

Finally, organic sulfur is determined by subtracting the sum of sulfate and pyritic sulfur from the total sulfur.

The results of a kinetic study on coal dusulfurization by chlorination in methylchloroform at 60°C are given in Table 11.

In reference to this table, the following observations can be made:

(1) Total-sulfur reduction increases with chlorine uptake in coal but reaches a plateau after a short reaction time, though chlorine uptake continues at a relatively high rate for long chlorination periods. The decrease in total-sulfur reduction after extended chlorination is probably due to the reintroduction of sulfur in the coal matrix by secondary reactions of sulfur compounds like sulfur monochloride with the coal (23,99):

$$\mathrm{Ar\,H + S_2Cl_2 \longrightarrow Ar{-}S{-}S{-}Cl + HCl}$$

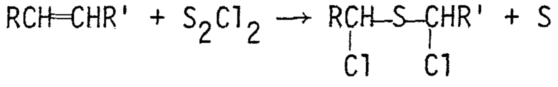

$$\mathrm{RCH{=}CHR' + S_2Cl_2 \longrightarrow \underset{\displaystyle Cl}{RCH}{-}S{-}\underset{\displaystyle Cl}{CHR'} + S}$$

The sulfur monochloride is formed during nonaqueous chlorination of pyrite (Section 4.1.2).

Table 11. Desulfurization versus reaction time in the slurry-phase chlorination of PSOC 190A coal in methylchloroform at 60°C.

Reaction Time (min)	Chlorine Uptake $\left(\frac{\text{g of chlorine}}{\text{g of raw dry coal}}\right)$	Total Sulfur Reduction[1,2] (%)		Pyritic Sulfur Increase[1,2] (%)
0	0		0	0
5	0.080		11.0	20
10	0.120		10.0	74
20	0.193	15.7±1.0	15.0	111
40	0.293		14.7	133
60	0.359		16.8	145
80	0.385		15.9	174
100	0.415		14.6	163
120	0.421		17.0	140
180	0.457		12.4	229

[1] Corrected for the different weight increase of each chlorinated coal sample over the raw coal.

[2] The precision of the ASTM sulfur determinations was ±0.05 wt.% sulfur. For the raw PSOC 190A coal, which has 2.49% total sulfur, 0.16% pyritic sulfur, 0.80% sulfate sulfur and 1.53% organic sulfur, this translates to ±2 in total-sulfur-reduction values and ±30 in pyritic-sulfur-increase values in the above table.

(2) There seems to be a considerable increase in the pyritic-sulfur content of the treated coal with chlorination time. Because there is no feasible way, at least by any known reaction, that pyrite (FeS_2) can be formed during coal chlorination, this effect must be an artifact of the analytical technique used for pyritic-sulfur determination on chlorinated coal samples.

In contrast with the total- and the sulfate-sulfur determinations, where sulfur is <u>directly</u> determined as SO_4^{2-}, the pyritic sulfur determination involves extraction of the sample which has already been extracted with d.HCl) with dilute nitric acid and determination of the iron in solution $\left(FeS_2 \xrightarrow{d.HNO_3} Fe^{3+}, SO_4^{2-}\right)$ as a measure of sulfur in the pyrite form.

Because the results indicate that pyritic sulfur in coal increases with reaction time, they imply that during the d.HNO_3 extraction of chlorinated samples, iron, not of the FeS_2 form and <u>not</u> extracted by dilute HCl, is being leached out and thus credited to pyritic sulfur in the subsequent iron determination. The amount of this nonpyritic iron, nonextractable with d.HCl, increases with chlorination time and can be attributed to the formation of complex Fe—S—Cl salts, stable enough to withstand d.HCl extraction in the coal matrix (<u>100</u>).

Finally, the use of other nonaqueous solvents (CCl_4, $CCl_2{=}CCl_2$) and different temperatures (30° - 100°C) did not improve significantly the overall coal desulfurization by chlorination (100).

5.2.2 Chlorinolysis of a high pyritic-sulfur coal

The objective here was to study the removal of pyritic sulfur from coal under chlorinolysis conditions. The PSOC 276 coal was selected for this study. This was a high-volatile Ohio #8 coal with the following distribution of sulfur forms:

Total sulfur	3.97 wt.%
Pyritic sulfur	2.60 wt.%
Sulfate sulfur	0.27 wt.%
Organic sulfur	1.10 wt.%

The moisture content of the coal was 2.3 wt.% and its heating value 12346 $\frac{\text{Btu}}{\text{lb}}$. The surface area, as determined by the BET dynamic technique (Section 3.2), was 1.5 $\frac{m^2}{g}$.

In a series of experiments, approximately 11.6 grams of raw PSOC 276 coal, 100 x 275 mesh size, were suspended in 350 ml of three different solvents (water, carbon tetrachloride, and a 50/50 volume mixture of carbon tetrachloride and methanol) and chlorinated for two hours at a chlorine flow rate of 0.3 g/min and at various temperatures. The slurry was then filtered, and the chlorinated coal was dried in vacuum at room temperature for 24 hours. In the cases of the nonaqueous runs (CCl_4 and CCl_4/MeOH), the dried chlorinated coal was then suspended in 350 ml of distilled water and hydrolyzed for two hours at 75°C. The chlorinated and hydrolyzed coal was filtered and dried for 24 hours in vacuum at room temperature.

The results for coal desulfurization by chlorinolysis of the PSOC 276 coal are given in Table 12.

In reference to this table, the following observations can be made:

(1) There is a very significant reduction in total-sulfur content for the coal chlorinated in water under the reaction conditions examined. This reduction (∿70%) comes mainly from the almost complete elimination of pyritic sulfur from coal. Pyritic-sulfur reduction decreases slightly with temperature.

Very low organic-sulfur reduction is observed in all three water runs. Lower temperatures seem to slightly favor the removal of organic sulfur from coal.

(2) Chlorine uptake in coal chlorinated in water decreases with temperature, obviously as a result of the significantly reduced solubility of chlorine at higher temperatures. Therefore, higher chlorination temperatures should be preferred here, because they can achieve the same level of desulfurization with less severe chlorination of the organic matrix.

(3) Chlorination of the coal in carbon tetrachloride followed by hydrolysis of the chlorinated coal results in significant total-sulfur reduction coming entirely from pyritic-sulfur elimination. No organic sulfur is removed. Pyritic-sulfur reduction is substantially lower in this anhydrous chlorination than in aqueous chlorination under similar reaction conditions, in agreement with the results of the model-reaction studies on pyrite chlorination (Section 4.1).

(This page is blank, due to error in numbering)

Table 12. Desulfurization of the PSOC 276 coal in a two-hour slurry-phase chlorination in various solvents and at various temperatures.

Solvent	Chlorination Temperature (°C)	Chlorine Uptake $\left(\frac{\text{g of chlorine}}{\text{g of raw dry coal}}\right)$	Total Sulfur Reduction (%)	Pyritic Sulfur Reduction (%)	Organic Sulfur Reduction (%)
H_2O	30	0.396	70.8	98.0	8.8
H_2O	60	0.376	69.9	97.5	∿0
H_2O	80	0.295	70.5	95.9	∿0
CCl_4[1]	60	0.115	53.6	73.7	∿0
CCl_4/MeOH[1]	50	0.310	79.8	98.3	30.8

[1] Chlorinated and hydrolyzed coal.

(4) Most of the chlorine uptaken in coal during chlorination in carbon tetrachloride is bound loosely in the hydrocarbon matrix and is readily removed during the subsequent hydrolysis.

(5) Though water is not present, chlorination of the coal in the CCl_4/MeOH mixture, followed by hydrolysis, results in complete elimination of pyritic sulfur (see Section 4.1.2) and great reduction in total sulfur for the treated coal. For the first time, organic-sulfur removal is also significant (∿31%).

(6) The chlorine uptake in coal increases considerably when the CCl_4/MeOH mixture, instead of CCl_4 alone, is employed as the solvent for the coal slurry. A large portion of the uptake of chlorine in this case is bound strongly in the coal matrix and survives the hydrolysis step.

Is important to note here that after chlorination, the liquid phase of CCl_4/MeOH possessed a black color indicative of significant amounts of coal extract dissolved in it. The chlorine and sulfur contents of this possible extract were not taken into account in calculating the data for Table 12. As we will show in the next section, the impressive coal-desulfurization results obtained in CCl_4/MeOH chlorination are due to the delaminating and extractive actions of methanol on the coal and not due to any chemical participation in the desulfurization scheme.

5.2.3 Chlorinolysis of a high organic-sulfur coal

The objective here was to study the removal of organic sulfur from coal under chlorinolysis conditions. The PSOC 190A coal, after physical cleaning to remove part of the ash and the inorganic sulfur, was used throughout this investigation. The distribution of the sulfur forms for this coal was as follows:

Total sulfur	2.36%
Pyritic sulfur	0.24%
Sulfate sulfur	0.31%
Organic sulfur	1.81%

The moisture content was 0.15%, and the heating value of the coal was 12096 $\frac{\text{Btu}}{\text{lb}}$. The surface area, as determined by the BET dynamic technique (Section 3.2), was 40.1 $\frac{m^2}{g}$.

In a series of experiments, approximately 10 g of this coal, 200 x 325 mesh size, were suspended in 350 ml of five different solvents (water, carbon tetrachloride, methanol, a 50/50 volume mixture of carbon tetrachloride and methanol, and a 50/50 volume mixture of water and methanol) and were chlorinated at 50°C for various periods of time at a chlorine flow rate of 0.3 g/min. The chlorinated coal was then filtered and dried in vacuum for 24 hours at room temperature. The solvent phase after chlorination was evaporated and any solid residue present was recovered and analyzed for chlorine and sulfur contents.

The results for coal desulfurization by chlorinolysis of the PSOC 190A coal are given in Table 13. These results characterize the chlorinated-coal samples and in the overall balances do not include any coal residue dissolved in the solvent phase at the end of chlorination.

In reference to Table 13, the following observations can be made:

Table 13. Desulfurization of the PSOC 190A coal in slurry-phase chlorination at 50°C in various solvents and for various reaction times.

Solvent	Reaction Time (min)	Chlorine Uptake (g/g)	Total Sulfur Reduction (%)	Pyritic Sulfur Reduction (%)	Organic Sulfur Reduction (%)	Residue after Evaporation[1] (%)	Heating Value Loss (%)
H_2O	8	0.070	13.3	13.4	11.8	<0.01	0.3
H_2O	20	0.216	25.5	38.6	24.6	<0.01	-0.9
H_2O	45	0.351	35.2	65.9	31.3	<0.01	0.4
H_2O	120	0.396	40.1	76.2	27.4	<0.01	4.8
H_2O/MeOH	120	0.348	43.1	75.9	28.9	<0.01	-3.2
MeOH	120	0.339	41.2	87.3	35.8	0.15	32.8
MeOH/CCl_4	120	0.289 (9.7%)[3]	55.5	85.1	44.0	0.49	20.1
CCl_4	120	0.413 (34.6%)[3]	16.6	32.9[2]	17.1[2]	0.03	-0.7

[1] Grams of residue per gram of raw coal.

[2] Estimated from sulfur analysis of the chlorinated <u>and</u> hydrolyzed sample.

[3] Percent of hydrolyzable (80°C, 3 hours) chlorine.

(1) Water

(i) Though both pyritic- and sulfate-sulfur reduction continue at a reasonable rate even after 120 minutes of chlorination, and the same is also true for the chlorine uptake in coal, organic-sulfur reduction reaches a plateau after short reaction times (∿40 minutes). In fact, a trend observed in earlier experiments (Section 5.2.1), namely, the slight increase in organic-sulfur content after extended chlorination, is present here too.

It is interesting to note that, under very similar reaction conditions, aqueous chlorination of the PSOC 190A coal results in significant organic-sulfur removal (∿28%; Table 13), while aqueous chlorination of the PSOC 276 coal gives absolutely no organic-sulfur removal (Table 12; Section 5.2.2). Because chlorine uptake and pyritic-sulfur reduction are approximately the same for the two coals, the difference in organic-sulfur removal is not due to any mass-transfer limitations (for example, surface area of PSOC 276: $1.5 \frac{m^2}{g}$; of PSOC 190A: $40.1 \frac{m^2}{g}$), but rather due to a thermodynamic constraint in the reaction of chlorine with the sulfur compounds in coal. It is very likely that the PSOC 276 coal has a much higher portion of the organic sulfur in dibenzothiophenic form than the PSOC 190A coal. As we have shown in Section 4.2.2, dibenzothiophenic sulfur is the most stable form of organic sulfur in coal and cannot be removed under the mild chlorinolysis conditions.

(ii) Heating-value losses for the chlorinated PSOC 190A coal are insignificant during the first hour of chlorination, while at the same time total-sulfur reduction and chlorine uptake in coal continue at a high rate. Only when chlorination and desulfurization rates considerably slow down, does the oxidation of the coal matrix (indicated by the ∿5% loss in heating value) become significant (35). This observation suggests the feasibility of optimizing the chlorination time for maximum chlorinolysis efficiency in terms of sulfur removal and heat-content losses. For example, the quantity:

$$F = \left(1 - \frac{S_f}{S_o}\right)\left(\frac{H_f}{H_o}\right)$$

may be used as the parameter to be optimized. $S_o(H_o)$ and $S_f(H_f)$ are the total-sulfur contents (heat contents) for the raw and the chlorinated coal, respectively. At reaction time $t_R = 0$, obviously $H_f = H_o$ and $S_f = S_o$, so that

$$F = \left[\left(1 - \frac{S_f}{S_o}\right)\left(\frac{H_f}{H_o}\right)\right]_{t_R=0} = 0$$

For any $t_R > 0$, in general

$$F = \left[\left(1 - \frac{S_f}{S_o}\right)\left(\frac{H_f}{H_o}\right)\right]_{t_R} > 0$$

Therefore, the objective is to maximize F with respect to t_R.

(2) Water-methanol mixture

Chlorinolysis of the PSOC 190A coal in a water-methanol mixture shows no significant differences in terms of sulfur removal (pyritic, organic or total) compared with the chlorinolysis of the same coal in water alone under the same reaction conditions. Chlorine uptake in coal is somewhat higher in water than in a water-methanol mixture. The drastic action of methanol during chlorination of coal in a carbon tetrachloride-methanol mixture (see below) does not seem to be present here.

(3) Carbon tetrachloride

Chlorination of the PSOC 190A coal in carbon tetrachloride displays the same characteristics already mentioned in previous sections, namely:

(i) High chlorine uptake in the coal matrix. A significant (∿35%) portion of this chlorine is loosely bound in the coal and is readily removed by mild hydrolysis in water at 80°C for three hours.

(ii) Chlorination of coal in anhydrous CCl_4 results in only a small reduction in total-sulfur content which comes from the removal of small amounts of pyritic and organic sulfur from coal, in agreement with the results of the model-reaction studies (Chapter 4).

(iii) Finally, chlorination of coal in carbon tetrachloride does not have any significant effect on the heat content of the coal. Subsequent hydrolysis though, results in considerable (∿5%) loss of heating value.

(4) Carbon tetrachloride-methanol mixture

Chlorination of the PSOC 190A coal in the carbon tetrachloride-methanol mixture results in high total-sulfur removal (∿56%) with so far the highest organic-sulfur removal (44%), in almost complete elimination of the pyritic and sulfate sulfur, but also in high heat-content losses (∿20%) and, for the first time, in a large amount of coal residue in the liquid phase (0.49 grams per gram of raw coal). These results are in complete agreement with the results on the coal/chlorine/CCl_4-MeOH system reported in Section 5.2.2 for the PSOC 276 coal.

The above picture is completely altered if one takes into account in the overall sulfur and chlorine mass balances the analyses of the considerable amount of coal residue. This residue, which represents an extraction product of the combined chlorine-MeOH/CCl_4 action on coal, should be considered together with the chlorinated coal in the overall balances.

Sulfur and chlorine analyses on the residue gave the following results:

Total sulfur	1.72 wt.%
Chlorine content	26.7 wt.%

If the residue is taken into account in the overall sulfur and chlorine mass balances, the combined total-sulfur reduction can be calculated to be 19.9% and the combined chlorine uptake to be $0.420 \frac{\text{g of chlorine}}{\text{g of raw coal}}$. These values are very close to the corresponding values for coal chlorination in carbon tetrachloride alone (16.6% and $0.413 \frac{\text{g of chlorine}}{\text{g of raw coal}}$, respectively), thus indicating that the spectacular results on sulfur reduction for the coal/chlorine/CCl_4-MeOH system (when the solid residue is <u>not</u> included in the calculations) are due to the delaminating and extracting action of methanol on the coal matrix (which yields a large amount of coal extract in the solvent phase), rather than due to some chemical participation of methanol in the desulfurization scheme. Complete penetration of the coal-pore structure by methanol may allow longer contact times of the reactant (chlorine) with the reactive sites of the coal surface, leading to higher extraction yields and also to more stable chlorination products. This last possibility is supported by the fact that only 9.7% of the chlorine taken up by the coal during chlorination in the CCl_4-MeOH mixture is removed by mild hydrolysis (80°C, 3 hours) compared with the 34.6% of hydrolyzable chlorine for coal chlorinated in CCl_4 alone.

Chlorination of coal in the CCl_4-MeOH mixture displays two additional, very interesting characteristics:

(i) If one calculates the sulfur-distribution coefficient at the end of the chlorination reaction, this number is found to be 1.42. The sulfur-distribution coefficient is defined as the ratio of the amount of sulfur in the coal residue over the amount of sulfur in the chlorinated coal divided by the ratio of the amount of coal material in the residue over the amount of coal material in the chlorinated coal. It is simply a measure of any preference of the sulfur in coal for the solvent phase over the solid coal phase. If no such preference existed, this coefficient should be equal to one. The value, as already mentioned, is 1.42, indicating a significant preference of the sulfur in the PSOC 190A coal for the solvent phase or, in other words, indicating selective sulfur extraction by the CCl_4-MeOH mixture during chlorinolysis.

(ii) The coal-extraction yield, not taking into account the chlorine incorporated in the coal matrix or in the coal residue, can be calculated to be 36%. This value is very impressive, because it shows that 36% of the coal material dissolves into the CCl_4-MeOH phase during chlorinolysis under very mild reaction conditions, namely, ambient pressure and 50°C. Under the same conditions the normal (i.e. in the absence of chlorine) extraction yield is about 5 - 10% only.

(5) Methanol

Chlorination of the PSOC 190A coal in methanol alone gives results comparable to the results of coal chlorination in the CCl_4/MeOH mixture, at least in terms of sulfur reduction. Chlorine uptake in coal is lower in methanol chlorination than in chlorination in carbon tetrachloride, obviously as a result of lower chlorine solubilty.

The amount of coal residue (0.15 grams per gram of raw coal) is significantly lower here than in the case of methanol-carbon tetrachloride (0.49 grams per gram) and the same is also true for the coal-extraction yield (12.1% compared with 36%). The sulfur-distribution coefficient in the pure-methanol case is determined to be 3.98. Selective sulfur extraction by methanol has also been observed in supercritical extraction of the PSOC 190A coal with toluene-methanol mixtures (101).

Chapter 6

SOLVENT EFFECTS IN COAL CHLORINOLYSIS

6.1 Introduction

In Section 5.2.3 we showed that the significantly increased sulfur removal in the CCl_4-MeOH chlorination of the PSOC 190A coal, over the pure-CCl_4 chlorination, is really an artifact of the delaminating and extractive action of methanol on the coal matrix, which results in a large amount of coal material being dissolved in the liquid phase. On the other hand though, this methanol-extraction effect occurs to only a limited extent in coal chlorinolysis in pure MeOH and is not present at all in MeOH-H_2O chlorinolysis. Thus, questions arise. Provided the above effect is a physical one (e.g. a solvent-extraction effect), which exactly is the physical parameter of the solvent (being extremely favorable for the coal/CCl_4-MeOH system but not so favorable for the coal/MeOH and completely unfavorable for the coal/MeOH-H_2O, coal/H_2O and coal/CCl_4 systems) that determines the extent of this solvent extraction? The solvent-solubility parameter is the most obvious candidate and has led us to the study of the solubility parameter for coal as described in the next sections.

6.2 The solubility-parameter concept

The one-dimensional solubility parameter of a liquid, δ, is defined (102) as the positive square root of its cohesive energy density, c, that is, of the potential energy E of a mole of material divided by the molar volume V:

$$\delta \triangleq c^{\frac{1}{2}} \triangleq \left(-\frac{E}{V}\right)^{\frac{1}{2}} \tag{1}$$

If the vapor phase of the liquid is assumed ideal, an approximate relation between solubility parameter and heat of vaporization of the liquid (ΔH_v) can be developed:

$$\delta^2 = \frac{\Delta H_v - RT}{V} \tag{2}$$

The unit for solubility parameter is $cal^{1/2}\ cm^{-3/2}$, the so-called Hildebrand (Hb).

The reason for the introduction of the solubility-parameter concept and the basic principle for the whole solubility-parameter theory lies on Hildebrand's assumption: *There is a correlation between cohesive energy density and mutual solubility.* It has been found that a good solvent for a certain (nonelectrolyte) solute such as a polymer has a solubility-parameter value close to that of the solute. Often a mixture of two solvents, one having a δ value higher and the other having a δ value lower than that of the solute, is a better solvent than the two components of the mixture (<u>102</u>).

The solubility parameter of a pure liquid can be calculated using a number of empirical correlations (<u>103</u>) which relate the solubility parameter to other physical parameters of the liquid, like the normal boiling point T_b(°K):

$$\delta^2 = \frac{\Delta H_v - RT}{V} \quad \text{and} \tag{2}$$

$$\Delta H_v\left(\frac{cal}{mole}\right) = 0.020\ T_b^2 + 23.7\ T_b - 2950 \tag{3}$$

(Hildebrand's relation),

the critical pressure P_c(atm):

$$\delta^2 = 1.25\ P_c\ , \tag{4}$$

the refractive index n:

$$\delta = 30.3\ \frac{n^2 - 1}{n^2 + 2}\ , \tag{5}$$

or the surface tension $\gamma\left(\frac{\text{dyne}}{\text{cm}}\right)$:

$$\delta = 4.1\left(\frac{\gamma}{V^{1/3}}\right)^{0.43}\ . \tag{6}$$

Solubility-parameter values can also be calculated using corrresponding-states and group-additivity methods. In some cases, three-dimensional solubility parameters have been introduced:

$$\delta_o^2 = \delta_d^2 + \delta_P^2 + \delta_H^2 \tag{7}$$

where δ_d, δ_P and δ_H are the dispersion, polar and hydrogen-bonding components, respectively, of the overall solubility parameter δ_o. Barton (102) has published an extensive compilation of single and three-dimensional solubility-parameter values for most organic liquids.

The effective solublity parameter δ_m of a solvent mixture can be calculated using Hildebrand's mixing rule:

$$\delta_m = \sum_i \phi_i \delta_i \tag{8}$$

where ϕ_i and δ_i are the volume fraction and the solubility parameter, respectively, of component i in the mixture.

For nonvolatile solutes such as polymers, it is not possible to determine solubility-parameter values directly using the above-mentioned methods, as is done for liquids. A solute-solubility parameter can be assumed to have exactly the same value as a solvent-solubility parameter in the ideal case in which the solute and solvent mix in all proportions without enthalpy or volume change and without specific chemical interactions (102). More generally and practically, a variety of approaches is used, common between them being the following two:

(1) Intrinsic viscosity. The intrinsic viscosity of the solute is measured in a series of solvents, and the value of the solute-solubility parameter is taken as equal to that of the solvent in which the solute-intrinsic viscosity has a maximum value.

(2) Polymer swelling. The swelling of a slightly cross-linked analog of the polymer of interest in a series of solvents is studied, and the polymer is assigned the δ value of the liquid which gives the maximum swelling coefficient.

This last method is simple and convenient experimentally, but suffers from two serious drawbacks:

(i) Because of the use of specific solvents in the swelling measurements, one cannot avoid steps or breaks in the solubility-parameter continuum.

(ii) As the Flory-Rehner equation for swelling of cross-linked polymers indicates (104), the degree of polymer swelling depends not only on the solubilty parameter of the solvent but also on its molar volume. And again, because of the use of specific solvents in the swelling measurements, breaks cannot be avoided in the molar-volume continuum.

These two disadvantages of the regular polymer-swelling method result in significant scatter in the experimental data, so that solubility-parameter values for nonvolatile solutes cannot be determined with any accuracy.

Using the same polymer-swelling principle for the determination of solubility parameters, Lawson et al. (105) developed the so-called "Solubility-Parameter Spectroscopy", which eliminates effectively the disadvantages of the regular polymer-swelling method. In this method, six specific solvents (1,3 perfluorodimethylcyclohexane, 2-methylpentane, cyclohexane, cyclohexanone, 2-hydroxyethyl methacrylate or hema, and water), carefully selected to satisfy a number of criteria (103), are used to prepare five overlapping solvent systems and seventy-one solvent pairs covering the range of solubility-parameter values from 5.8 to 23.2 Hb at a step of 0.25 Hb per pair. The molar volumes of the solvent pairs change in a regular fashion from high molar volumes at low δ values to low molar volumes at high δ values. Because one of the two solvents in each of the five solvent systems is the same as one of the two solvents in the preceding system, steps or breaks in both the molar-volume and the solubility-parameter continuua are avoided. The making of this so-called "Mark III solvent system" is depicted in Figure 11.

The solubility-parameter spectra of three polymers (fluorosilicone rubber, polyurethane and a styrene-butadiene copolymer) obtained by the polymer-swelling method using the above solvent system (103) are depicted in Figures 12, 13 and 14, respectively. It is clear from these figures that experimental scattering in the swelling data is completely

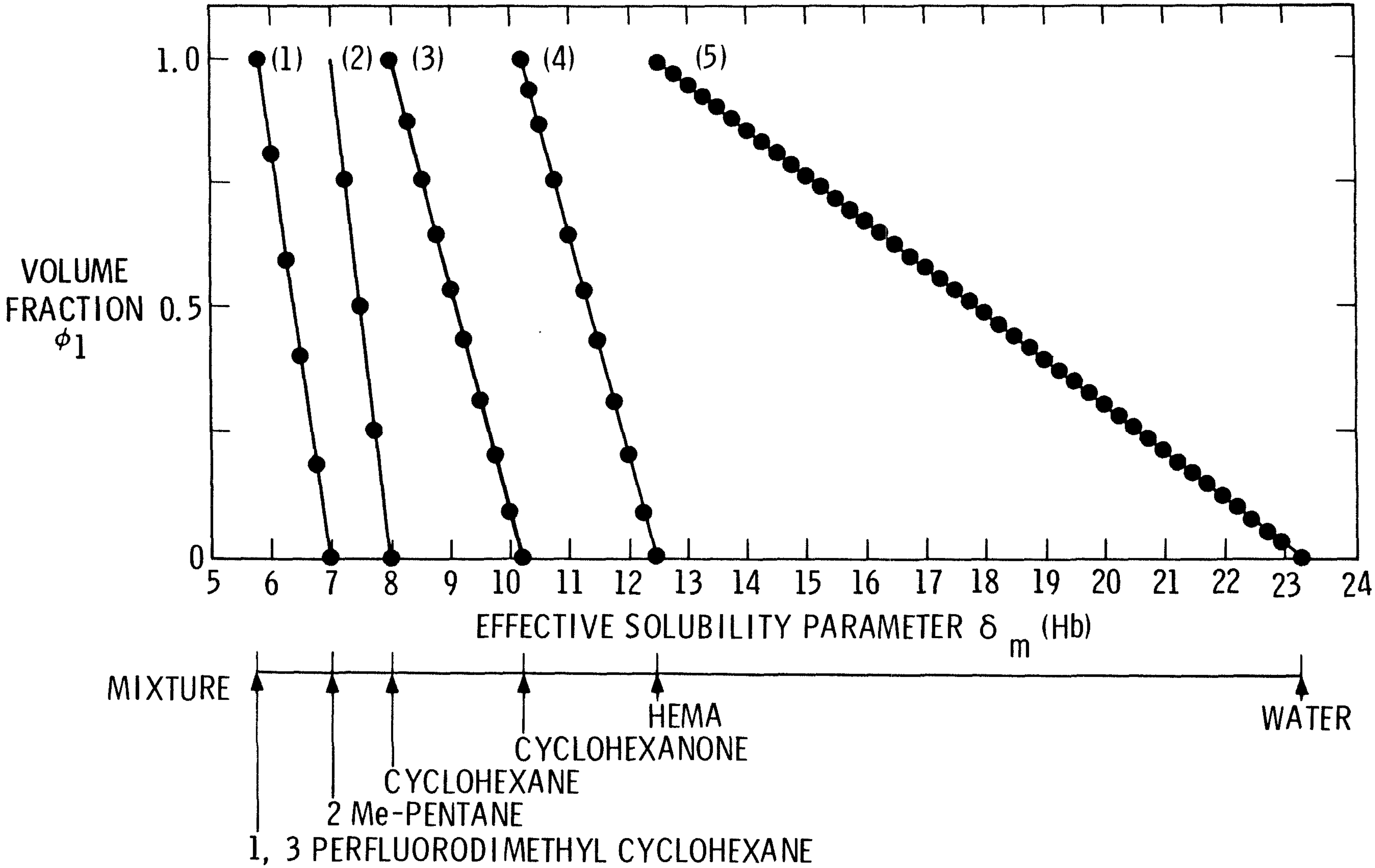

Figure 11. The Mark-III solvent system for Solubility-Parameter Spectroscopy.

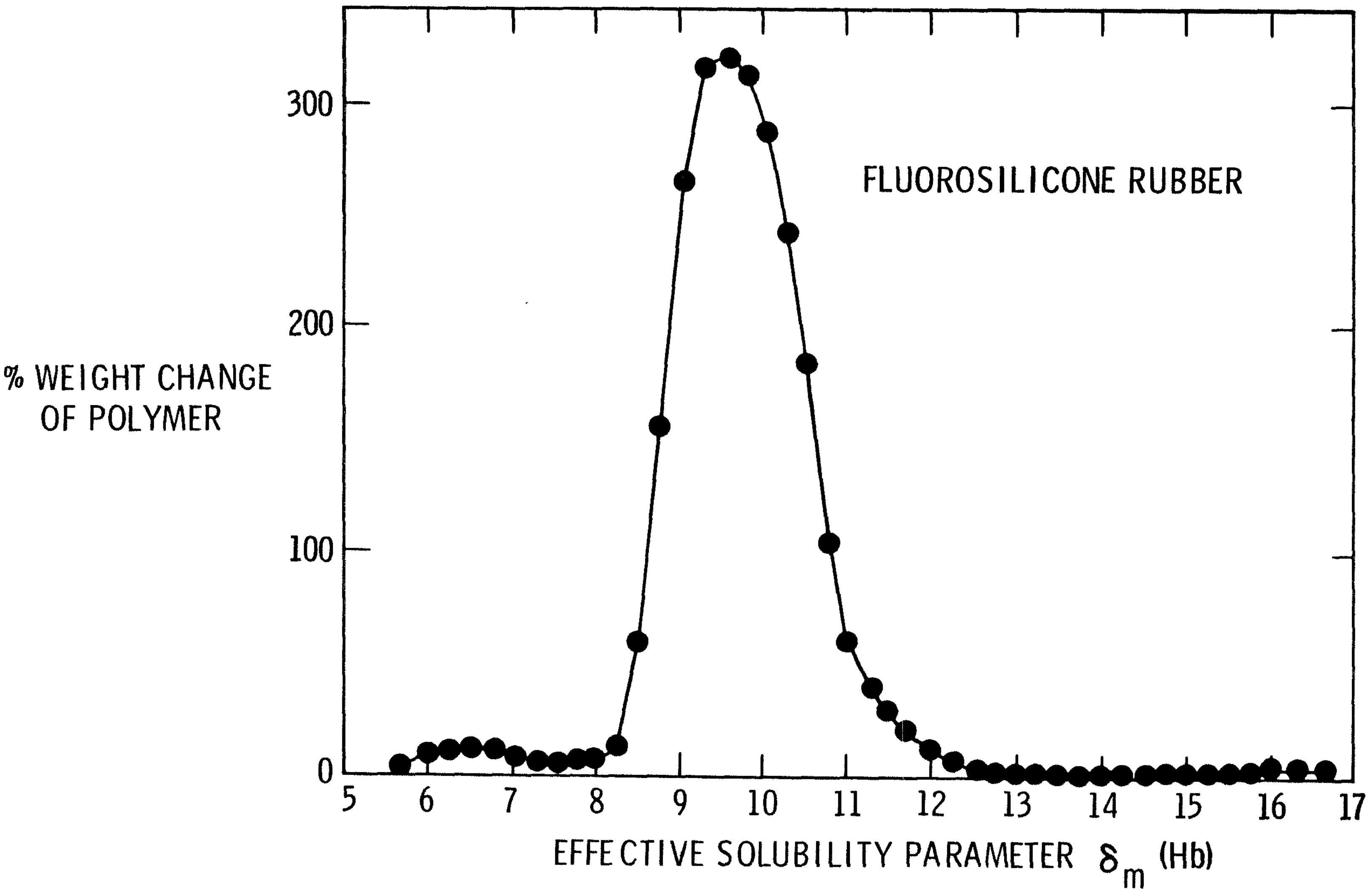

Figure 12. The solubility-parameter spectrum of a fluorosilicone rubber.

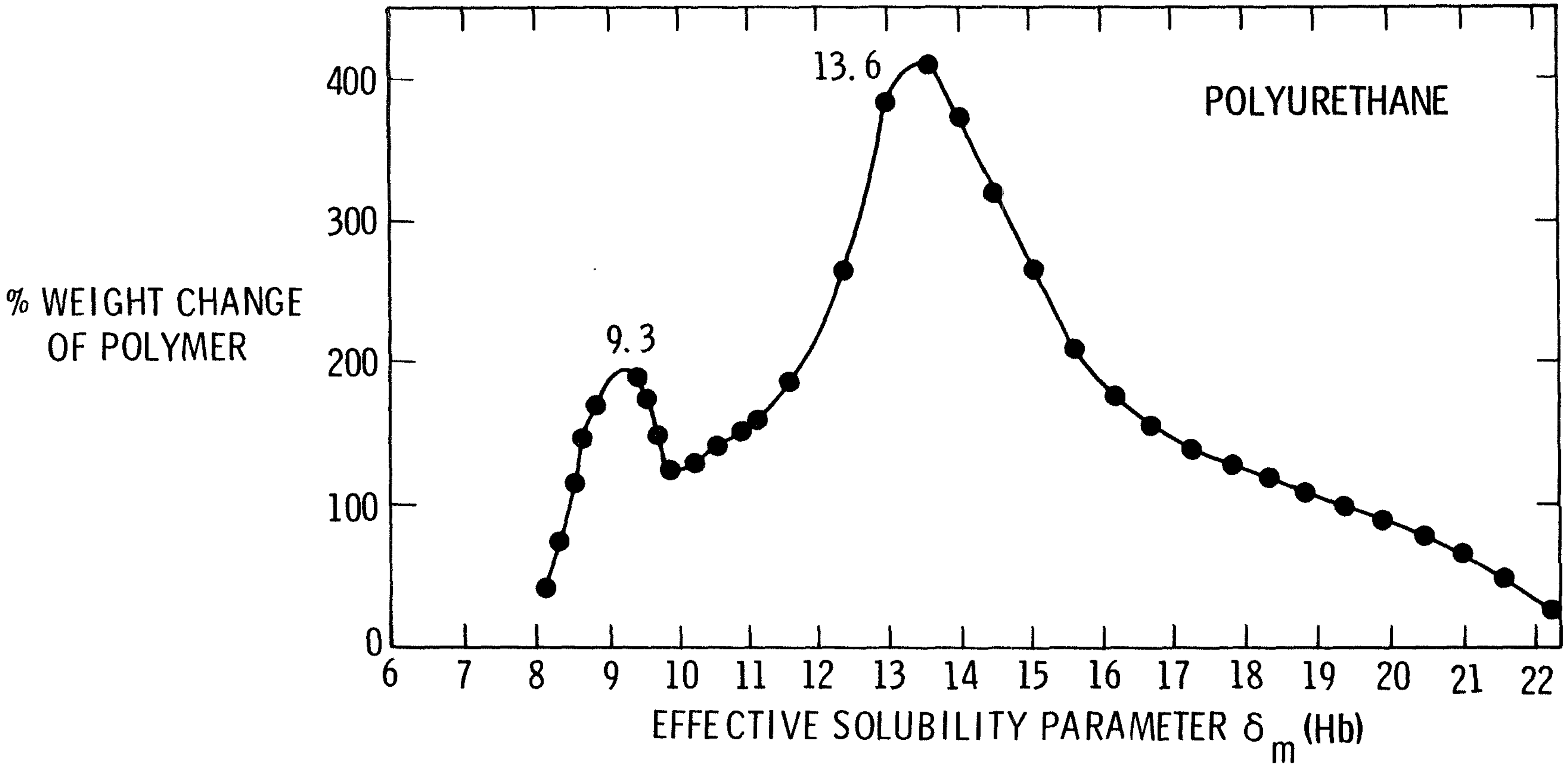

Figure 13. The solubility-parameter spectrum of a polyurethane polymer.

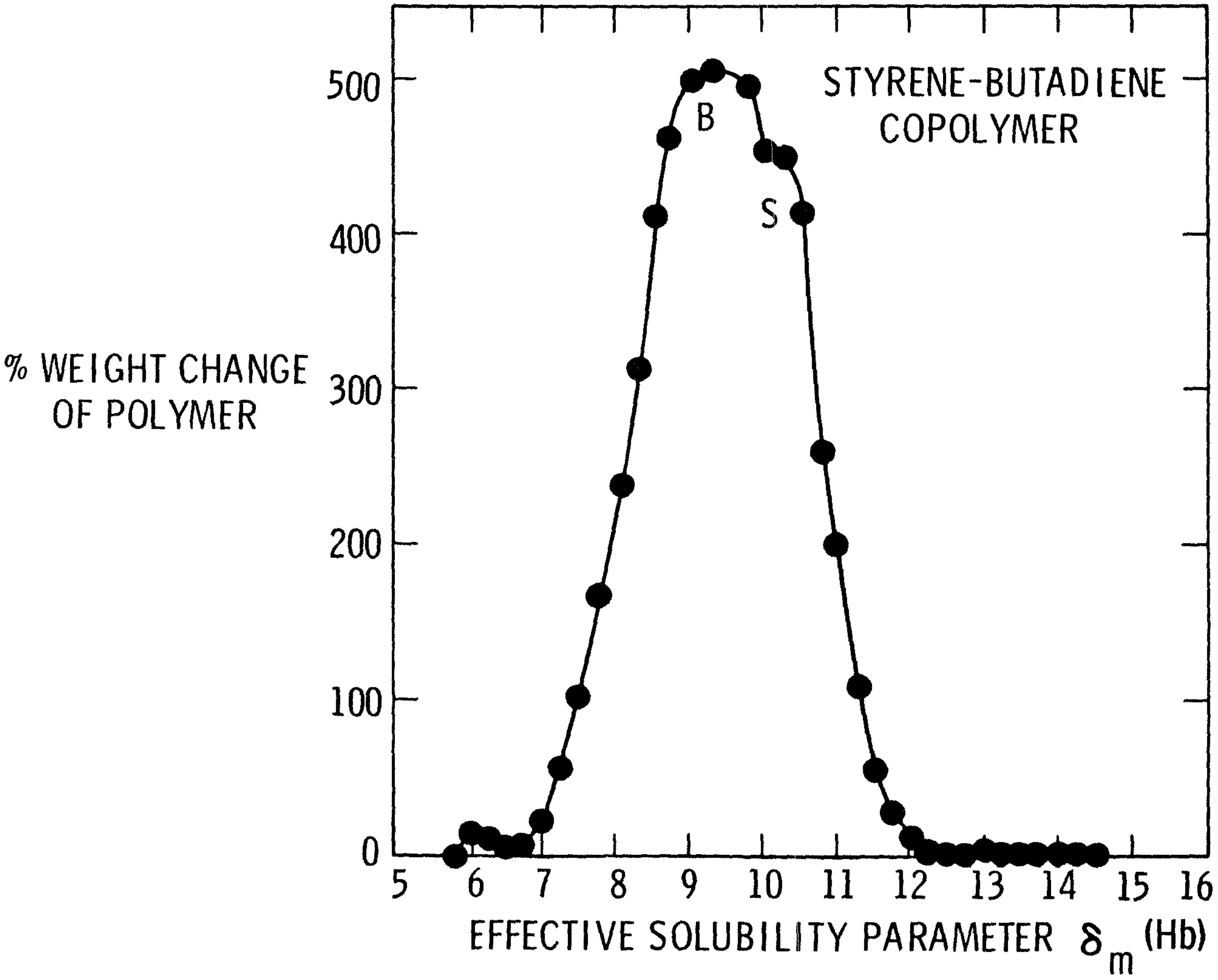

Figure 14. The solubility-parameter spectrum of a styrene-butadiene copolymer.

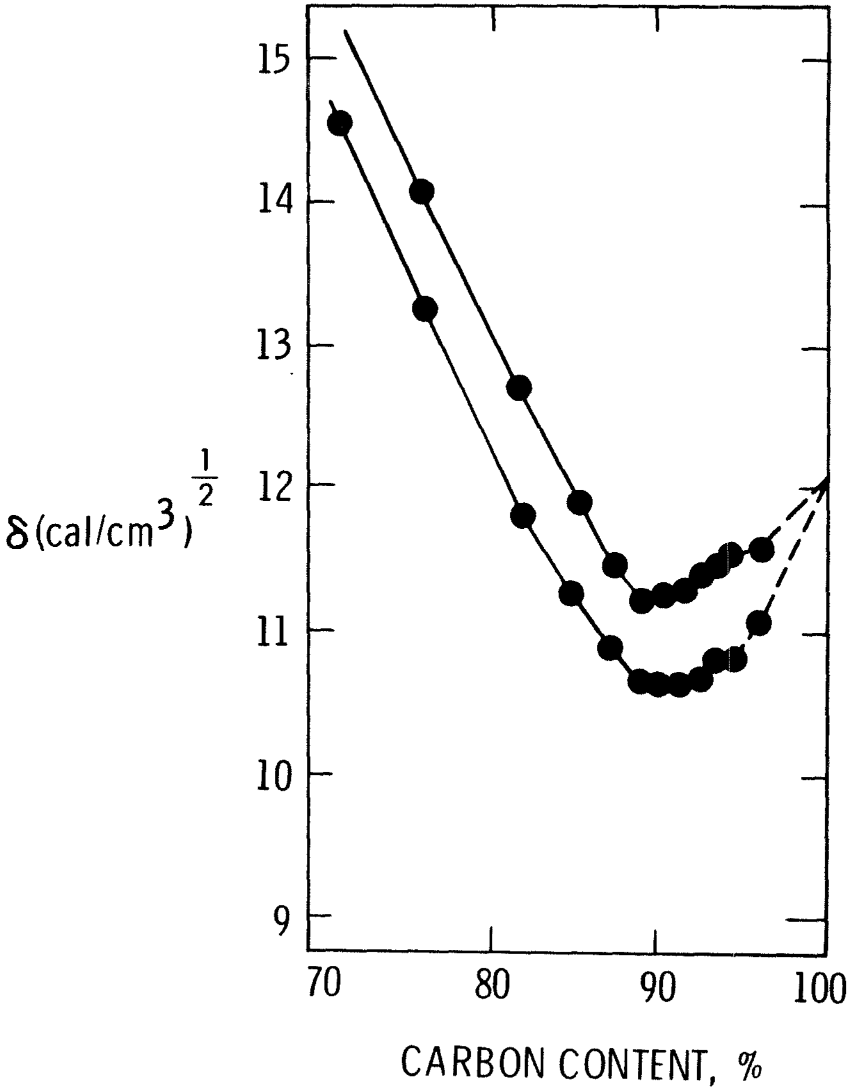

Figure 15. The solubility parameter of coal as a function of its rank.

eliminated in the Solubility-Parameter Spectroscopy, thus enabling the solubility parameter to be determined accurately. It should be noted also that the method is a spectroscopic method in the true sense of the word, because one can develop a library of single solubility-parameter values for known monomers and use it for identifying specific peaks on the solubility-parameter spectra of unknown polymers like, for example, the so-called soft and hard monomeric blocks in the polyurethane molecule (see Figure 13).

6.3 Solubility parameter of coal

6.3.1 Introduction

Cohesive energy densities and solubility-parameter values for coals and related materials have been calculated by van Krevelen (106) using a group-contribution method first proposed by Small (107). The results of these calculations are depicted in Figure 15 as upper and lower bounds for the (single) solubility parameter of coal as a function of its rank (carbon content). As can be seen from this figure, the solubility parameter of coal shows a distinct minimum at about 88.5% carbon content.

If a solubility-parameter value is to be assigned experimentally to a coal sample by the polymer-swelling method, then it must be established that a cross-linked system exists in coal and that the theory of swelling is applicable. Physical methods of analysis including NMR spectra, hardness, creep properties and dilation and the close correlation between the behavior of coal and a system that has undergone trifunctional polycondensation (106) have demonstrated that, indeed, coal has properties normally associated with a cross-linked system (108).

Sanada and Honda (109) studied the equilibrium swelling of coal in various solvents. For brown and bituminous coals, the equilibrium degree of swelling was found to increase with increasing solubility parameter of the solvent, reacting a maximum at about $\delta = 10.8$ and then decreasing with further increase of δ. Strongly coking coal and anthracite did not swell at all in the solvents tested. In agreement with van Krevelen's prediction, they found that cohesive forces in coals show a distinct minimum at about 85 to 87% carbon content.

Kirov et al. (108) compared coal-solubility parameters evaluated both indirectly, by van Krevelen's method, and experimentally, either by the polymer-swelling method or from solubility measurements. Reasonable agreement was found between the δ values for a coal of 88% carbon content; but with decrease in rank, the values obtained by van Krevelen's methods increased, whereas the values from the experimental methods remained approximately constant.

Finally, Yen et al. (110) obtained solubility-parameter spectra for raw and extracted coals employing Lawson's method (105) and used them to demonstrate the feasibility of a novel coal-conversion process, where low-molecular-weight species can be released from the relatively H-poor portion of the coal.

6.3.2 Solubility-parameter spectroscopy on raw and chlorinated PSOC 190A coal

Solubility-parameter spectra of raw and chlorinated PSOC 190A coal samples were obtained using Lawson's version of the polymer-swelling method. The experimental procedure involved suspending approximately one gram of coal, 50 x 100 mesh size, in 10 ml of each of the seventy-one solvent pairs and allowing the system to reach equilibrium swelling for five days. The weight increase of the coal because of swelling was then determined and plotted against the solubility parameter of the solvent pair.

The solubility-parameter spectrum of the raw PSOC 190A coal was obtained this way and is depicted in Figure 16. The spectrum shows two distinct peaks, one at $\delta \sim 10.7$ Hb and one at $\delta \sim 15.2$ Hb. Using van Krevelen's calculations (Figure 15), one can identify the first peak (10.7) with a coal material very rich in carbon (∼90% carbon content) and the second peak (15.2) with a coal material more or less representative of the PSOC 190A coal as a whole (∼70% carbon content).

The spectrum of the raw PSOC 190A coal can be utilized to explain the results of the experimental study on the extractive action of various solvents and solvent mixtures on this coal during chlorinolysis (Section 5.2.3). Those results indicated that, while CCl_4 ($\delta = 8.6$), H_2O ($\delta = 23.2$) and a 50/50-by-volume MeOH-H_2O mixture ($\delta_m = 18.9$) show very little extractive action on coal during chlorination, methanol ($\delta = 14.5$) displays moderate extractive action and a 50/50-by-volume MeOH-CCl_4 mixture ($\delta_m = 11.5$) displays a very significant extractive action under similar chlorination conditions.

In the solubility-parameter spectrum, CCl_4 and H_2O are remote from the two peaks and they show very low swelling. Therefore, they are

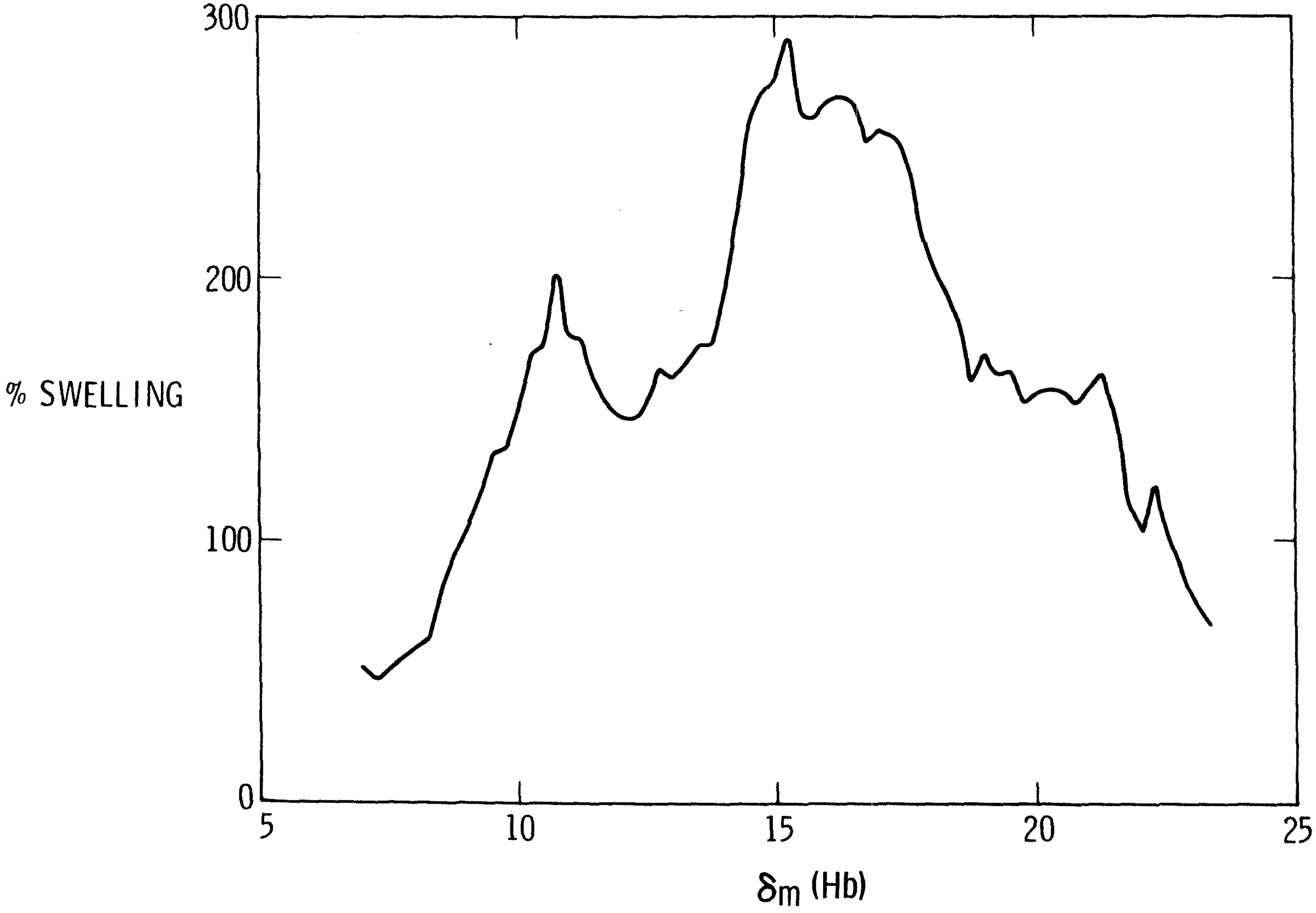

Figure 16. The solubility-parameter spectrum of raw PSOC 190A coal.

expected to display a low degree of coal-solvent interaction and this is, indeed, the case in the very low extraction yields obtained when coal was chlorinated in these two solvents.

For the MeOH-H_2O and MeOH-CCl_4 mixtures, though, the solubility-parameter spectrum gives approximately the same degree of swelling (160 - 170%). Therefore, one should expect the same extraction characteristics towards coal by these two solvent systems during chlorination. But this result is not the case because, as discussed already, MeOH-H_2O yields almost no extract in coal chlorination, and MeOH-CCl_4 yields a very significant amount of extract.

The apparent failure of the solubility-parameter approach can be overcome if one assumes that *the two peaks on the solubility-parameter spectrum of the raw coal represent two different mechanisms of coal-solvent interaction.* The first peak ($\delta \sim 10.7$) corresponds to a coal constituent (either petrographic or chemical, see Section 6.4) for which the dominant interaction path with the solvent is extraction, that is, dissolution prevails over swelling. The second peak ($\delta \sim 15.2$) corresponds to a coal constituent for which swelling, prevailing over dissolution, is the dominant solvent-interaction path. These assumptions are totally supported by the results of the chlorinolysis experiment with pure methanol. Methanol, with a solubility parameter very close to the second peak ($\simeq$ swelling path), shows a very high degree of coal swelling ($\sim$260%), but the extraction yield under chlorinolysis conditions is substantially less than the extraction yield for the CCl_4-MeOH mixture (Table 13).

For comparison purposes, the solubility-parameter spectrum of a chlorinated* PSOC 190A coal sample, 50 x 100 mesh size, was also obtained and is depicted in Figure 17. The composite picture for spectra of both the raw and the chlorinated coal is depicted in Figure 18. Reference to Figure 18 shows two characteristic differences between the spectra of the raw and the chlorinated coal:

(i) The two distinct peaks present on the spectrum of the raw coal have been more or less washed out on the spectrum of the chlorinated coal so that for the chlorinated coal there exists a wider range of solubility-parameter values (10 - 20 Hb) for solvents showing approximately the same degree of swelling (∿200%).

(ii) For the chlorinated coal, the dissolution part of the spectrum has increased and the swelling part has decreased when compared with the corresponding parts on the spectrum of the raw coal.

The two characteristic differences between the spectra of the raw and the chlorinated coal give another good indication of the validity of the assumption made on page 119, because they demonstrate nicely two well-known facts in the literature of chlorinated coal (37), namely, that chlorinated coal is much more soluble in a given set of solvents than raw coal (the dissolution part of the spectrum increases) and that chlorinated coal is more condensed than raw coal in terms of the number

---

*Chlorinated in carbon tetrachloride at room temperature. Weight increase because of chlorination: 39.6%.

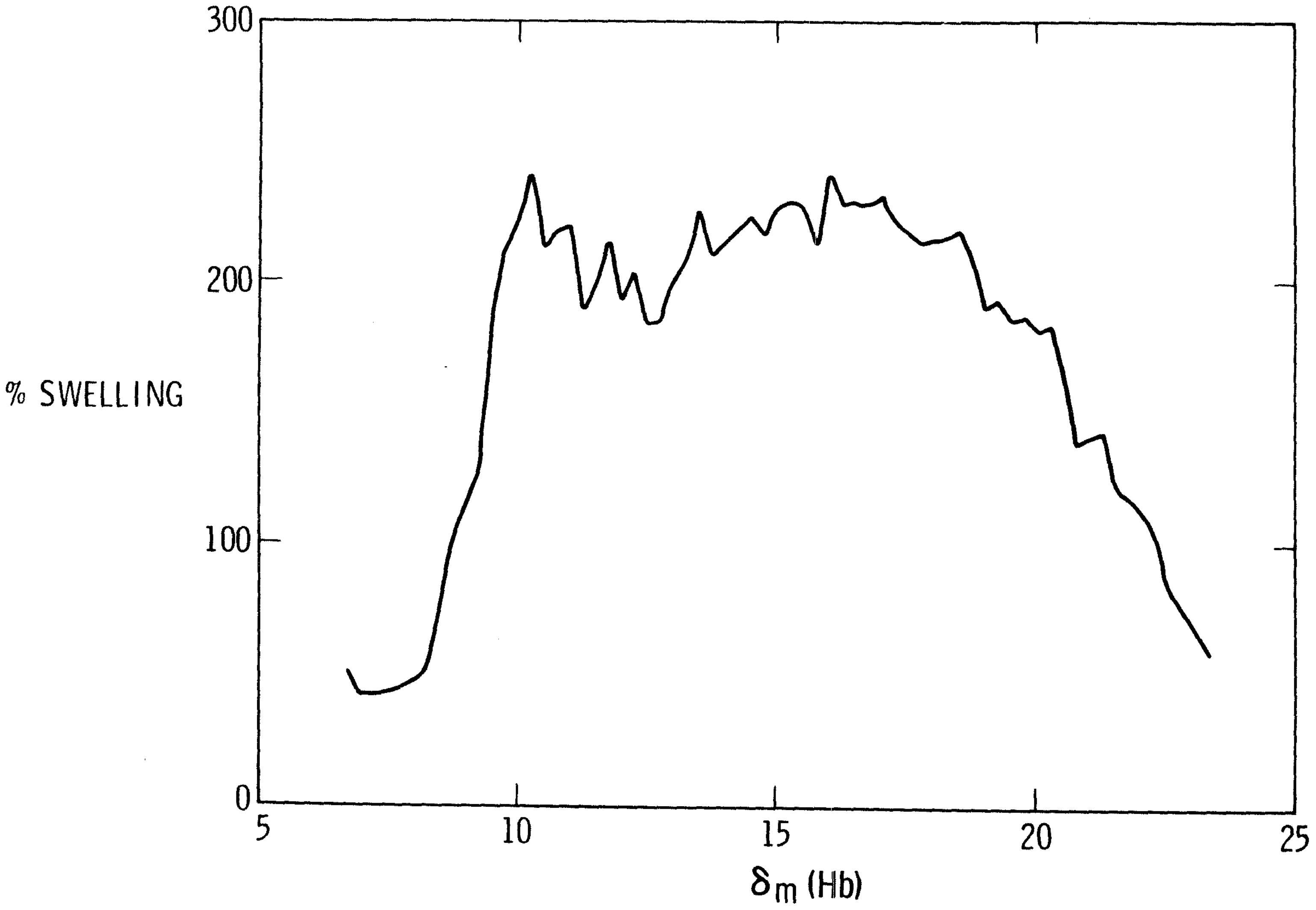

Figure 17. The solubility-parameter spectrum of a chlorinated PSOC 190A coal sample.

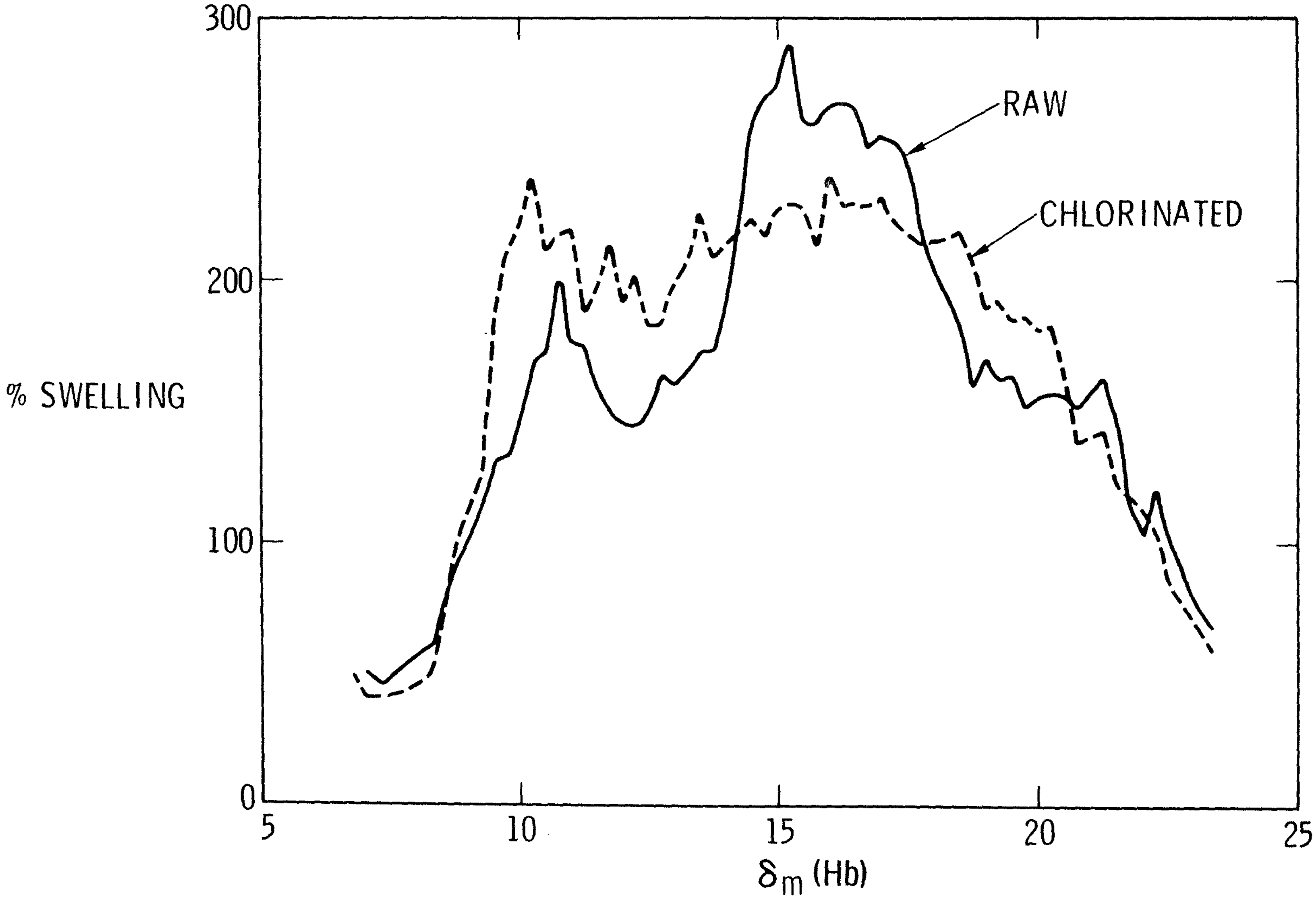

Figure 18. The solubility-parameter spectra of raw and chlorinated PSOC 190A coal.

of cross-linkages between molecular chains per unit volume (the swelling part of the spectrum decreases).

6.4 Discussion

The discussion in Section 6.3.2 suggests that solubility-parameter spectroscopy of coal may be a valuable tool for further studies in the following areas:

(1) Coal characterization. Determination of single solubility-parameter values for model constituents of the coal matrix (mainly petrographic, like vitrinite or fusinite (110) but also chemical, like anthracene) will eventually lead to identification of the peaks on raw-coal spectra with specific coal materials and will provide a better understanding of the coal-solvent interactions. Lawson's current work on obtaining the solubility parameter for pure vitrinite (111) can be extended to other coal macerals and bears the implication that the types of coal-solvent interactions (swelling, dissolution, etc.) are determined by the various petrographic entities in the coal rather than by its chemical structure.

(2) Coal treatment. High-resolution solubility-parameter spectroscopy can be used to obtain additional information about the history of any coal treatment, like the chlorinolysis or the coal-pump process (112). Determination and analysis of the solubility-parameter spectra of the coal, both raw and processed, is important as a measure of possible changes in the

petrography and the chemical structure that occur due to various treatments.

(3) Coal processing. The solubility-parameter spectrum can also be utilized as an additional screening tool for solvent selection in any coal beneficiation process that uses a solvent (chlorinolysis, extraction, liquefaction, etc.). Solvents with solubility parameters close to the peak values on the spectrum will cause maximum swelling or maximum dissolution of the coal material and this condition will have a direct effect on the efficiency of the beneficiation process.

Maximum swelling may increase the desulfurization efficiency of chlorinolysis by providing an alternative path for the reactant (chlorine) to reach the reactive sites of the internal surface of the coal. These sites would otherwise be very difficult or impossible to reach through the network of micropores because of the severe pore blocking occurring during coal chlorination (Section 3.3). The alternative path involves transfer of the reactant with the solvent through the swollen coal material, that is, through the solid coal structure. Of course, maximum swelling can work also in exactly the opposite way from the one just mentioned, by further closing down the micropores because of excessive pore-wall expansion, thus further reducing the mass-transfer of chlorine to the reactive sites of the coal surface. But, either way, swelling will have significant effect on the chlorinolysis efficiency.

Maximum dissolution, on the other hand, is of great importance in extraction and liquefaction processes. Angelovich et al. (113) have stressed the importance of the (nonpolar) solubility parameter of the solvent in determining the liquefaction yield in the liquid-phase catalytic hydrogenation of coal. Fong and Pichaichanarong (101) obtained maximum yields in methanol-toluene-supercritical extraction of the PSOC 190A coal when they used mixtures of the two solvents having effective solubility parameters close to the peak values on the spectrum of Figure 16.

Chapter 7

SUMMARY AND RECOMMENDATIONS

7.1 Summary and conclusions

7.1.1 Chlorination of coal

(1) The slurry-phase chlorination of coal in carbon tetrachloride at $25^{\circ}C$ was examined. Chemical reaction was found to be the rate-determining step for coal particles less than about 150 μ in diameter. For larger particle sizes, a transition from chemical to intraparticle-mass-transfer control was observed.

(2) The chlorine taken up by the coal is either chemically bound in the organostructure, physically adsorbed in the pores, or "dissolved" in molecular configuration in the solid matrix. The amount of the physically adsorbed or dissolved chlorine in chlorinated coal is believed to be small. The total chlorine uptake, Q, in the PSOC 190 coal for the -400 mesh particle size (where chemical rates prevail) was very satisfactorily described by an Elovitch-type equation:

$$\frac{dQ}{dt} = A\, e^{-BQ}$$

with

$$A \simeq 3.7 \, \frac{\text{g of chlorine}}{\text{(g of raw dry coal)(min)}}$$

$$B \simeq 30.4 \, \frac{\text{g of raw dry coal}}{\text{g of chlorine}}$$

The equilibrium value of chlorine uptake for the 25^{o}C reaction in carbon tetrachloride was determined to be about $0.34 \frac{\text{g of chlorine}}{\text{g of raw(dry)PSOC 190 coal}}$.

(3) The chlorination reaction results in extensive fracturing and size reduction of the coal particles and also in significant loss of porosity as revealed by a steep decrease in the nitrogen-surface area of the coal after chlorination. After one hour of chlorination of the PSOC 190 coal in methyl chloroform at 60^{o}C, almost 89% of its original surface area $\left(70.6 \frac{m^2}{g}\right)$ became inaccessible for nitrogen adsorption. The loss of porosity is probably a result of swelling at the pore walls because of the considerable chlorine uptake in the coal matrix and decreases with increasing reaction temperature. The effect is independent of the amount of chlorine taken up by the coal. Chlorine uptake for the PSOC 190 coal was higher $\left(0.344 \frac{\text{g chlorine}}{\text{g coal}}\right)$ in the chlorination in carbon tetrachloride at 60^{o}C than at 30^{o}C $\left(0.334 \frac{\text{g chlorine}}{\text{g coal}}\right)$, but the resulting surface area of the chlorinated coal at 60^{o}C $\left(15.8 \frac{m^2}{g}\right)$ was more than twice that at 30^{o}C $\left(7.0 \frac{m^2}{g}\right)$. The reduced blocking at higher temperatures can be explained by the significantly increased intrinsic reaction rate at higher temperatures. Chlorine is readily consumed at the entrance of the larger pores before diffusing into the apertures and causing extensive blocking. In contrast, at low temperatures, chlorine has enough time to diffuse

into the smaller pores before being completely reacted, so that a more uniform and severe blocking of the pores occurs. Surface areas obtained using carbon dioxide as the adsorbate show different trends in slurry-phase chlorination of coal from those obtained by nitrogen adsorption. A sample of the PSOC 190 coal chlorinated in carbon tetrachloride at 60°C showed a 75.9% decrease in available surface area using nitrogen adsorption and a 5.5% increase using carbon-dioxide adsorption. This result seems to support the possibility that CO_2 adsorption in coal includes direct permeation through the coal matrix, and, of course, this adsorption component is not affected by pore blocking.

7.1.2 Model-reaction studies

(1) The chlorination of iron pyrite in an organic solvent is a mass-transfer-limited reaction because of the very small solubility of the reaction products ($FeCl_3$, S_2Cl_2) in the organic phase. The inability of the organic solvent to dissolve appreciable amounts of $FeCl_3$ results in the fast formation of a $FeCl_3$ layer on the pyrite surface which prohibits the exposure of fresh pyrite for further chlorination. The situation is improved considerably by the use of solvents like methanol or water in which the chlorination products are readily soluble. Under the same reaction conditions (60°C, 2 hours), the extent of pyrite chlorination was only 1.6% in carbon tetrachloride but it was 35% in a 50/50 volume mixture of methanol and carbon tetrachloride.

(2) The aqueous chlorination of iron pyrite is a thermodynamically favorable, very exothermic ($\Delta H^o = -390 \frac{\text{Kcal}}{\text{mole}}$) reaction with a low activation energy and with liquid diffusion of chlorine as the rate-controlling step. The reaction can be described by first-order kinetics:

$$\frac{dX}{dt} = k[Cl_2]$$

where

X = pyrite conversion (%).
t = reaction time, min.
k = rate constant, min^{-1}.
$[Cl_2]$ = concentration of molecular chlorine in the aqueous solution, $\frac{\text{cm}^3 \text{ chlorine}}{\text{cm}^3 \text{ water}}$.

Reduction of the experimental data gave the following Arrhenius expression for k:

$$\ln k = 12.97 - \frac{7,384}{RT},$$

$$T = \text{reaction temperature, } {}^oK.$$

(3) Sulfones are the final products of chlorinolysis ($T < 100^oC$) for the more stable organic sulfur compounds (dibenzothiophene, phenyl sulfide). They can be obtained in high yields through oxidation at higher-than-room temperatures in the aqueous chlorination of the corresponding sulfides. Slurry-phase chlorination of dibenzothiophene in water at 70°C gave the corresponding sulfone as the only product in very high yield (∿94% of the theoretical).

Chlorination of the aromatic nucleus was not observed in aqueous chlorinolysis of either dibenzothiophene or phenyl sulfide at temperatures below 100°C but it was significant for both compounds in carbon-tetrachloride chlorination even at room temperature.

(4) More severe reaction conditions have to be applied to carry the oxidation of the organic sulfur beyond the sulfone state, to breaking of carbon-sulfur bonds, and eventually to complete desulfurization. Of special interest among these conditions are those of hydrolysis reactions of the oxidized sulfur at temperatures higher than 200°C. An alternative desulfurization path also exists which involves rupture of carbon-sulfur bonds at the state of the sulfide rather than of the sulfone and leads to the same final chlorinolysis products. Complete desulfurization under uncatalyzed chlorinolysis conditions was demonstrated only for simple aliphatic sulfides. Aqueous chlorination of tert-butyl sulfide at 60°C and up to a point of slight chlorine excess over the stoichiometric requirement for complete desulfurization resulted in 60% conversion of the sulfide to water-soluble sulfate ions.

7.1.3 Coal desulfurization by chlorinolysis

(1) Pyritic sulfur can be easily and almost quantitatively removed from coal under mild chlorinolysis conditions. Aqueous chlorination, for example, of the PSOC 276 coal, a high (2.60%) pyritic-sulfur coal, for two hours at 30°C resulted in 98% removal of pyritic sulfur.

(2) Under the same reaction conditions (60°C, 2 hours), aqueous chlorination of the PSOC 190 coal gave significant ($\sim$28%) organic-sulfur reduction while PSOC 276 coal showed no organic-sulfur reduction at all in spite of comparable pyritic-sulfur reductions and chlorine uptakes for the two coals. This result is probably due to a higher portion of organic sulfur existing in stable thiophenic and aryl-sulfide forms in the PSOC 276 coal than in the PSOC 190 coal. It also suggests that there is an upper limit on the amount of organic sulfur that can be removed from coal under mild chlorinolysis conditions, namely, atmospheric pressure and temperatures less than 100°C.

(3) Under similar reaction conditions, aqueous coal chlorinolysis is superior (in terms of level of desulfurization) to the chlorination in an organic solvent followed by hydrolysis of the chlorinated coal, in agreement with the results of the model-reaction studies. Higher-than-room temperatures in aqueous chlorination are to be preferred because they favor increased sulfur removal from coal and also significantly reduced uptake of chlorine in the organic matrix. The increased sulfur removal is a result of higher desulfurization rates in iron-pyrite chlorination at higher temperatures (paragraph 7.1.2) and of higher organic-sulfur removal because of the temperature-promoted hydrolysis reactions.

7.1.4 Solvent effects in coal chlorinolysis

(1) The solvent-solubility parameter, defined as the positive square

root of the solvent's cohesive energy density, that is the potential energy per unit volume, can be used along with solubility-parameter spectra of raw coal (Figure 16, page 118) to predict possible swelling and extractive actions on coal during chlorinolysis. Matching of the solubility-parameter values for the solvent and certain peaks on the spectra will lead to either maximum swelling or maximum dissolution of coal in processing. Thus, the solubility parameter can serve as an additional screening tool for optimal selection of solvent systems for a given coal-beneficiation process.

(2) Methanol displays remarkable capabilities both in terms of selective sulfur extraction from coal and high liquefaction yields of coal material when combined with other solvents in certain beneficiation processes like chlorinolysis or supercritical extraction. Chlorination of the PSOC 190 coal in a 50/50 volume mixture of methanol and carbon tetrachloride for two hours at 50°C resulted in 36% of the coal material being dissolved into the CCl_4-MeOH phase (compared with ∿5% in the absence of the chlorination reaction) and 1.42 times more sulfur in excess of the extraction yield passing into this phase than remaining in the coal matrix. The selectivity of sulfur extraction was even higher (3.98 compared with 1.42) when the same coal was chlorinated in methanol alone under similar reaction conditions.

7.2 Recommendations

The research work analyzed in Chapters 2 - 6 covered the basic topics in the coal-chlorinolysis area. Various aspects of this research can be explored further and studies of new specialized topics can be initiated. The following suggestions illustrate possible research areas for future work in the coal-chlorinolysis project (114):

(1) One can study the effect of the combined attack of chlorine with other gaseous oxidizing agents, like nitrogen dioxide, on the extent of coal-chlorination and sulfur removal. In particular, the possibly large perturbation effects that the presence of trace quantities of oxygen in the gaseous stream may generate (115) should be examined. On the other hand, chlorinating agents like SO_2Cl_2 or liquid chlorine may be considered as well.

(2) Similarly, one can study the effect of catalysts (especially iron and aluminum compounds) in chlorine-promoted desulfurization of coal, as well as the role of certain additives, such as peroxyacids (116), present in low concentrations in the liquid phase of a coal-water slurry.

(3) The effect of certain physicochemical parameters of the solvent system, such as interfacial tension on coal or volume expansivities $\left(\frac{\partial V}{\partial T}\right)_P$ and $\left(\frac{\partial V}{\partial P}\right)_T$, on the desulfurization efficiency of chlorinolysis should be examined further (26). Mixed solvents may provide a more complete set of character-

istics needed for process optimization. The delaminating action of methanol on the coal matrix (Section 5.2.3) can be possibly extended to other similar solvents, like acetone. Pretreatment of the coal with such solvents may yield a material more susceptible to the chlorination-desulfurization attack (117).

(4) It would be interesting to obtain kinetic curves on chlorine uptake for various coal-particle sizes (Section 2.3.2) at chlorination temperatures higher than 25°C to determine whether a change in reaction mechanism (from chemical to mass-transfer control), like the one observed by Ball and Mitchell (38), takes place at these higher temperatures.

(5) Chlorinolysis pressures higher than atmospheric may prove beneficial both in maintaining the (solvent-assisted) structural integrity of the coal matrix, leading to improved mass-transfer rates (20,26,27), and in promoting desulfurization reactions beyond the sulfone stage (Section 4.2.3).

(6) One can also determine directly the overall rate of penetration of the reacting species (Cl_2) in the coal particle. The mechanism of this penetration involves pore diffusion or permeation through the solid coal matrix or a combination of the two. The use of the SEM/EDAX microprobe is particularly suited for such a study. One can subject a chunk of coal on the order of centimeters to chlorinolysis conditions, cut

suitable cross-sections and analyze for chlorine-concentration profiles. This work should also prove useful for determining the chlorine effect on iron and sulfur compounds at the same time because many elements can be analyzed at once. Alternatively, normal-size coal particles (100 x 200 mesh) can be suspended in a matrix which is then cut to expose some particle cross-sections. Because the larger chunks may exhibit different swelling tendencies with respect to chlorine than the particles, the latter method may be more representative of the true situation (114,118).

(7) One can study the chlorine types in chlorinated-coal extracts by carbon 13 - NMR and other analytical techniques. Presence of aryl chlorides would indicate additional difficulties in the dechlorination step. The aliphatic/aromatic chlorine ratio is therefore an important parameter which should be considered together with desulfurization in optimizing the chlorinolysis conditions.

(8) Finally, chlorinolysis of sulfur compounds under controlled conditions may provide additional information on their relative susceptibility to chlorine attack and on the role of certain reaction parameters, like temperature, solvent and catalyst present, in enhancing the yield of desulfurized products. These controlled conditions may include model-reaction studies (Chapter 4), chlorinolysis of solutions of SRC I and SRC II coal products in tetrahydrofuran, or even

desulfurization of fuel oil in emulsion-phase chlorination. Sulfur compounds of various organic-sulfur forms (R—S—R', R—S—Ar, Ar—S—Ar', R—S—H, Ar—S—H, R—S—S—R', thiophenes, etc.) and at various sulfur-oxidation states (, 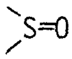, 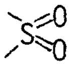, 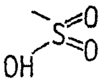, etc.) should be considered here.

References

1. Balzhiser, R. E., Chemical Engineering 84, 72 (1977).
2. Van Krevelen, D. W., "Coal", Elsevier Publishing Co., New York (1961).
3. Tabler, S. K., Journal of the Air Pollution Control Association 29, 803 (1979).
4. Attar, A., "The Chemistry of Selective Oxidation of Sulfur Compounds and Its Relation to Fuel Desulfurization", PhD Thesis, California Institute of Technology, 1977.
5. Deurbruck, A. W., "Sulfur Reduction Potential of the Coals of the United States", U.S. Bureau of Mines RI7633, Washington, D.C., 1972.
6. Attar, A. and Corcoran, W. H., Ind. Eng. Chem. Prod. Res. Dev. 16, 168 (1977).
7. Bootent, D. A. D. and Phillips, C. R., Fuel 55, 318 (1976).
8. Kalvinskas, J. J., et al., "Coal Desulfurization by Low Temperature Chlorinolysis", Jet Propulsion Laboratory, proposal prepared for the U.S. Bureau of Mines, December 1976.
9. Schmit, G. C. A. and Grates, B. C., AIChE J. 19, 417 (1976).
10. du Fresne, E. R., "Coal Cleaning versus Flue-Gas Desulfurization in Meeting New Proposed Air Pollution Standards", Assessment Report, Jet Propulsion Laboratory, May 1979.
11. Meyers, R. A., Hydrocarbon Process 54, 93 (1975).
12. Meyers, R. A., "Coal Desulfurization", Marcel Dekker Inc., New York (1977).

13. Stambaugh, E. P., et al., Hydrocarbon Process 54, 115 (1975).

14. McCandless, L. C. and Contos, G. V., "Current States on Chemical Coal Cleaning Process — An Overview", presented at EPA Symposium on "Coal Cleaning to Achieve Energy and Environmental Goals", Hollywood, Florida, September 11 - 15, 1979.

15. Guth, E. D., "Oxidative Coal Desulfurization Using Nitrogen Oxides — The KVB Process", EPA Symposium at Hollywood, Florida.

16. Teichman, D. P., "Desulfurization of Coal by Oxidation with Nitrogen Oxides", M.S. Thesis, California Institute of Technology, 1977.

17. Kralik, J. G., "The Selective Oxidation of Sulfur Compounds Found in Coal", Candidacy Report, California Institute of Technology, March 1978.

18. Hsu, G. C., et al., "Coal Desulfurization by Low Temperature Chlorinolysis", reprint from ACS Symposium Series No. 64, Coal Desulfurization, 1977.

19. Wheelock, T. D. (ed.), "Coal Desulfurization", ACS Symposium Series No. 64, 1977.

20. Corcoran, W. H., "Combined Mass Transfer and Chemical Reaction Rate Effects in Desulfurization of Coal in the Slurry State", research proposal submitted to the Jet Propulsion Laboratory, December 1977.

21. Hsu, G. C., et al., U.S. Patent 4,081,250, March 28, 1978.

22. Jet Propulsion Laboratory, "Coal Desulfurization by Low Temperature Chlorinolysis", progress report submitted to the U.S. Bureau of Mines, September 1977.

23. Kalvinskas, J. J. and Hsu, G. C., "JPL Coal Desulfurization Process by Low Temperature Chlorinolysis", presented at EPA Symposium on "Coal Cleaning to Achieve Energy and Environmental Goals", Hollywood, Florida, September 11-15, 1978.

24. Kalvinskas, J. J., et al., "Final Report for Phase II — Coal Desulfurization by Low Temperature Chlorinolysis", Jet Propulsion Laboratory Publication 80-15, January 1980.

25. Vasilakos, N. P., "Coal Desulfurization Processes", Candidacy Report, California Institute of Technology, March 1978.

26. Corcoran, W. H., "Physical and Chemical Rate Studies in the Use of Chlorine to Desulfurize Coal in the Slurry State", research proposal submitted to the Jet Propulsion Laboratory, January 1979.

27. Corcoran, W. H., "Desulfurization of Coal and the Effects of Solvents and Solvent Mixtures on Physical and Chemical Rates at Temperatures Less than 250°C and at Moderate Pressures", research proposal submitted to the Jet Propulsion Laboratory, March 1977.

28. Wang, J. K. and Corcoran, W. H., "Solvent Effects on Coal Chlorinolysis: A Study of Contact Angles and Interfacial Tensions of Organic Solvents on Coal", Chemical Engineering Laboratory report, California Institute of Technology, March 1978.

29. (i) McCulloch, A., et al., J. Soc. Chem. Ind. 48, 167T (1929).
    (ii) ibid. 49, 377T (1930).
    (iii) ibid. 51, 49T (1932).
    (iv) ibid. 51, 186T (1932).
    (v) ibid. 52, 47T (1933).

30. Beyers,E. and van Rooyen, D., J. S. African Chem. Inst. 4, 97 (1951).

31. Weiler, J. F., Fuel 14, 190 (1935).

32. Kung, F. E., Fuel 43, 225 (1964).

33. Boyk, S. and Hass, H. B., Ind. Eng. Chem. 38, 745 (1946).

34. (i) Pinchin, F. J., Fuel 37, 293 (1958).
    (ii) ibid. 38, 147 (1959).

35. Moschopedis, S. E., *et al.*, Fuel 42, 338 (1963).

36. Wielopolski, A., *et al.*, Bull. Acad. Polon. Sci. 13, 135 (1965).

37. (i) Macrae, J. C. and Oxtoby, R., Fuel 44, 395 (1965).
    (ii) ibid. 44, 409 (1965).
    (iii) Oxtoby, R., ibid. 45, 457 (1966).

38. Ball, D. R. and Mitchell, S. C., Fuel 57, 365 (1978).

39. Russ, J. C., in "Energy Dispersion X-Ray Analysis: X-Ray and Electron Probe Analysis", ASTM Special Technical Publication No. 485 (1971).

40. Marsh, H., *et al.*, Carbon 13, 103 (1975).

41. (i) Brunauer, S., Emmett, P. H. and Teller, E., J. Am. Chem. Soc. 60, 309 (1938).
    (ii) Emmett, P. H. (ed.), "Catalysis", Vol. 1 (Chapter 2), Reinhold Pub. Corp., New York (1954).

42. (i) Dubinin, M. M., Ind. Carbon and Graphite, 272 (1958).
    (ii) Dubinin, M. M., Chem. Rev. 60, 235 (1960).

43. Zwietering, P. and Van Krevelen, D. W., Fuel 33, 331 (1954).

44. Medeiros, D. J. and Petersen, E. E., Lawrence Berkeley Laboratory Rep. LBL-4439, University of California, Berkeley, 1975.

45. Gan, H., Nandi, S. P. and Walker, P. L., Fuel 51, 272 (1972).

46. Lamond, T. G. and Marsh, H., Carbon 1, 281 (1964).

47. Anderson, R. B., et al., J. Phys. Chem. 60, 1548 (1956).

48. Walker, P. L., Austin, L. G. and Nandi, S. P., in "Chemistry and Physics of Carbon", Vol. 2 (ed. P. L. Walker), Marcel Dekker, New York (1966), pp. 257-371.

49. (i) Kamishita, M., et al., Fuel 56, 444 (1977).
    (ii) Mahajan, O. P. and Walker, P. L., Fuel 58, 333 (1979).

50. Lahiri, A., et al., Fuel 35, 71 (1956).

51. Kini, K. A., Fuel 43, 173 (1964).

52. Nandi, S. P. and Walker, P. L., Fuel 43, 385 (1964).

53. Anderson, R. B., et al., Fuel 41, 559 (1962).

54. Walker, P. L. and Geller, I., Nature 178, 1001 (1956).

55. Metcalfe, J. E., et al., Fuel 42, 233 (1963).

56. (i) Nelson, F. M. and Eggertsen, F. T., Anal. Chem. 30, 1387 (1958).
    (ii) Masamune, S. and Smith, J. M., AIChE J. 10, 246 (1964).

57. Lopez-Gonzalez, J. de D., et al., J. Res. Nat. Bur. Stand. 55, 11 (1955).

58. Kralik, J. G., private communication.

59. Mellor, J. W., "A Comprehensive Treatise on Inorganic and Theoretical Chemistry", Vol. XIV, p. 227, Longmans, Green and Co., New York (1934).

60. (i) Brown, A. P., Proc. Amer. Phil. Soc. 33, 225 (1894).
    (ii) Brown, A. P., Chem. News 71, 120,130,144,155,171,179 (1895).
61. Crookes, W., Trans. Roy. Soc. (London) 163, 307 (1873).
62. Deville, H. S. C., Ann. Chim. Phys. 61, 309 (1861).
63. Rivot, L. E., *et al.*, Ann. Mines 4, 221 (1853).
64. Kangro, W. and Flügge, R., Zeit. Elektrochem. 35, 189 (1929). .
65. Ezdakov, V. I., Chem. Abstr. 35, 4555 (1941).
66. Luft, N. and Todhunter, K., British patent 749,078; CA. 50, 13707h (1956).
67. (i) Manyaka, R. T. and Iwasaki, I., Trans. Soc. Mining Eng., AIME, 254, 37 (1973).
    (ii) Hohn, H., *et al.*, Austrian patent 179,095; CA. 48, 9303e (1954).
    (iii) Ishikawa, T. and Yoshizawa, S., Kogyo Kagaku Zasshi 66, 342 (1963).
68. (i) McElroy, R. and Peters, E., Canadian patent 923,682, April 3, 1973.
    (ii) McElroy, R. and Peters, E., "Chlorination of Pyrites in Chlorinated Hydrocarbon Solvents", presented at the 7th Annual Conference of Metallurgists, Vancouver, British Columbia, 1968.
69. Boros, J., *et al.*, "Oxidation of Pyrites in Chlorinated Solvents", EPA report R2-72-069, November 1972.
70. Fortunatov, N. S., *et al.*, Ukr. Khim. Zh. 32, 900 (1966); CA. 65, 19504a (1966).

71. (i) Sherman, M. I. and Strickland, J. D. H., J. of Metals, Trans. AIME 9, 1386 (1957).

(ii) Jackson, K. J. and Strickland, J. D. H., Transactions of the Metallurgical Society of AIME, June 1958, p. 373.

72. Yoshiro Amio, Chem. Abstr. 51, 18514d (1957).

73. Lopatin, A. G. and Girdasova, Z. M., Chem. Abstr. 69, 98598y (1968).

74. Vasilakos, N., Research Progress Report, California Institute of Technology, June 1979, p. 39.

75. Stephen, H. and Stephen, T. (ed.), "Solubilities of Inorganic and Organic Compounds", Vol. 1 (Part 1), Pergamon Press, New York (1963), p. 92.

76. (i) Yakovkin, A., J. Russ. Phys.-Chem. Soc. 32, 673 (1900).

(ii) Arkadiev, V., ibid. 50, 205 (1918).

(iii) Adams, F. W. and Edmonds, R. G., Ind. Eng. Chem. 29, 447 (1937).

(iv) Whitney, R. P. and Vivian, J. E., ibid. 33, 741 (1941).

77. Reid, E. E., "Organic Chemistry of Bivalent Sulfur", Vol. 2, pp. 48-52, Chemical Publishing Co., New York (1960).

78. Pierre, J. I., Jahresber. 1948-9, 686 (1851).

79. Spring, W. and Lecrenier, A., Bull. Soc. Chim. 48, 623 (1887).

80. Fries, K. and Vogt, W., Ann. 381, 337-46 (1911).

81. Lee, S. W. and Dougherty, G., J. Org. Chem. 5, 81 (1940).

82. Dronov, V. I., *et al*., "Chemistry of Organic Sulfur Compounds in Petroleum and Petroleum Products", Akademiya Nauk SSSR, Vol. 6, 1964. Translated from Russian, Jerusalem 1967, p. 316.

83. (i) Zincke and Frohneberg, Ber. 42, 2728 (1909).

(ii) Douglass, I. B. and Johnson, T. B., J. Am. Chem. Soc. 60, 1486 (1938).

(iii) Ziegler, C. and Sprague, J. M., J. Org. Chem. 16, 621 (1951).

(iv) Truce, W. E. and Milionis, J. P., J. Am. Chem. Soc. 74, 974 (1952).

84. Wood, A. E. and Travis, E. G., J. Am. Chem. Soc. 50, 1226 (1928).

85. Ardagh, E. G. R., *et al.*, J. Soc. Chem. Ind. 59, 27 (1940).

86. Vasilakos, N. P., Bone, R. L. and Corcoran, W. H., Ind. Eng. Chem. Prod. Res. Dev., submitted for publication, 1980.

87. Brown, R. K., *et al.*, J. Am. Chem. Soc. 70, 1748 (1948).

88. Attar, A. and Corcoran, W. H., Ind. Eng. Chem. Prod. Res. Dev. 17, 102 (1978).

89. Baciocchi, E. and Mandolini, L., Ric. Sci. 37, 863 (1967).

90. Dronov, V. I., *et al.*, Khim. Seraorg. Soedin., Soderzh. Neftyakh Nefteprod 9, 158 (1972); Chem. Abstr. 79, 115388f (1973).

91. (i) Otto and Ostrop, Ann. 141, 96 (1867).

(ii) Otto, ibid. 136, 154 (1865).

92. (i) Lecher, H. and Holschneider, F., Ber. 57B, 755 (1924).

(ii) Lecher, H., *et al.*, Ber. 58B, 409 (1925).

93. Nelson, H. W., *et al.*, Ind. Eng. Chem. 25, 1355 (1933).

94. Ochi, S., J. Fuel Soc. Japan 9, 246 (1930).

95. Sun, S. C. and Wu, M. T., preprint, AIME annual meeting, Dallas, Texas, February 1974.

96. Mukai, Shigeru, *et al.*, Nenryo Kyokai-Shi 48, 905 (1960).

97. Vasilakos, N. P., et al., "Desulfurization of Coal by Aqueous Chlorination", U.S. Patent pending.

98. Lowry, H. H. (ed.), "Chemistry of Coal Utilization", supplementary volume, pp. 215-9, John Wiley and Sons Inc., New York (1963).

99. Wiles, L. A. and Ariyan, Z. S., Chemistry & Industry, Dec. 1962, pp. 2102-5.

100. Vasilakos, N. P., Research Progress Report, California Institute of Technology, March 1979, pp. 6-7.

101. Fong, W. and Pichaichanarong, P., Research Progress Report, California Institue of Technology, August 1980.

102. Barton, A. F. M., Chem. Rev. 75, 731 (1975).

103. Lawson, D. D., "Solubility Parameters as Related to Coal Technology", Jet Propulsion Laboratory Seminar, December 1979.

104. Flory, P. J. and Rehner, J., J. Chem. Phys. 11, 521 (1942).

105. Lawson, D. D., et al., "Solubility Parameter Spectroscopy", 18th Canadian High Polymer Forum, 1975.

106. Van Krevelen, D. W., Fuel 44, 229 (1965).

107. Small, P. A., J. Appl. Chem. 3, 71 (1953).

108. Kirov, N. Y., et al., Fuel 46, 415 (1967).

109. (i) Sanada, Y. and Honda, H., Fuel 45, 295 (1966).
  (ii) ibid. 45, 451 (1966).

110. (i) Yen, T. F. and Lee, W. C., Proc. Intersoc. Energy Convers. Eng. Conf., 1979, 14th (Vol. 1), pp. 832-6.
  (ii) Weinberg, V. L. and Yen, T. F., Fuel 59, 287 (1980).

111. Lawson, D. D., private communication.

112. Reeder, J. and Kushida, R., Interoffice memorandum 346-216-JR/RK, Jet Propulsion Laboratory, June 1980.

113. Angelovich, J. M., et al., Ind. Eng. Chem. Process Des. Develop. 9, 106 (1970).

114. Vasilakos, N., "Suggestions for Future Studies in the Coal Chlorinolysis Program", report submitted to the Jet Propulsion Laboratory, September 1979.

115. Blakemore, J. E., et al., Ind. Eng. Chem. Fundam. 12, 147 (1973).

116. Bone, R. L., "Application of Selective Oxidation to the Desulfurization of Fuel Oil", PhD Thesis, California Institute of Technology, 1981.

117. Vasilakos, N. and Corcoran, W. H., "Beneficiation of Coal in a Methanol-Water Slurry", October 1979, U.S. Patent pending.

118. Kralik, J. G., research proposal, California Institute of Technology, September 1979.

119. Wood, T. J., Appl. Chem. 8, 565 (1958).

120. Levenspiel, O., "Chemical Reaction Engineering", pp. 361-377, John Wiley and Sons Inc., New York (1972).

121. Crank, J., "Mathematics of Diffusion", p. 86, Oxford Un. Press, 1956.

122. Smith, J. M., "Chemical Engineering Kinetics", pp. 400-23, Mc Graw Hill, New York (1970).

123. Perry, R. H. and Chilton, C. H. (ed.), "Chemical Engineer's Handbook", pp. 3-224/6, McGraw Hill, Fifth Edition, New York (1975).

124. (i) Taylor, N. and Hildebrand, J. H., J. Am. Chem. Soc. 45, 682 (1923).

(ii) Hildebrand, J. H. and Gjaldbaek, J. C., ibid. 72, 609 (1950).